



NTNU – Trondheim
Norwegian University of
Science and Technology

Grounding of Outdoor High Voltage Substation

Samnanger Substation

Anders Morstad

Master of Science in Electric Power Engineering

Submission date: June 2012

Supervisor: Hans Kristian Høidalen, ELKRAFT

Norwegian University of Science and Technology
Department of Electric Power Engineering

PREFACE

This report presents my master thesis work conducted at the Norwegian University of Science and Technology during the spring 2012.

The nomenclature list explains abbreviations and technical terms necessary to know to gain optimal understanding of the report content.

When the reference is listed before the sentence period it applies only to that sentence. If the reference is listed after the sentence period it applies to all text in the previous paragraph. All references are listed in a separate reference list.

It must be emphasized that Samnanger substation is only used as an example, and simplifications made in simulations may not correspond with reality.

I would like to thank Professor Hans Kristian Høidalen for being willing to be my mentor on this master thesis and for his valuable inputs during discussions. Arne Petter Brede at Sintef also deserves thanks for responding quickly to my questions, and challenging me to look deeper into different phenomenon occurring during my work. Also many thanks to Helge Kvale at BKK who provided me with valuable information and insight about the Samnanger substation and the network connected to it.

For giving me the opportunity to write about substation grounding, I would like to thank Øyvind Ølstad and ABB in Oslo.

The front page picture is downloaded from: <http://www.esgroundingsolutions.com/about-electrical-grounding/what-is-ground-potential-rise.php>

Veme, 05.06.2012

Anders Morstad

SUMMARY

The subsurface grounding network of high voltage substations is installed as a protective measure to prevent dangerous touch- and step voltages inside the substation area. The main objective of this master thesis is to map the different parameters that will influence the performance of the grounding system, and to what extent the performance will be affected. Samnanger substation and the electrical network connected to it are used as a basis for the simulations conducted in CDEGS – AutoGrid Pro.

Two different networks were used in the simulations; Network 1 with a specified two layer soil model, and Network 2 with a specified grounding network resistance to earth of 2Ω . Network 1 was used where the simulation objective was to investigate how the resistance to earth changed with varying parameters, while Network 2 was used for all other simulations.

Thirteen different simulations were conducted: Initial modeling, Insulating surface layer modeling, Varying fault duration, Varying soil conditions at Samnanger substation, Varying R_E at adjacent substations, Varying R_t for overhead line towers, Varying mesh density, Varying cross sectional value of earth electrodes, Meshed network including vertical rods, Meshed network including vertical rods embedded in conductive additives, Disconnection of overhead line earth conductors, Increased single-phase-to-earth short circuit current, and Three phase short circuit current.

The simulations showed that:

- $U_T < U_{Tp}$ inside the switchyard bays during normal conditions when $t_{\text{fault}} = 1$ second, but in some of the “open” areas inside the substation $U_T > U_{Tp}$. Using a $3000 \Omega\text{m}$ -10 cm insulating surface layer and $t_{\text{fault}} = 0.06$ second eliminates all dangerous U_T for an I_{k1} fault. Same effect for I_{k3} using $3500 \Omega\text{m}$ -20 cm surface layer and $t_{\text{fault}} = 0.06$ second
- $U_S < U_{Sp}$ for all simulations
- The soil resistivity and its composition is decisive when it comes to U_T and U_S
- The value of R_E of adjacent substations have very little to neglectable effect on the grounding network performance at Samnanger
- The value of R_t has a large effect on the grounding network performance at Samnanger and adjacent substations
- Based on conditions used in this master thesis, Statnett Earthing Guidelines with respect to mesh density seems too conservative when considering 50 Hz grounding. Transient conditions have not been simulated
- The cross sectional value of the grounding network electrodes has little effect on the grounding network performance
- Vertical grounding rods have little effect in soils with high resistivity
- Vertical rods embedded in conductive additives were ineffective using the recommended modeling method in AutoGrid Pro

NOMENCLATURE LIST

Earth conductor	Conductor which provides a conductive path, or part of the conductive path, between a given point in a system or in an installation or in equipment and an earth electrode
Earth electrode	Conductive part, which may be embedded in a specific conductive medium, e.g. in concrete or coke, in electric contact with the Earth
Earth fault current (I_g)	Current which flows from the main circuit to earth or earthed parts at the fault location (earth fault location)
Earth Potential Rise (EPR)	Voltage between an earthing system and remote earth
Electric resistivity of soil (ρ_E)	Resistivity of a typical sample of soil
Grounding system	Arrangement of connections and devices necessary to earth equipment or a system separately or jointly
Impedance to earth (Z_E)	Impedance at a given frequency between a specified point in a system, or in an installation or in equipment, and reference earth
(Local) earth	Part of the Earth which is in electric contact with an earth electrode and the electric potential of which is not necessarily equal to zero
Protective bonding conductor	Protective conductor for ensuring equipotential bonding
Remote earth	Part of the Earth considered as conductive, the electrical potential of which is conventionally taken as zero, being outside the zone of influence of the relevant earthing arrangement
Resistance to earth (R_E)	Real part of the impedance to earth
Permissible step voltage (U_{Sp})	The maximum value allowed for step voltages to ensure that auricular fibrillation does not occur
Permissible touch voltage (U_{Tp})	The maximum value allowed for touch voltages to ensure that auricular fibrillation does not occur

Step voltage (U_S)	Voltage between two points on the Earth's surface that are 1 m distant from each other, which is considered to be the stride length of a person
Substation	Part of a power system, concentrated in a given place, including mainly the terminations of transmission or distribution lines, switchgear and housing and which may also include transformers. It generally includes facilities necessary for system security and control (e.g. the protective devices)
Touch voltage (U_T)	Part of the potential rise during an earth fault which can affect a person by the current flowing through the body from hand to foot. 1 meter horizontal distance from exposed-conductive-part.

TABLE OF CONTENTS

1	Introduction	1
2	Theory and method	3
2.1	Substation grounding theory	3
2.1.1	<i>Earth potential rise</i>	3
2.1.2	<i>Touch voltage</i>	4
2.1.3	<i>Step voltage</i>	5
2.1.4	<i>Dimensioning of the grounding system</i>	5
2.1.5	<i>Substation grounding electrodes</i>	7
2.1.6	<i>Transients and lightning</i>	8
2.1.7	<i>Soil conditions</i>	9
2.2	Grounding system modeling in CDEGS	10
2.2.1	<i>Safety module</i>	10
2.2.2	<i>Report module</i>	11
2.2.3	<i>Soil module</i>	12
2.2.4	<i>Circuit module</i>	13
2.2.5	<i>Process module</i>	14
3	Statnett Earthing Guidelines	15
4	Samnanger substation	17
4.1	Substation overview	17
4.2	Soil conditions	19
4.3	Grounding network	19
4.4	Adjacent substations	19
4.5	Power lines connected to Samnanger	20
4.6	Single phase short circuit values at Samnanger	22
5	Modeling and simulation results	23
5.1	Initial modeling	23
5.1.1	<i>Soil modeling</i>	24
5.1.2	<i>Grounding network modeling</i>	25
5.1.3	<i>Circuit modeling</i>	26
5.1.4	<i>Initial modeling results</i>	26
5.2	Insulating surface layer	31
5.3	Varying fault duration	32
5.4	Varying soil conditions at Samnanger substation	32
5.4.1	<i>Scenario 1</i>	33
5.4.2	<i>Scenario 2</i>	35
5.4.3	<i>Scenario 3</i>	35
5.4.4	<i>Scenario 4</i>	36
5.5	Varying R_E at adjacent substations	37
5.5.1	<i>Scenario 5</i>	38
5.5.2	<i>Scenario 6</i>	39
5.5.3	<i>Scenario 7</i>	39

5.6 Varying R_t for overhead line towers.....	39
5.6.1 Scenario 8	40
5.6.2 Scenario 9	41
5.6.3 Scenario 10.....	42
5.7 Mesh density	44
5.7.1 Scenario 11.....	44
5.7.2 Scenario 12.....	45
5.8 Cross sectional value of earth electrodes	46
5.9 Vertical rods	47
5.10 Conductive additives.....	49
5.11 Overhead earth conductors	51
5.12 Increased single-phase-to-earth current	54
5.13 Three phase short circuit current	55
6 Discussion.....	59
6.1 Initial modeling	59
6.2 Insulating surface layer.....	59
6.3 Varying fault duration	60
6.4 Varying soil conditions at Samnanger substation	60
6.4.1 Scenario 1	60
6.4.2 Scenario 2	60
6.4.3 Scenario 3	61
6.4.4 Scenario 4	61
6.5 Varying R_E at adjacent substations	62
6.5.1 Scenario 5	62
6.5.2 Scenario 6	62
6.5.3 Scenario 7	62
6.6 Varying R_t for overhead line towers.....	63
6.6.1 Scenario 8	63
6.6.2 Scenario 9	63
6.6.3 Scenario 10.....	63
6.7 Mesh density	64
6.8 Cross sectional value of earth electrodes	64
6.9 Vertical grounding rods	65
6.10 Conductive additives.....	65
6.11 Overhead line earth conductors	66
6.12 Increased single-phase-to-earth current	66
6.13 Three phase short circuit current	67
7 Conclusion.....	69
8 Future work.....	71
References.....	73
Figure list.....	75
Table list.....	77

Appendices	79
Appendix A	81
Appendix B	83
Appendix C	85
Appendix D	87
Appendix E	89
Appendix F	91

1 INTRODUCTION

Grounding of high voltage substations is a very important subject in electric power technology since it is decisive when it comes to touch and step voltages that will arise within a substation area during an earth fault. High voltage substation grounding has previously been an experienced based field of work, thus it is of interest to acquire a more theoretical approach to dimensioning of high voltage substation grounding. This to ensure that safety issues are taken care of without constructing an over dimensioned, and more expensive than necessary, system.

In the past it has been common that the transmission system operator (TSO) and the regional network operator (RNO) engineered the grounding system of a new power substation themselves, but lately engineering companies like ABB have experienced that this task has been included in the request for offer. Thus, ABB feel the need to strengthen their theoretical knowledge within the field of high voltage substation grounding through initiating a master thesis subject in cooperation with NTNU.

The main objective of this master thesis work is to map the different parameters that will influence the performance of the grounding system, and to what extent the grounding system performance is influenced. The scenario used in this master thesis is an existing grounding network at the Samnanger substation, which is connecting the well known monster tower line to Sima. The grounding network for Samnanger substation is developed by Statnett and is used as a basis for the simulations carried out by the use of CDEGS – Safe Engineering Services & technologies ltd.

To ensure a good understanding of the results presented in this master thesis report chapter two presents the basic theory behind substation grounding, with special emphasis on safety aspects like step and touch voltage. A short presentation of the simulation software is also presented in chapter two. Statnett have published Earthing Guidelines for their substations and these are presented in short in chapter three, where they are compared to legal and standard earthing requirements. Chapter four presents Samnanger substation, including the soil composition, adjacent substations and power lines connected to Samnanger. Modeling and simulation results are presented in chapter five. The discussion of results will be presented in chapter six. Chapter seven includes the conclusions of the master thesis work, while chapter eight presents potential future work that can be conducted.

2 THEORY AND METHOD

The following subchapters include the theory concerning substation grounding, and a presentation of the simulation program CDEGS – AutoGrid Pro. The substation grounding theory includes the most important issues regarding safety, dimensioning and soil characteristics. Only the typical earth electrodes used in substation grounding are presented, and it is referred to [1] for more information about other types of electrodes.

2.1 Substation grounding theory

The substation grounding system shall be dimensioned and installed in such a way that during a fault in the electrical installation, no danger to life, health or material shall occur neither inside nor outside the installation. The grounding system shall be constructed to fulfill the following demands, which apply to all voltage levels: [2]

- Provide personnel safety against dangerous touch voltages including at highest earth fault current
- Prevent damage to property and installations
- Be dimensioned to withstand corrosion and mechanical stress during the entire lifetime of the installation
- Be dimensioned to withstand the thermal stress from fault currents

The risk connected to electric shock to human beings is primarily connected to current flowing through the heart region and of a magnitude large enough to cause auricular fibrillation. The “current-through-body” limit, see Appendix A, is transformed into voltage limits in order to be compared to calculated step and touch voltages when considering the following factors:

- The amount of current flowing through the heart region
- The body impedance along the current path
- The resistance between the contact spot of the body and for example a metal construction against the hand including glove, or feet including shoes or shingle towards remote earth
- The duration of the fault

One must consider that the fault frequency, magnitude of the current, fault duration and presence of human beings are probabilistic factors [3].

2.1.1 Earth potential rise

The earth potential rise (EPR) is defined as the voltage between a grounding system and remote earth [3]. When electricity enters the earth as a result of a phase-to-earth fault or a lightning stroke, both the grounding system and the surrounding soil will rise in electrical potential leading

to potential differences along the surface which may cause hazardous step and touch voltages. The initial design of a grounding system can be based on the EPR, which can be calculated from (2-1).

$$U_E = R_E \cdot I_E \quad (2-1)$$

U_E Resistance to earth, calculated or measured [Ω]

I_E Fault current to earth [A]

2.1.2 Touch voltage

The permissible touch voltage (U_{Tp}) is a measure on how large a potential rise a human being can endure during an earth fault. According to NEK 440:2011 the U_{Tp} is calculated based on the maximum permissible current through the body, the current through the heart during a fault, the body impedance and stating that the probability of auricular fibrillation should be less than 5 %. The body impedance is assumed not to be exceeded by 50 % of the population. [3] The U_{Tp} is a function of fault time, and reduces with increasing time as shown in Figure 2-1. The duration of fault is dependent on the system protection, but there is a demand that earth faults shall be disconnected automatically or manually to ensure touch voltages to be time-limited [2].

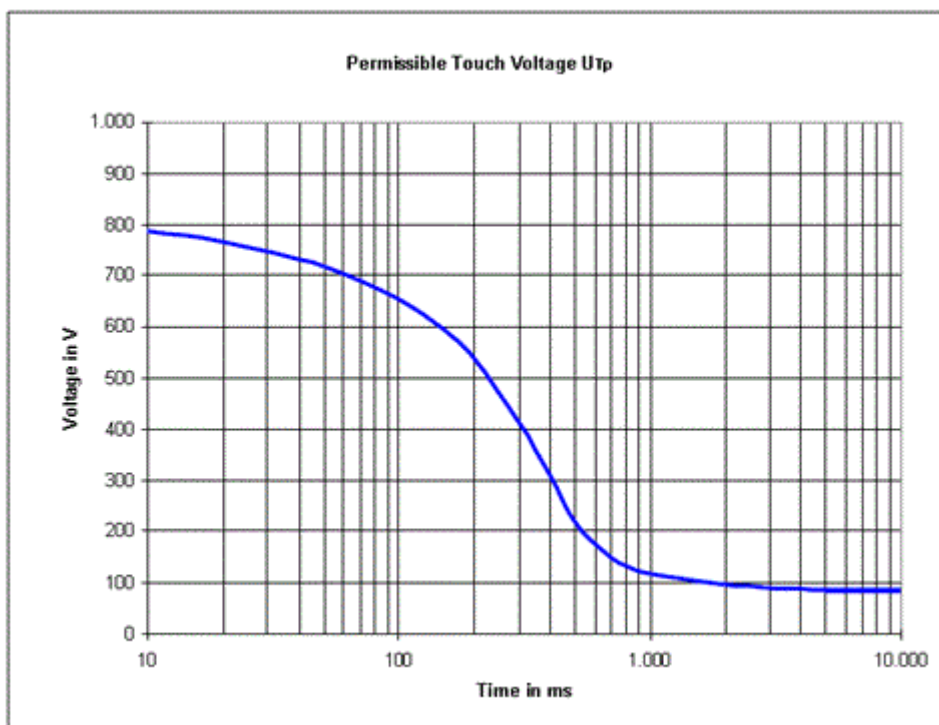


Figure 2-1 Permissible touch voltage U_{Tp} [3]

Figure 2-1 states the maximum permissible voltage between bare hands and feet, but this value can be increased by applying additional resistances like the resistance of footwear and gloves. The most common measure to increase U_{Tp} is to apply an insulating surface layer of high resistivity at the substation site. This top layer is normally 10 – 20 cm thick made up of crushed rock and acts as an “insulating” surface. For a top layer to have any effect its resistivity must be higher than the resistivity of the soil it is installed upon.

The potential touch voltage (U_T) shall be less than U_{Tp} , and is assumed to be so if one of the following conditions is met:

- The grounding system is part of a global grounding system
- The EPR during an earth fault is less than $2xU_{Tp}$
- The EPR during an earth fault is less than $4xU_{Tp}$, if measures to reduce the touch voltage are implemented. These measures are described in FEF 2006 - §4-11.

If neither of these conditions is met, U_T shall be calculated or measured. The maximum permissible R_E can be found from (2-2).

$$R_E = \frac{U_{Tp}}{I_E} \quad (2-2)$$

2.1.3 Step voltage

It is considered unnecessary to calculate values for the step voltage (U_S) inside the fence of the substation, since the permissible values of U_S are higher than U_{Tp} . Grounding systems that satisfies the demands for touch voltages will thus automatically satisfy the demands for step voltages. U_S just outside the fence of the substation must however be calculated to ensure that danger to human beings is not present. [3]

2.1.4 Dimensioning of the grounding system

The following subchapter is based on [3].

The grounding system shall be dimensioned to withstand corrosion and mechanical stress throughout the lifetime of the electrical installation. Relevant parameters for dimensioning of grounding systems are:

- Value of fault current
- Fault duration
- Soil properties

Fault current value and fault duration are dependent on the neutral point connection to earth of the high voltage installation.

The grounding system comprises earth electrodes, earth conductors and protective bonding conductors.

2.1.4.1 Earth electrodes

The material of electrodes in direct contact with the soil shall be corrosion resistant, and the electrodes must withstand the mechanical stress it is subjected to during installation and normal service [3]. Earth electrodes shall be made up of copper, steel, or copper coated steel [2]. Steel armoring in concrete foundations, steel poles or other natural earth electrodes may be used as a part of the grounding system [3]. The minimum cross section of earth electrodes in Norway shall be 25 mm² Cu or 50 mm² steel, but it is the material's mechanical strength and resistance to corrosion that decides the dimensions of earth electrodes [2], as shown in Appendix B.

2.1.4.2 Earth conductors

Earth conductors and protective bonding conductors shall be made up of copper, steel, aluminum or copper coated steel. As for earth electrodes, both earth conductors and protective bonding conductors shall withstand corrosion and mechanical stress throughout the entire lifetime of the electrical installation [2]. To meet these demands the minimum cross section for the above mentioned conductors shall be 16 mm² Cu, 35 mm² Al, or 50 mm² steel. [3]

2.1.4.3 Thermal dimensioning

The following subchapter is based on [3]

The current flowing through earth conductors and electrodes shall not cause deterioration of the conductors or cause harm to surroundings due to heating of the conductor. Thermal dimensioning of earth conductors and earth electrodes shall be based on the currents shown in Appendix C. In some cases it may also be necessary to take into consideration the stationary zero sequence current, and one should also consider that the fault current may be elevated in the future due to voltage upgrading of the transmission lines. It is possible to dimension the earth electrodes and conductors for only parts of the fault current since the current often is divided. Experience has shown that temperature rise in the surrounding soil has little affection and does not have to be considered during the dimensioning process.

Calculation of cross section from value and duration of fault can be calculated, and the process is shown in NEK 440: 2011 - Appendix D. It is emphasized that minimum dimensions as described in 2.1.4.1 and 2.1.4.2 must be kept.

A flow chart showing how a grounding system shall be dimensioned is shown in Appendix D.

2.1.5 Substation grounding electrodes

A grounding system generally comprises several horizontal, vertical or inclined electrodes buried or driven into the earth to reduce the 50 Hz power-frequency earth resistance. The grounding system design of a substation depends largely on the voltage level and the size of the station, and the most common types of electrodes are vertical rods, horizontal earth conductors radiating from one common point, or a meshed network. It is common to combine these types of design if the soil conditions within the substation area vary substantially, and to optimize the performance of the grounding system. [4] The most common grounding design for outdoor substations is a meshed network, often combined with vertical rods. Rods driven vertically or inclined into the earth are advantageous when the resistivity of the earth decreases with increasing depth. In the initial planning phase of a grounding system one can use analytical formulas to calculate the R_E for a meshed network, as shown in (2-3). It must be emphasized that (2-3) is only an approximation and does not provide very accurate results, but it is nevertheless useful in the initial planning phase as a basis for computer assisted design and simulation. The area of the meshed network is decisive when it comes to the resulting R_E , but also the size and number of meshes must be considered.

$$R_E = \frac{\rho}{4} \sqrt{\frac{\pi}{A}} + \frac{\rho}{L} \quad (2-3)$$

A Area of the meshed network [m²]

L Total length of horizontal electrodes [m]

For a meshed network with vertical ground electrodes (2-4) and (2-5) can be used to approximate the resistance to earth.

$$R_E = \rho \left[\frac{1 + \frac{r}{r + 2.5h}}{8rK_R} + \frac{1}{L} \right] \quad (2-4)$$

$$K_R = 1 + \frac{n_R l_R^2}{10r^2} \quad (2-5)$$

r Radius of a circle with area equivalent to the meshed network [m]

h Installation depth of meshed network [m]

L	Total length of horizontal and vertical electrodes [m]
K_R	Constant dependent of the number, position and length of vertical electrodes
l_R	Length of a single vertical electrode [m]
n_R	The sum of vertical electrodes along the circumference of the meshed network and half of the remaining vertical electrodes in the rest of the meshed network

At substation sites where the soil consists largely of rock it is common to drill holes in the ground and fill them with a filling compound with low resistivity, such as bentonite or petroleum coke. Vertical rods can then be driven into the holes. For additional information regarding substation grounding electrodes, see [4].

2.1.6 Transients and lightning

Lightning strokes and switching of breakers are sources to high- and low frequent currents and voltages. Switching transients typically stem from switching of long cable sections, GIS disconnectors, and capacitor banks. The transients from lightning strokes and switching operations need to be damped, and this is achieved by increasing the density of grounding electrodes, or impulse electrodes, around feeding points. The increased density will handle the high frequency currents, while the meshed grounding network will handle the low frequency currents. [3] Statnett recommend that the meshed network is denser around surge arresters, and voltage- and current transformers [5].

It is impossible to completely prevent damages caused by lightning strokes, but a generally agreed practice is to provide lightning protection systems for outdoor switchgear installations and for buildings of indoor switchboards. Overhead line earth conductors and lightning rods can be used as protection against direct lightning strokes, as surge arresters generally only protect against incoming atmospheric overvoltages caused by a lightning stroke far from the substation. These methods provide an almost complete protection against lightning strokes, they are simple methods, and are the standard solutions for installations up to 420 kV. [6] For additional information regarding transient and lightning protection of substations, see NEK 440:2011, Part 1, Appendix E.

2.1.7 Soil conditions

The following subchapter is based on [7].

The specific resistance (ρ_E) of the soil varies considerably depending on the type of soil, granularity, temperature, and the density- and humidity content. This is due to the fact that the soil consists mainly of silicon- and aluminum oxide which act as insulators, thus the electric conductivity of the soil is dependent on the salts and moisture between these materials since the electrical conduction in the soil is mainly electrolytic. Quite large deviations in specific resistance can be observed due to temperature changes and humidity content throughout a year.

The soil at any given substation site is often non-homogenous due to the fact that the soil normally consists of several layers. It is considered appropriate to approximate the soil characteristics by assuming that the soil consists of two layers; a top layer of resistivity ρ_1 and thickness d_1 , and a bottom layer with resistivity ρ_2 and infinite depth as illustrated in Figure 2-2.

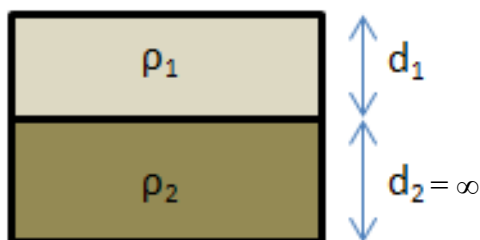


Figure 2-2 Two layer soil model

The specific resistance of the soil can normally be measured by using a four probe method called the Wenner method, to determine the resistance to earth (R_E) for earth electrodes. Table 2-1 shows the guidance values for the specific resistance of different soils.

Table 2-1 Specific resistance of different soils

Type of soil	Specific resistance of the soil [Ωm]
Boggy soil	5 – 40
Clay, loam, humus	20 – 200
Peat, mould	50 – 250
Sand	200 – 2500
Gravel	2000 – 3000
Weathered rock	< 1000

Sandstone	2000 – 3000
Ground moraine	< 30000
Granite	< 50000

2.2 Grounding system modeling in CDEGS

The CDEGS software package (Current Distribution, Electromagnetic fields, Grounding and Soil structure analysis) is a simulation tool used to analyze projects involving grounding, electromagnetic fields, and electromagnetic interference, during normal, fault, lightning and transient conditions. The CDEGS sub package AutoGrid Pro is used for modeling and simulation of the substation grounding system in this master thesis. AutoGrid Pro computes the following:

- R_E for the grounding system
- Earth potentials inside and outside the installation
- EPR of the grounding system and nearby buried metallic structures
- U_T and U_S for the grounding system
- Fault current distribution
- Amount of material used

The user interface consists of a CAD drawing module for the design of the grounding network, along with the most important integrated modules; Safety, Report, Soil, Circuit and Process module.

2.2.1 Safety module

The criteria that should be used during the safety analysis of the grounding installation shall be defined in the Safety module. Based on either IEEE or IEC standards the limits for the touch and step voltages can be derived. The limits for touch and step voltages are, as explained in 2.1.2 and 2.1.3, a function of the fault time, but also an insulating surface of relatively high resistivity will contribute to higher limits.

As can be seen in Figure 2-3 it is possible to define the initial safety criteria in the “Safe Allowable Values” box. The safe step and touch voltage values are based on the “Fibrillation Current Calculation Method” in the “Safety (Advanced)” window. The Norwegian standard is based on the C2-IEC curve and that the curve is exceeded by 50 % of the population.

It is also possible to define three scenarios of fault clearing time with the results being presented in the written part of the Report module, see Figure 2-3. In this way it is possible to see how the step and touch voltages change with increasing fault clearing time.

To see how the step and touch voltage limits change with increasing surface layer resistivity, it is possible to define the number of scenarios to be investigated, surface layer thickness, starting surface resistivity and incremental surface resistivity. The results can be presented in table form in the written part of the Report module.

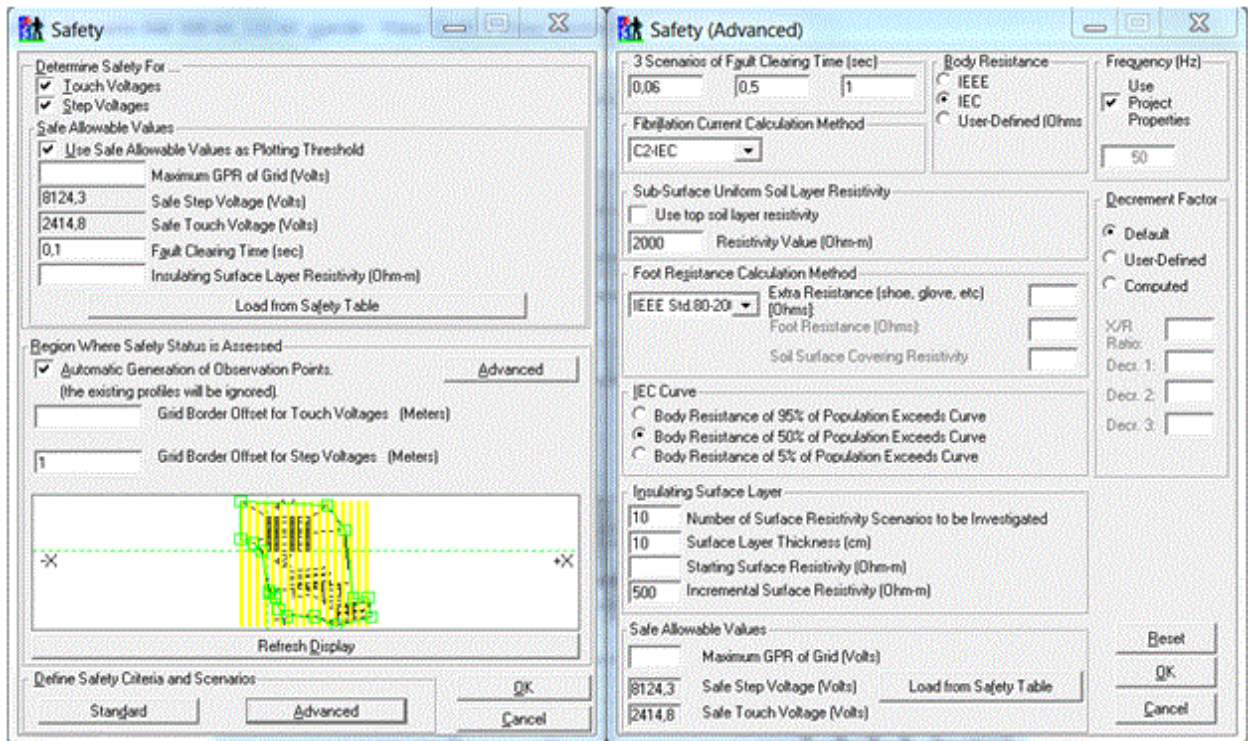


Figure 2-3 User interface of the Safety module

2.2.2 Report module

The Report module can provide both written and graphical reports presenting the results of the simulations. The written report can, in addition to the computation results and input data summary, present a list of materials. It is very beneficial that the list of materials can be a part of the simulation reporting since it shall be included in the grounding network documentation.

The graphical part of the Report module can present computation plots as 2D Spot, 2D curve, 2D contour and 3D perspective plots. The computation plots can present touch and step voltages, scalar potential, soil resistivity and fault current distribution. Grounding system- and electric network configuration can be presented in configuration plots as 3D perspective, side- and top view. Figure 2-4 shows the user interface of the Report module.

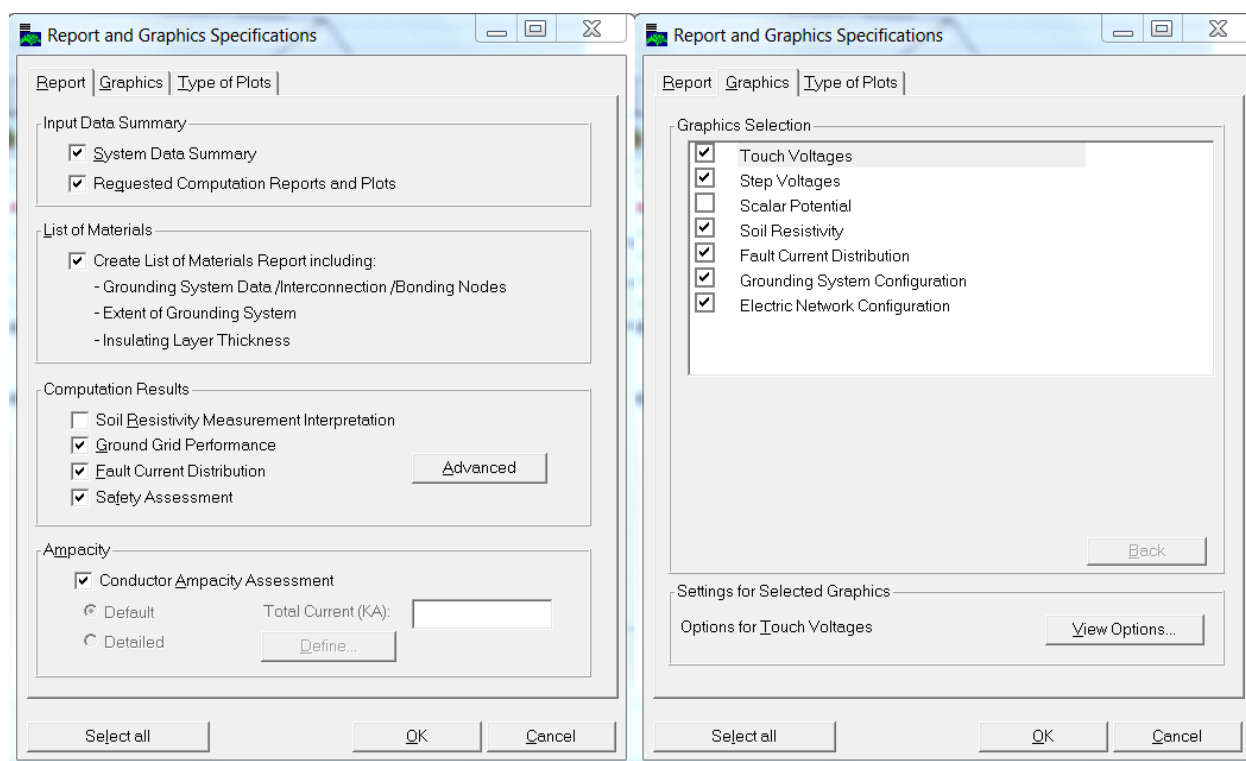


Figure 2-4 Report module interface

2.2.3 Soil module

The Soil module is used to define the characteristics of the soil where the grounding network is installed. The soil characteristics can be defined using specified soil structure characteristics, or deduced from field resistivity measurements.

When specifying a soil structure one can choose between uniform soil, horizontal and vertical multilayer soil, and arbitrary heterogeneities. It is also possible to simulate hemispherical or cylindrical shapes of different resistivity than the rest of the soil. For most cases it is sufficient to simulate a two-layer horizontal soil to achieve realistic results. It is evident that the more complex soil type simulated, the more time demanding the simulation will be.

To achieve the most precise presentation of the soil characteristics one should deduce the soil structure from field resistivity measurements. The most correct resistivity measurements are obtained after the substation area has been leveled out, since the soil structure and characteristics often change substantially during the engineering process. It is however in most cases not possible to wait with the grounding network engineering until the substation area has been leveled out.

In the Soil module it is possible to choose between five measurement methods: General, Schlumberger, Unipolar, Dipole-dipole, and the most common; Wenner. The needed input data are probe spacing, depth of probes and apparent resistance/resistivity. In the Advanced tab it is

possible to determine whether the program shall deduce the number of soil layers, or set a user defined number of layers. Figure 2-5 shows the Soil module interface.

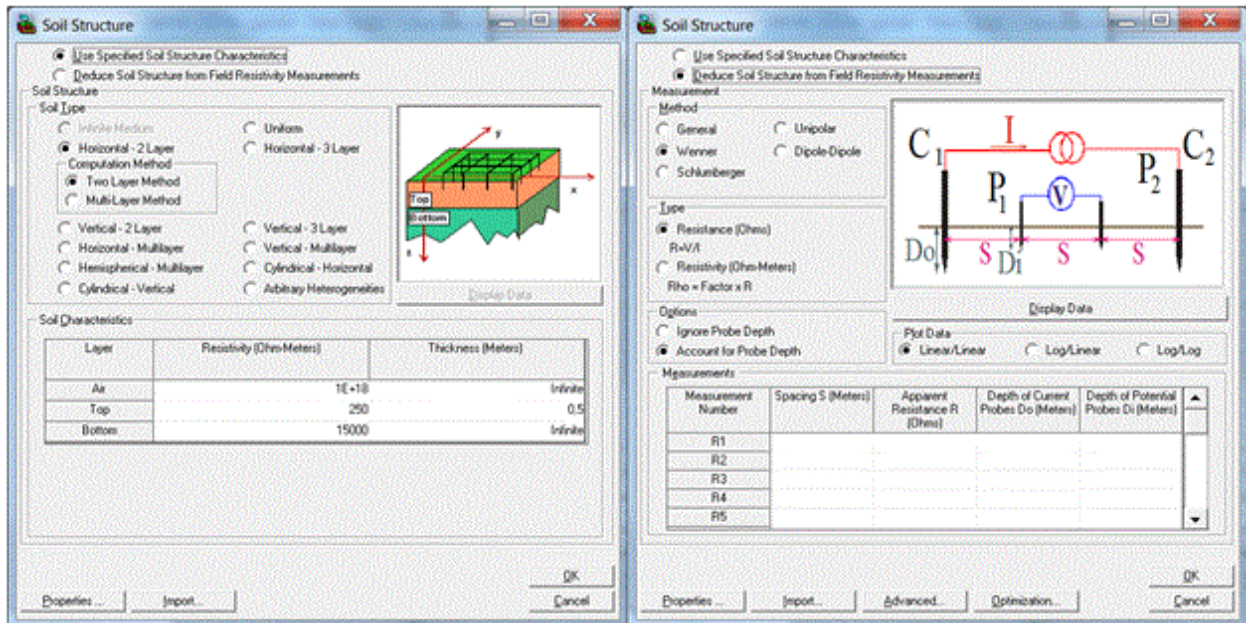


Figure 2-5 Soil module interface

2.2.4 Circuit module

Normally a substation is connected to several other substations through overhead power lines or cables. These adjacent substations contribute to the total short circuit current during a fault, but they will also absorb some of the fault current through the overhead line earth conductors and the grounding networks of the substations.

The Circuit module contains two tabs: Central site and Terminals. In the Central site tab the only things to specify are the substation name and the average soil characteristics in the region covered by the electrical network. One can also choose to specify a value for the substation ground impedance, but this is normally deduced from grounding computations done by the program.

In the Terminals tab the first things to specify are the terminal name, ground impedance and the short circuit contribution from the terminal. The number of sections, section length and tower impedance of the overhead line are specified under the Section tab in Terminals. In addition it is possible to define the impedance of the neutral-to-terminal connection depending on the transformer neutral grounding arrangement. Lastly the overhead line including any earth conductors must be defined. It is sufficient to model the overhead line earth conductors and the phase line furthest away from the earth conductors. The characteristics of the overhead line earth

conductors can be imported from the simulation software abundant database, or it can be defined by the user. Figure 2-6 shows parts of the Circuit module interface.

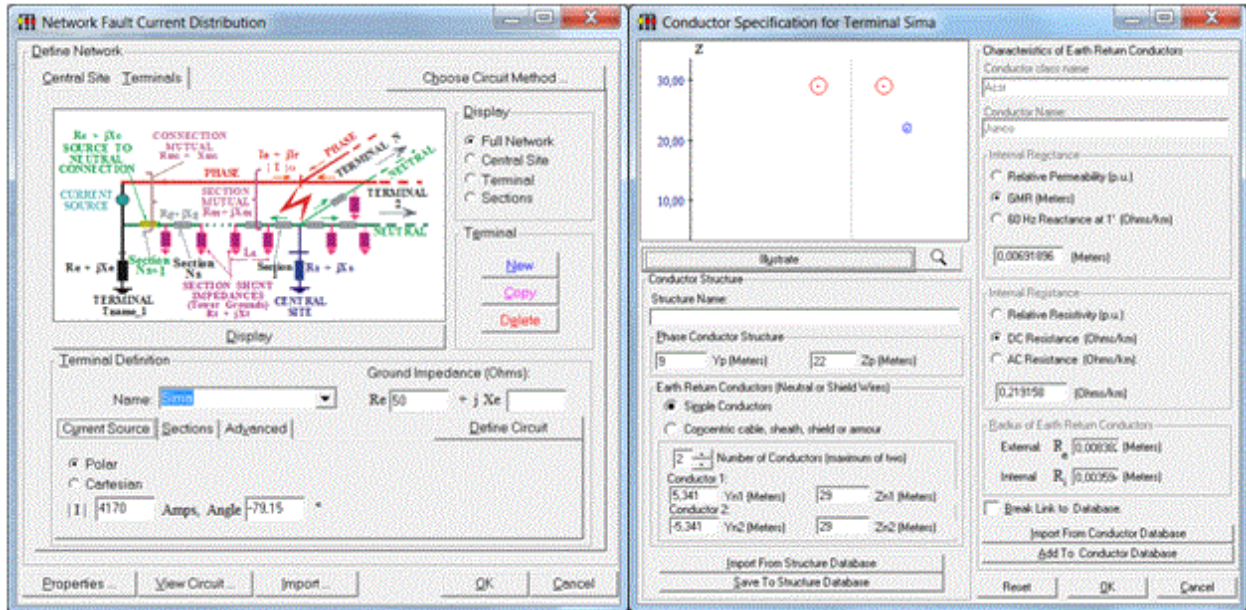


Figure 2-6 Circuit module interface

2.2.5 Process module

The Process module interprets the user settings and simulates the grounding network case thereafter. Based on the settings made in the Report module the Process module presents the simulation results in both written and graphical form, which can be used in the grounding network documentation.

3 STATNETT EARTHING GUIDELINES

The Grid Construction Division (N: Divisjon Nettutbygging) at the Norwegian transmission system operator Statnett has issued a guide for grounding of their substations. The guide is mainly based on publications from Sintef (EFI), IEEE, FEF 2006 and Statnett documents. This chapter will briefly compare the most important Statnett earthing guidelines for subsurface grounding with legal and standard requirements found in FEF 2006 and NEK 440:2011.

Table 3-1 shows the most important Statnett guidelines compared to FEF 2006 regulations and NEK 440:2011 norms.

Table 3-1 Comparison of Statnett guidelines and norms and regulations

	Statnett	FEF 2006/NEK 440:2011
Meshed network	<ul style="list-style-type: none"> - 70 – 120 mm² Cu - ≈ Square meshes <ul style="list-style-type: none"> ○ ≤ bay width between conductors ○ Preferably 4x4 – 5x5 m - d = 0.5 – 1.0 m 	<ul style="list-style-type: none"> - 25 mm² Cu - No special shape instruction <ul style="list-style-type: none"> ○ ≤ 10x50 m ○ The mesh size should be decreased in areas where large transients are probable - d = 0.5 – 1.0 m
Fences	<ul style="list-style-type: none"> - ≥ 70 mm² Cu line installed at ca. 0.3 m depth, one meter outside fence - Connected to every other fence pole and every gate pole - Cu line should normally be connected to the rest of the grounding network - Extra Cu line in the gate area, connected to the Cu line surrounding the fence 	<ul style="list-style-type: none"> - Bare metal fences shall be grounded - Earth electrode installed at ca. 0.5 m depth, one meter outside fence - A sufficient amount of earthing points shall be used, for example at every corner - In accordance with local conditions the fence should be connected to the high voltage grounding network or to separate electrodes. - Potential grading in gate area if the gate is connected to the grounding network
Measuring transformers and surge arresters	<ul style="list-style-type: none"> - Extra transverse earth conductors → extra fine meshed network 	<ul style="list-style-type: none"> - Mesh size should be reduced

4 SAMNANGER SUBSTATION

The Samnanger substation is located in Samnanger municipality, about 30 km straight east from Bergen city centre, as seen in Figure 4-1. Samnanger substation is owned and run by Bergenshalvøen kommunale kraftselskap (BKK) which is the territorial concessionaire of the regional network in 16 municipalities around Bergen.

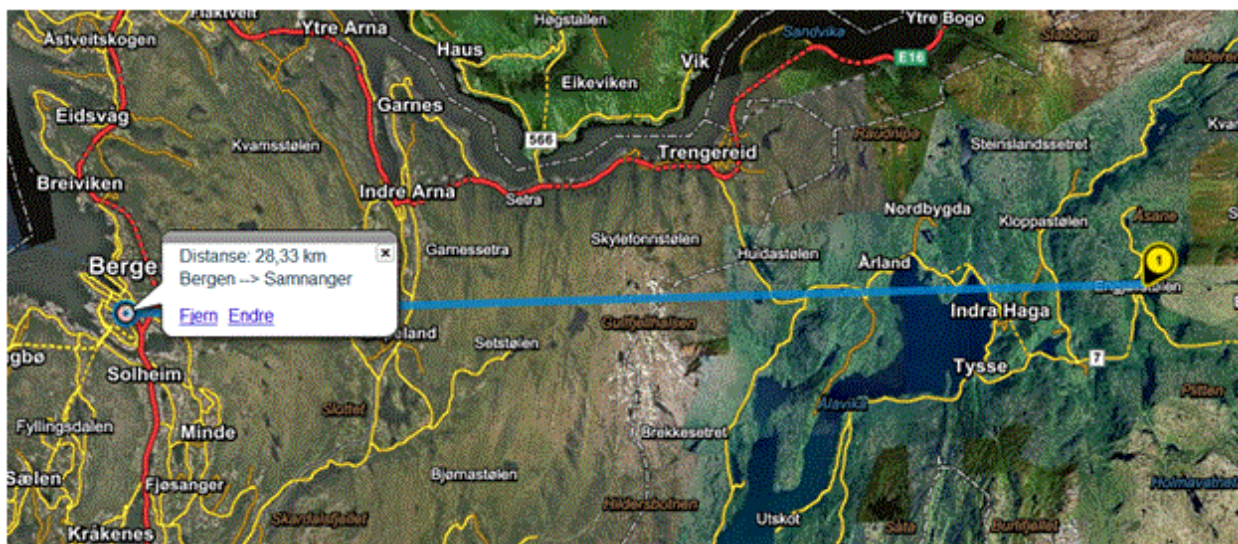


Figure 4-1 Location of Samnanger substation in relation to Bergen city centre

4.1 Substation overview

The substation is located in the bottom of a valley with steep hills on all sides, especially on the east and west side. Today the substation is equipped with switchgear for 300 kV and 132 kV, 300 kV/132 kV transformation equipment, and a control house. The 300 kV network has an effectively earthed neutral, while the 132 kV network has an isolated neutral.

There are three overhead lines connected to the 300 kV going to/from Evanger, Mauranger and Fana, and two overhead lines connected to the 132 kV going to/from Norheimsund and Frøland. At present Samnanger substation is expanded with four 420 kV switchgear sections. Connected to the 420 kV switchgear will be the Sima – Samnanger overhead line, one reactor section and one transformer section. The fourth section is reserved for future voltage upgrading of the 300 kV Samnanger – Mauranger overhead line. Future plans also show a voltage upgrading of the 300 kV Samnanger – Fana and Samnanger - Evanger overhead lines.

The 420 kV Sima – Samnanger and 300 kV Mauranger – Samnanger lines are owned by Statnett, while the remaining lines are owned by BKK Nett. An overview of the complete Samnanger substation is shown on the next page.

4.2 Soil conditions

Resistivity measurements of the soil at Samnanger substation does, to the author's knowledge, not exist. Correspondence with representatives from BKK shows that the soil at Samnanger substation consists of bedrock with a layer of earth of different thickness, but also bare rock. For the part of the 420 kV substation area that is leveled out the earth layer is considered to be 0.5 meter. The meshed network will be installed on top of blasted bedrock of relatively high resistivity. It is assumed for simulation reasons that the existing meshed grounding network at the 300 kV and 132 kV is installed the same way. See Table 2-1 for typical specific resistance of different soils.

4.3 Grounding network

The existing 300/132 kV grounding network at Samnanger substation was installed in the late 80's, when the substation was built. It consists of horizontal 70 mm² Cu earth electrodes arranged as a meshed network, the meshes being relatively large compared to today's guidelines from Statnett. Earth electrodes are installed along the dividing line between each switchyard bay and along the outer edges of the switchyard. Crossing earth electrodes are installed perpendicularly across the bay, close to the measuring transformers. See Appendix E for technical drawing of the grounding network.

The 420 kV grounding network is installed during the spring of 2012, and consists of horizontal 120 mm² Cu earth electrodes arranged as a meshed network. Looking at the technical drawing in Appendix E, one can see that the electrodes are more or less evenly spaced from left to right by approximately 5 meters. Across the switchyard bays there are only four electrodes unevenly spaced, making the meshes larger than the Statnett guidelines.

4.4 Adjacent substations

There are six substations connected to Samnanger substation, through over head power lines, shown in Table 4-1. It is assumed that these substations have similar soil conditions as Samnanger substation.

Table 4-1 Substations connected to Samnanger substation

Substation	Upper voltage level
Sima	420 kV
Mauranger	300 kV
Evanger	300 kV
Fana	300 kV
Norheimsund	132 kV
Frøland	132 kV

4.5 Power lines connected to Samnanger

The overhead power lines connected to Samnanger vary in voltage level between 132 kV to 420 kV, thus the material of the power lines and earth conductors will also vary depending on the voltage level. Table 4-2 shows the composition of the different overhead power lines, which is needed for simulation reasons.

L Length of line [km]

d_{pl} Distance between phase lines [m]

d_{gc} Distance between ground conductors [m]

h_{pl} Average height above ground for phase lines [m]

Table 4-2 Overhead lines connected to Samnanger substation

Going to	L [km]	No. of towers	d_{pl} [m]	Type of phase lines	h_{pl} [m]	d_{gc} [m]	Type of ground conductors
Sima	92.3	265	9	3x2 x ACSR Parrot special 863.1 mm ² , ϕ 38.3 mm	22	10.7	1. AACSR Sveid 261.5 mm ² , ϕ 21 mm 2. OPGW Sveid eqv. 244.7 mm ² , ϕ 21 mm
Mauranger	47.6	118	9	3 x FeAl nr. 480 Parrot 863.1 mm ² , ϕ 38.3 mm	16	9.0	1. Fe 85 mm ² , ϕ 12 mm 2. Fe 135 mm ² , ϕ 15.05 mm
Evanger	57.7	97	9/10	Section 1-50	20	10.4	1-16, 90-97
							2 x FeAl 53 Gondul
				Section 50-90			16-49
							2 x FeAl 69 Sveid, ϕ 21
				Section 90-97			49-50
							Buried electrodes
				Section 90-97			50-79
							2 x Fe 85 mm ² , ϕ 15 mm
							79-90
							2xFe 135 mm ² , ϕ 15 mm
Fana	32.9	71	9/10	Section 1-24, 26-71	20	10.4	2 x FeAl 53-Gondul, ϕ 18.27 mm
				Section 24-26			
				Section 24-26			Sea electrodes
				3 x FeAl nr. 1022, 15/37 Hubro			
Norheimsund	15.1	56	5	3 x FeAl 150 mm ² 26/7	12	5.2	2 x Fe 50 mm ² , ϕ 9 mm
Frøland	2.3	10	5	3 x FeAl 150 mm ² 26/7	12	5.2	2 x Fe 50 mm ² , ϕ 9 mm

4.6 Single phase short circuit values at Samnanger

The short circuit calculations at Samnanger are based on the new 420 kV installation with short circuit contribution from Sima and the 300 kV installation via a 1000 MVA autotransformer. Future voltage upgrading of the 300 kV overhead lines will contribute to an increase in the short circuit values.

The following assumptions are made for the short circuit calculations:

- The calculations are based on network model Norden 2010 which includes the 420 kV Sima – Samnanger overhead line.
- The short circuit current is based on transient reactances X_d' in the network model.
- The short circuit current is a calculated value, and some margin should be added to take into consideration the calculation uncertainty.

A single phase short circuit on the 420 kV busbar at the Samnanger substation results in a short circuit current of 10.63 kA $\angle -79.52^\circ$. The contributions are as follows:

Sima - 4.17 kA $\angle -79.15^\circ$

300 kV via autotransformer - 6.46 kA $\angle -79.76^\circ$

5 MODELING AND SIMULATION RESULTS

There is a continuous need to improve the performance of electrical installations while at the same time focus on keeping the costs at reasonable levels. By using simulation programs in the planning phase of grounding system design it is possible to increase the efficiency of the planning process, and design a grounding system which ensures the safety of the electrical installation and human beings at the most optimal cost.

As a basis for the simulations the designed and existing grounding system at Samnanger will be used, before different parameters will be changed and varied to see how they contribute to the grounding system performance.

The simulation results are discussed in chapter 6.

5.1 Initial modeling

The modeling and simulation of the grounding network is carried out in AutoGrid Pro which is a package in the CDEGS software. Before modeling of the soil, grid and external circuit can commence, the project settings must be decided. These settings include measuring units, nominal frequency, reporting type of results and safety settings. Table 5-1 shows the initial settings.

Table 5-1 Project settings

Measuring unit	- Meters
Frequency	- 50 Hz
Reports	<ul style="list-style-type: none"> - System data summary - Requested computation reports and plots - List of materials including: <ul style="list-style-type: none"> ○ Grounding system data/Interconnection/bonding nodes ○ Extent of grounding system ○ Insulating layer thickness - Ground grid performance - Fault current distribution - Safety assessment

Graphics	<ul style="list-style-type: none"> - Touch voltages - Step voltages - Soil resistivity - Fault current distribution - Grounding system distribution - Electric network configuration
Type of plots	<ul style="list-style-type: none"> - 2D Spot - 3D Perspective
Safety settings	<ul style="list-style-type: none"> - $t_{\text{fault}} = 1$ second (As stated in [3] and [5]) - Three additional scenarios of fault clearing time [s] <ul style="list-style-type: none"> o 0.06 o 0.1 o 8 - C2-IEC – Fibrillation current calculation method - IEC body impedance curve exceeded by 50 % of the population - Insulating surface layer for report comparison <ul style="list-style-type: none"> o 10 surface resistivity scenarios to be investigated o 10 cm surface layer thickness o 500 Ωm starting surface resistivity o 500 Ωm incremental surface resistivity - 1000 Ω shoe resistance (old and wet shoes)

5.1.1 Soil modeling

Based on the soil conditions at Samnanger described in 4.2, the soil is modeled and computed using the horizontal two layer method. The initial values of the layers are shown in, Table 5-2 based on typical resistivity values listed in Table 2-1.

Table 5-2 Values of soil layers

	Resistivity [Ωm]	Thickness [m]
Top layer	250	0.5
Bottom layer	10000	∞

5.1.2 Grounding network modeling

The grounding network was modeled based on the technical drawings shown in Appendix E. The 300/132 kV network was modeled as 70 mm² electrodes, while the rest of the network was modeled as 120 mm² electrodes, including 420 kV network, fence connectors and internal connectors. The installation depth of the grounding network is set to 0.5 meters. The complete modeled subsurface grounding network for Samnanger substation is shown in Figure 5-1.

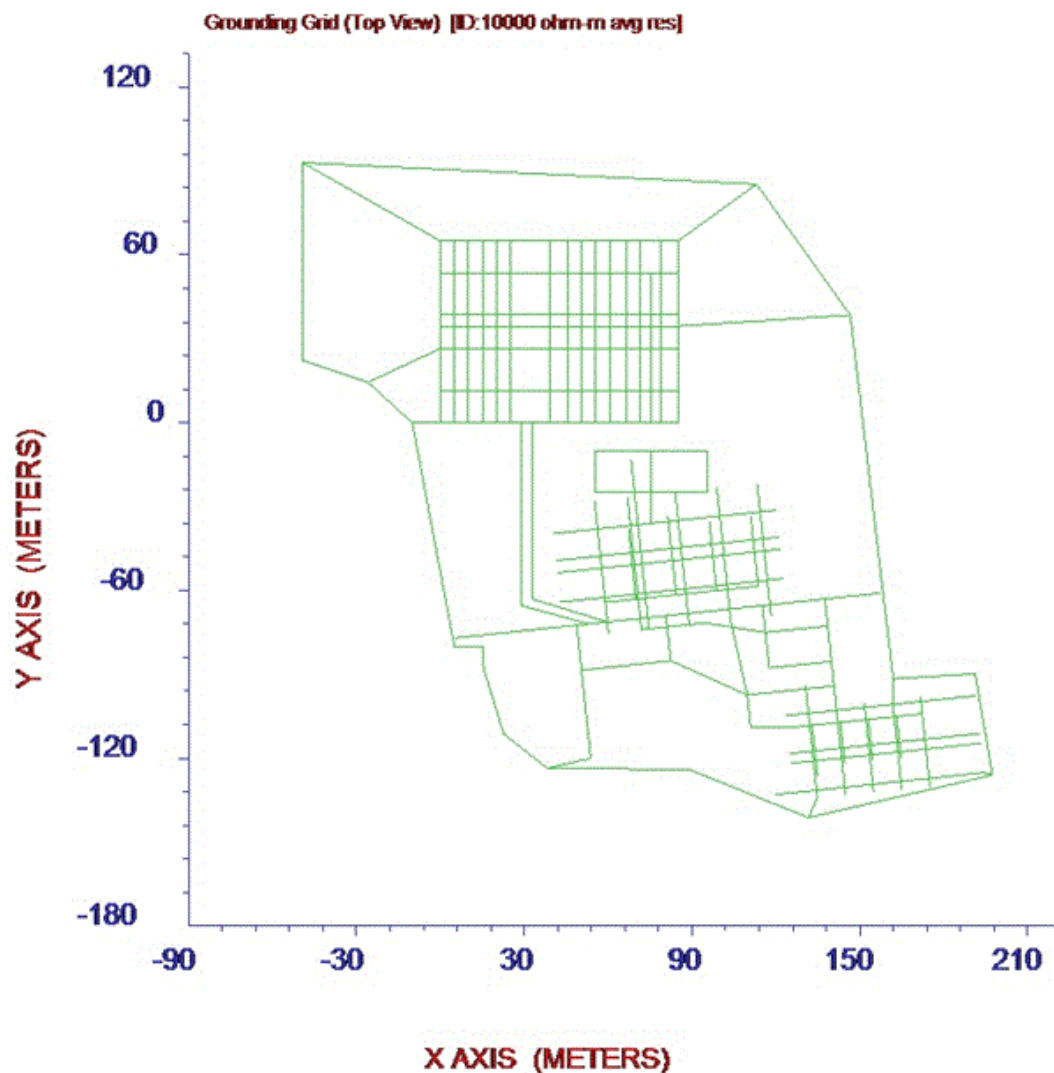


Figure 5-1 Grounding network as modeled in CDEGS

5.1.3 Circuit modeling

To achieve as correct results as possible the adjacent terminals and connected overhead power lines must be modeled. The average resistivity along the electric lines is based on the fact that the majority of the overhead power lines have rock foundations. The resistivity is set to 10000 Ωm , a typical value for bare rock. The short circuit currents described in 4.6 have been evenly distributed to the different terminals based on voltage level for simulation simplicity. The terminal data input is shown in Table 5-3. The average section length, L_s , is based on the number of towers and the length of the line, not considering any fjord spans.

Table 5-3 Terminal data input

	$I_{k1\text{ph-earth}}$ [A]	$R_{E\text{-terminal}}$ [Ω]	R_{tower} [Ω]	L_s [m]
Sima	4170 <-79.15	2	60	349.6
Mauranger	1615 <-79.76	2	60	406.8
Evanger	1615 <-79.76	2	60	393.8
Fana	1615 <-79.76	2	60	470.0
Norheimsund	807.5 <-79.76	2	60	274.5
Frøland	807.5 <-79.76	2	60	255.6

The initial $R_{E\text{-terminal}}$ value for the substations is based on resistance to earth measurements of various substations in Norway. Typical R_E values for Norwegian substations vary between 0.1 Ω and 2 Ω , and the most conservative value is chosen for these simulations due to the difficult grounding conditions in the substation areas.

It is assumed that the highest fault current discharged into the ground at the Samnanger substation occurs during a single-phase-to-earth fault on the phase furthest from the overhead line earth conductors. The magnetic field induction between the faulted phase and the earth conductors will be lowest in this case. It is sufficient to model the overhead line earth conductors and the faulted phase.

5.1.4 Initial modeling results

By using the settings in Table 5-1 and Table 5-2 the values for permissible touch (U_{Tp}) and step voltages (U_{Sp}) are 155.2 V and 347.5 V respectively. These values are listed in the written report

from the simulation; the complete written report is shown as an example in Appendix F. Figure 5-2 shows how the touch voltages are distributed inside the substation.

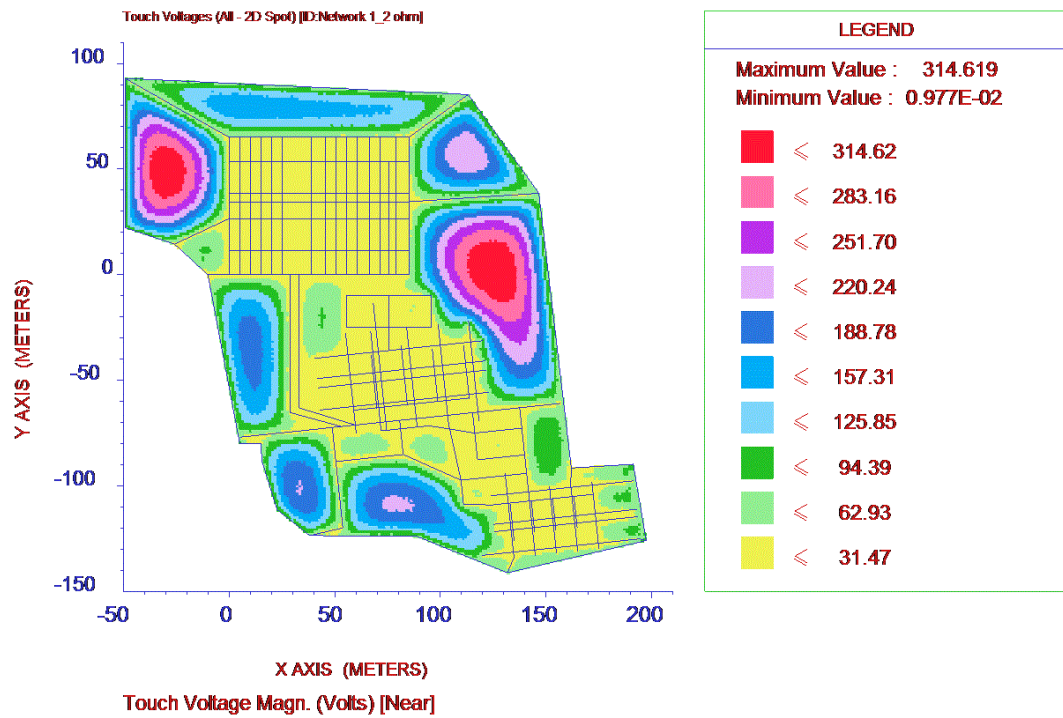


Figure 5-2 Initial modeling U_T inside substation area

It is evident that the touch voltages inside the switchyard area are lower than U_{Tp} , but in some of the “open” areas within the substation the touch voltages exceed U_{Tp} by up to approximately 159.4 V. The areas where $U_T > U_{Tp}$ are shown in Figure 5-3.

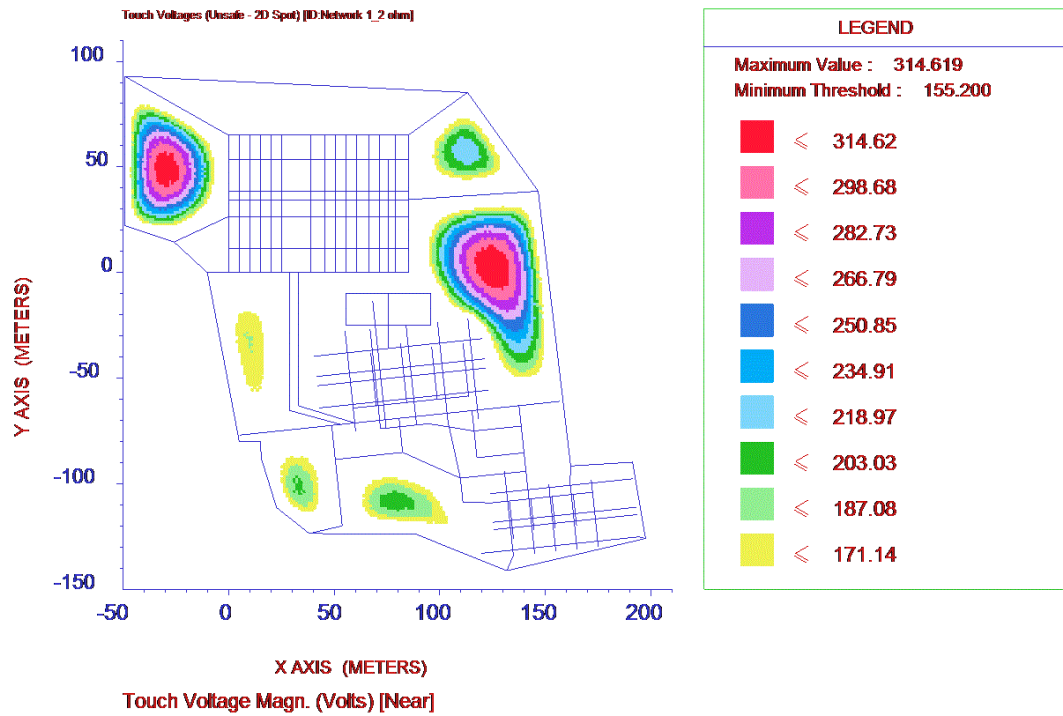


Figure 5-3 $U_T > U_{Tp}$ inside substation area

A common phenomenon regarding substation grounding is that the step voltages within the substation area are within permissible step voltages, but the touch voltages exceed U_{Tp} . This is also the case for the initial modeling of the Samnanger grounding network, as can be seen in Figure 5-4 showing the step voltages over an area extending up to three meters outside the grid. The highest U_s -values are found around the corners of the substation, with $U_{s\ max} = 144.21\ V$. This is well inside the $U_{Sp} = 347.5\ V$.

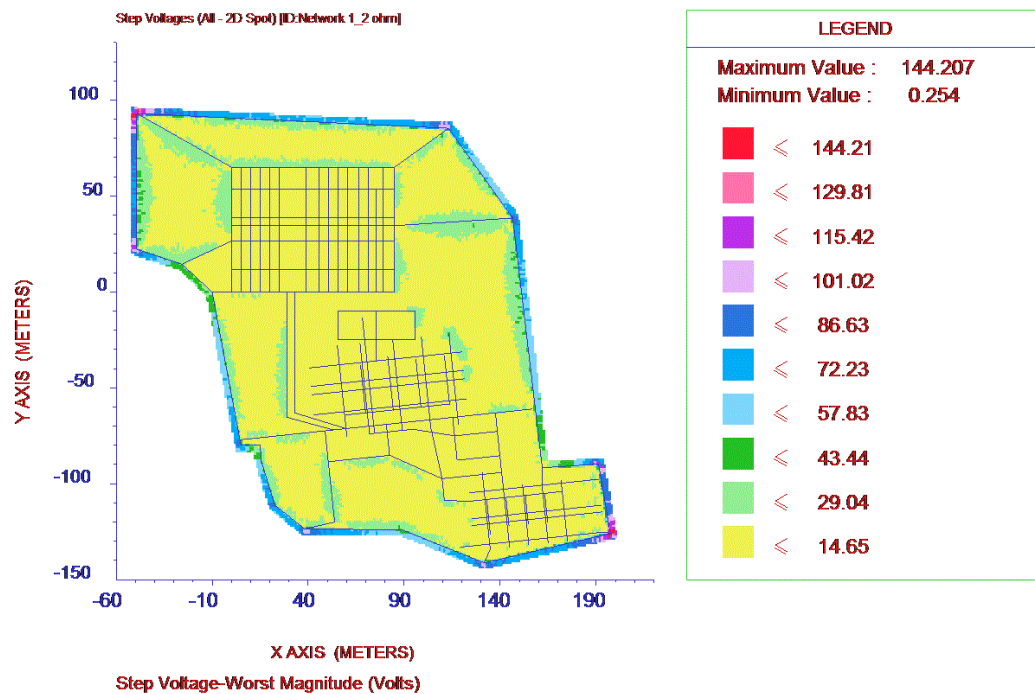


Figure 5-4 U_S within the substation area

The current flowing in the grounding network, which causes the touch- and step voltages, is calculated to 250.17 A, while the resistance of the electrode system is calculated to 18.06 Ω . This value of R_E is extremely high compared to typical values of R_E , thus it is suspected that the two layer model used in these simulations is insufficient. It is however, based on the soil composition at Samnanger substation, doubtful that the real R_E will have a value as low as 2 Ω .

A simulation setting $R_E = 2 \Omega$, based on R_E measurements of grounding networks in Norwegian substations, was carried out. Figure 5-5, Figure 5-6 and Figure 5-7 show the distribution of U_T , $U_{T_{\text{unsafe}}}$ and U_S , respectively. An insulating surface layer of $\rho = 3000 \Omega\text{m}$ is used, yielding $U_{T_p} = 369.3 \text{ V}$ and $U_{S_p} = 1203.9 \text{ V}$.

Figure 5-6 shows that $U_T < U_{T_p}$ inside the switchyard bays, but in the “open” areas extreme values of $U_{T_{\text{max}}} = 2136.11 \text{ V}$ occurs. Figure 5-7 shows that $U_S < U_{S_p}$.

It is decided to use both these networks as a basis in the remaining simulations, called Network 1 and Network 2, depending on the simulation objective. Network 1 is used in simulations where a change in R_E as a function of varying a parameter is interesting. Network 2 is used for all other simulations. Even though neither of the two networks may be in accordance with the real network with respect to R_E , a change as a function of varying a parameter will be evident.

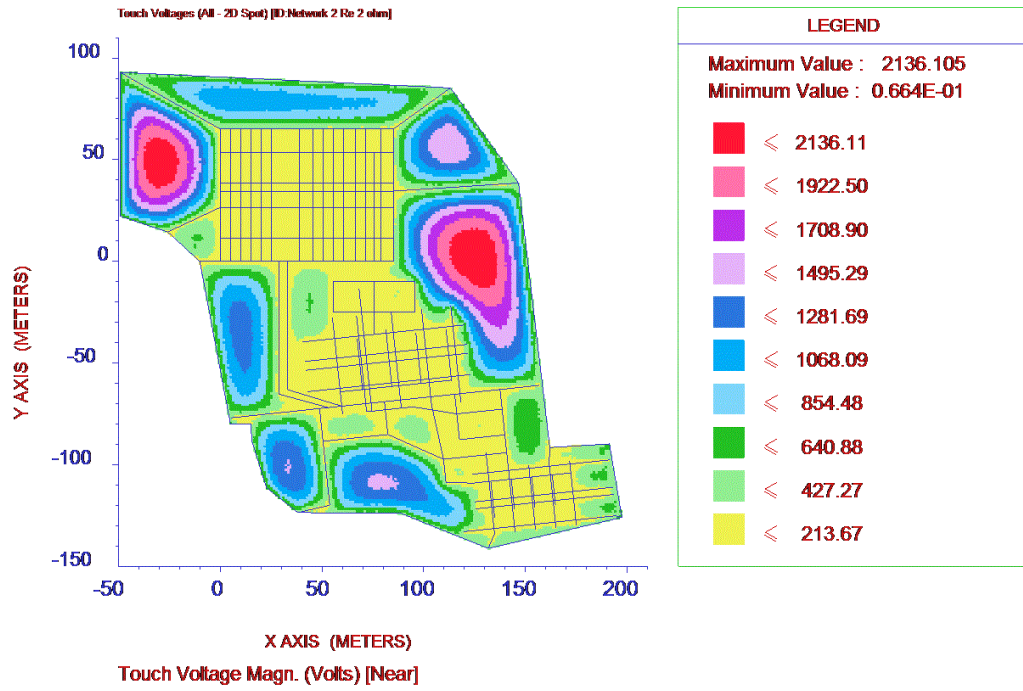


Figure 5-5 U_T within the substation area when $R_E = 2 \Omega$

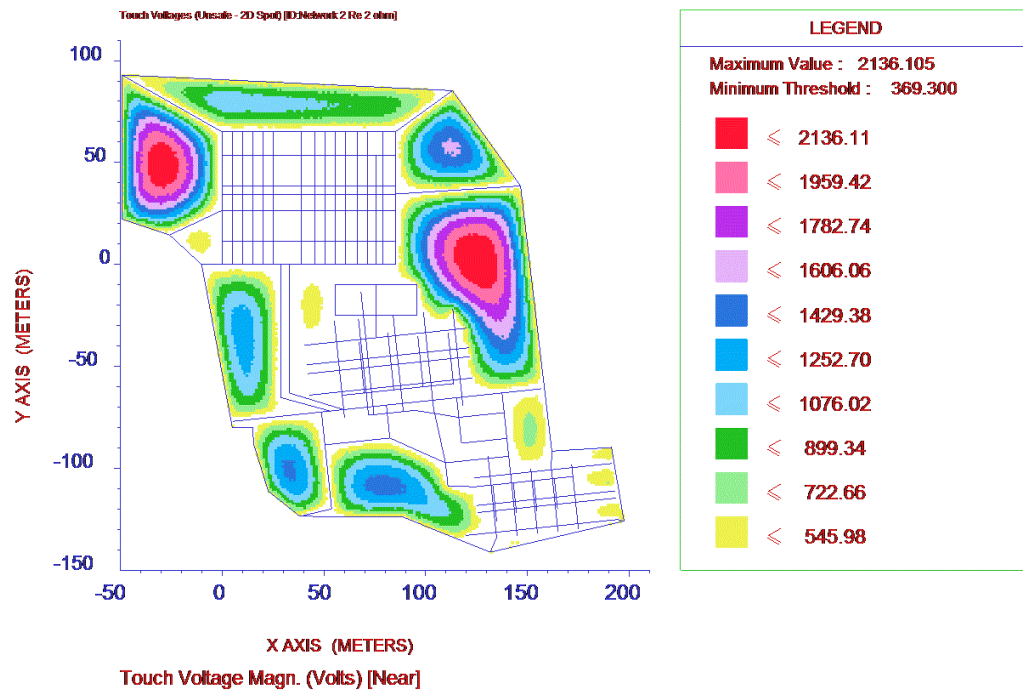


Figure 5-6 $U_{Tunsafe}$ within the substation area when $R_E = 2 \Omega$

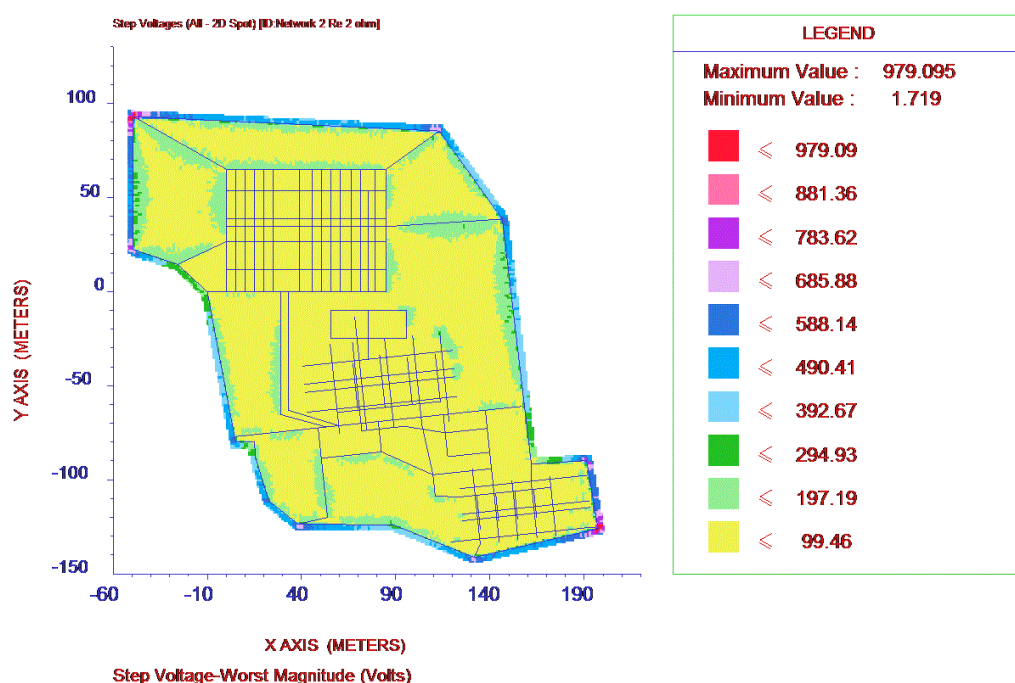


Figure 5-7 U_S within the substation area when $R_E = 2 \Omega$

5.2 Insulating surface layer

The touch and step voltage limits are, among other things, a function of foot contact resistance. Decisive of the foot contact resistance are the resistivity of the material on which a person is standing, its thickness and the subsurface soil resistivity. An increase in the foot contact resistance will lead to an increase of the U_{Tp} value, as shown in ([3], Part 2, Appendix B), and this is normally done by installing a crushed rock surface layer on the surface of the substation. This top layer should have a higher resistivity than the underlying soil layer in order to function as an insulating barrier. The potential touch and step voltages will not be reduced as a result of the top layer, but the U_{Tp} and U_{Sp} values will increase since a higher foot resistance will lead to a reduced current through the body.

Typical values for the top layer are 2000 – 3000 Ωm , which is equivalent to gravel. Using a 10 cm thick top layer of $\rho = 3000 \Omega\text{m}$ in Network 1 leads to $U_{Tp} = 369.3 \text{ V}$ and $U_{Sp} = 1203.9 \text{ V}$; now $U_{Tp} > U_T$ all over. Figure 5-8 shows how U_{Tp} and U_{Sp} changes with increasing top layer resistivity for Network 1. A linear increase can be seen for both voltages from a top layer resistivity of 500 Ωm .

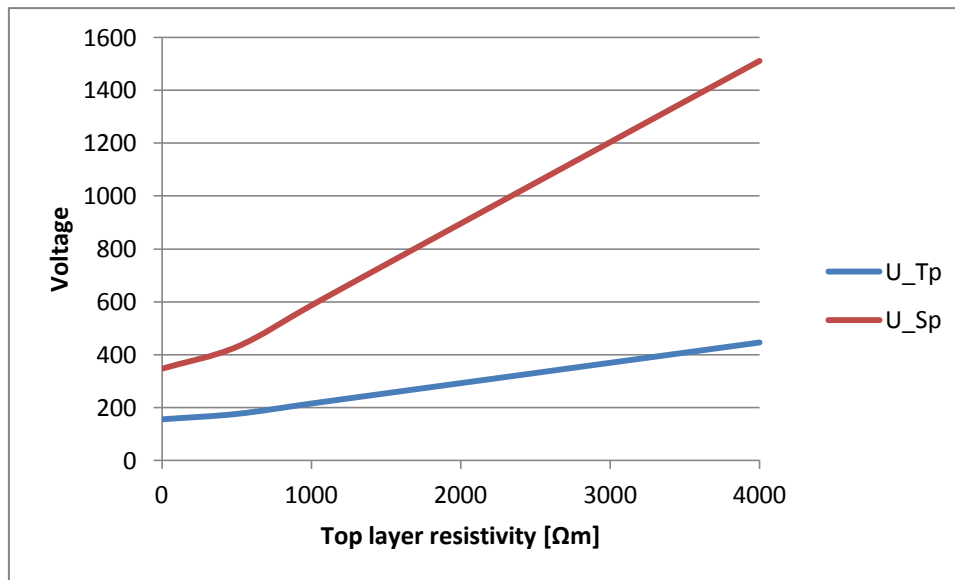


Figure 5-8 U_{Tp} and U_{Sp} as a function of 10 cm top layer resistivity

5.3 Varying fault duration

The duration of the fault, i.e. how long it takes for a fault to be detected and cleared by the system, is decisive when it comes to touch- and step voltage limits. The evolution of U_{Tp} and U_{Sp} as a function of fault duration are shown in Figure 5-9. Network 1 is used as a basis.

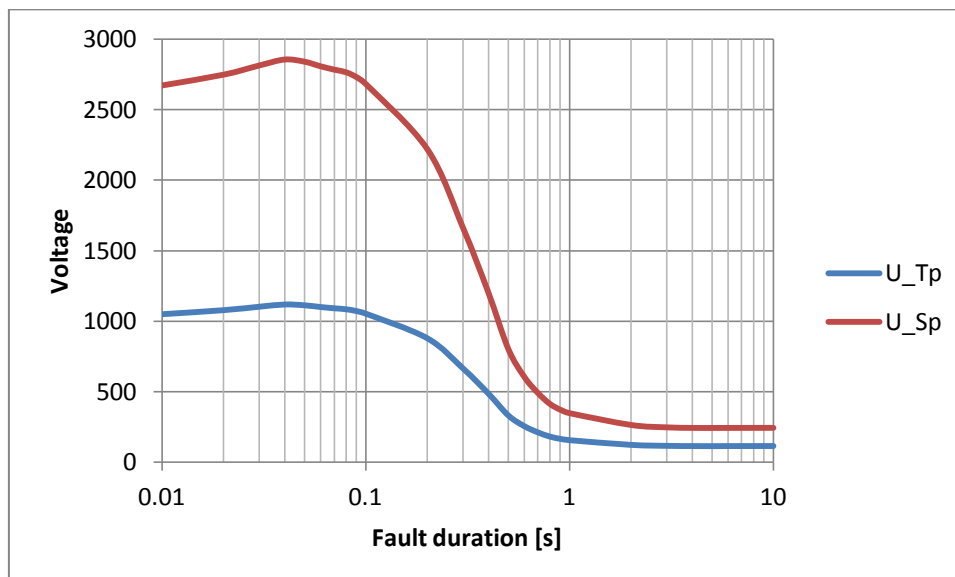


Figure 5-9 U_{Tp} and U_{Sp} as a function of fault duration

5.4 Varying soil conditions at Samnanger substation

The soil conditions at any given substation are decisive when it comes to the resulting potential touch and step voltages. By using Network 1 as a basis for the simulations the impact on the

grounding network performance by varying the soil conditions will be presented. Four scenarios have been developed and are described in Table 5-4.

Table 5-4 Varying soil scenarios at Samnanger

Scenario 1	Two layer soil: $\rho_1 = 250 \Omega\text{m}$, $\rho_2 = 15000 \Omega\text{m}$
Scenario 2	Two layer soil: $\rho_1 = 2000 \Omega\text{m}$, $\rho_2 = 10000 \Omega\text{m}$
Scenario 3	Two layer soil: $\rho_1 = 300 \Omega\text{m}$, $\rho_2 = 65 \Omega\text{m}$
Scenario 4	Uniform layer soil: $\rho = 250 \Omega\text{m}$

5.4.1 Scenario 1

The resistivity of the bottom soil layer was increased by $5000 \Omega\text{m}$ compared to Network 1. According to theory one should expect an increase in touch and step voltages, as well as the resistance to earth, when increasing the resistivity of the soil. However, one should keep in mind that the Samnanger substation is not an isolated system, and the network connected to it will play a role in the simulation results. The values for U_{Tp} and U_{Sp} are unchanged compared to Network 1. Figure 5-10 shows the distribution of the touch voltages within the substation area.

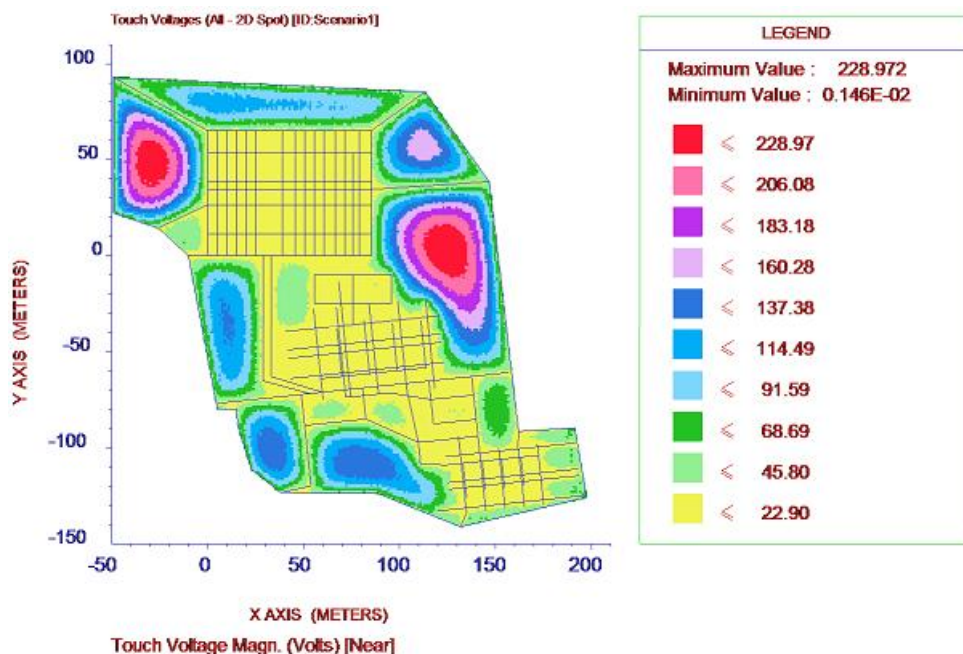


Figure 5-10 Scenario 1 U_T inside substation area

The maximum U_T for Scenario 1 is 228.97 V, which is a reduction of 85.65 V compared to Network 1. The maximum U_S for Scenario 1 is 125.27 V, a reduction of 18.94 V. Figure 5-11 shows how the U_T changes with increasing bottom soil layer resistivity. It is evident that an

increase in bottom soil resistivity leads to a decrease in U_{Tmax} , which is opposite to what should be expected according to theory. The results are discussed in 6.4.1.

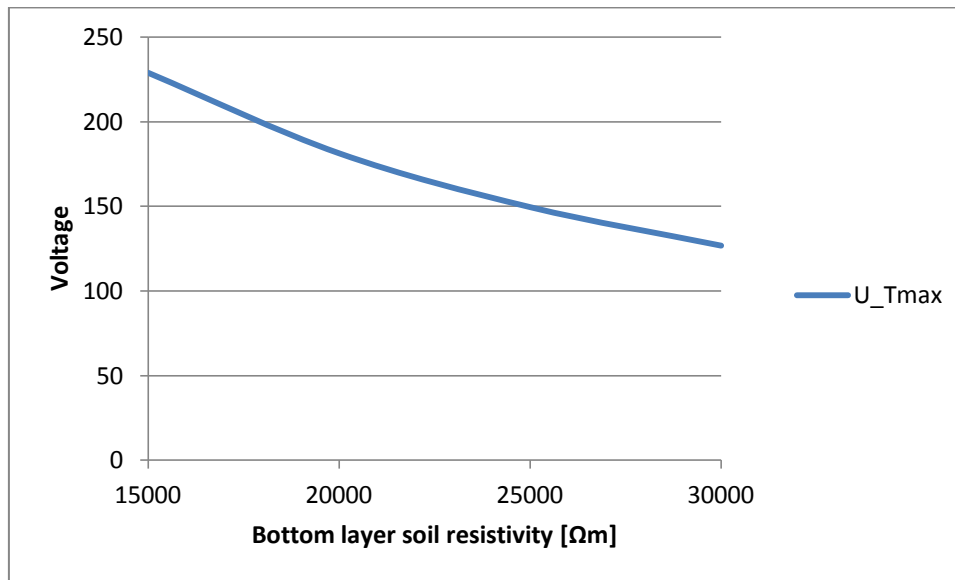


Figure 5-11 Change of U_{Tmax} as a function of bottom layer resistivity

Figure 5-12 shows the change in R_E and I_g as a function of bottom layer soil resistivity. The R_E has close to a linear increase with increasing resistivity, as should be expected. The current flowing in the grounding network, I_g , has a more exponential decrease with increasing resistivity, as the curve tends to flatten out.

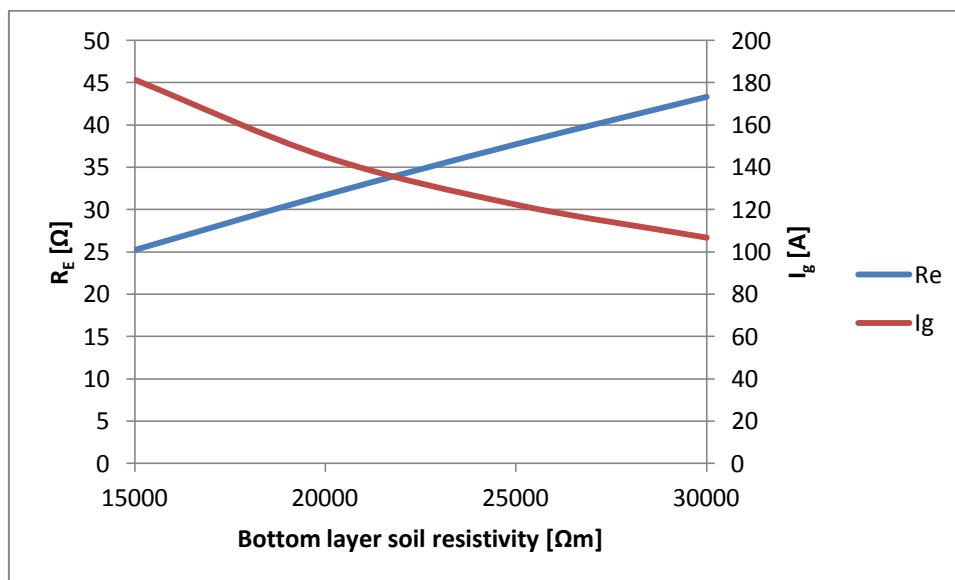


Figure 5-12 Change of R_E and I_g as a function of bottom layer resistivity

5.4.2 Scenario 2

The resistivity of the bottom soil layer was kept at $10000 \Omega\text{m}$ as in Network 1, while the upper soil layer was given a resistivity of $2000 \Omega\text{m}$. This upper layer is not to be confused with an insulating surface top layer, even though it will lead to higher values of U_{Tp} and U_{Sp} compared to Network 1. According to theory it is expected an increase in U_T , U_S and R_E , while I_g should be decreased compared to Network 1. The distribution of touch voltages within the substation area is shown in Figure 5-13.

For Scenario 2, $U_{Tp} = 352 \text{ V}$ and $U_{Sp} = 1135.1 \text{ V}$ with $t_{\text{fault}} = 1 \text{ second}$. Figure 5-13 shows that the touch voltages inside the switchyard bays are lower than U_{Tp} , but as much as 616.21 V higher than U_{Tp} outside. The highest step voltages are found at the corners of the substation area with $U_{S_{\text{max}}} = 285.24 \text{ V}$, which is lower than U_{Sp} .

R_E is calculated to 22.67Ω while I_g is calculated to 200.84 A .

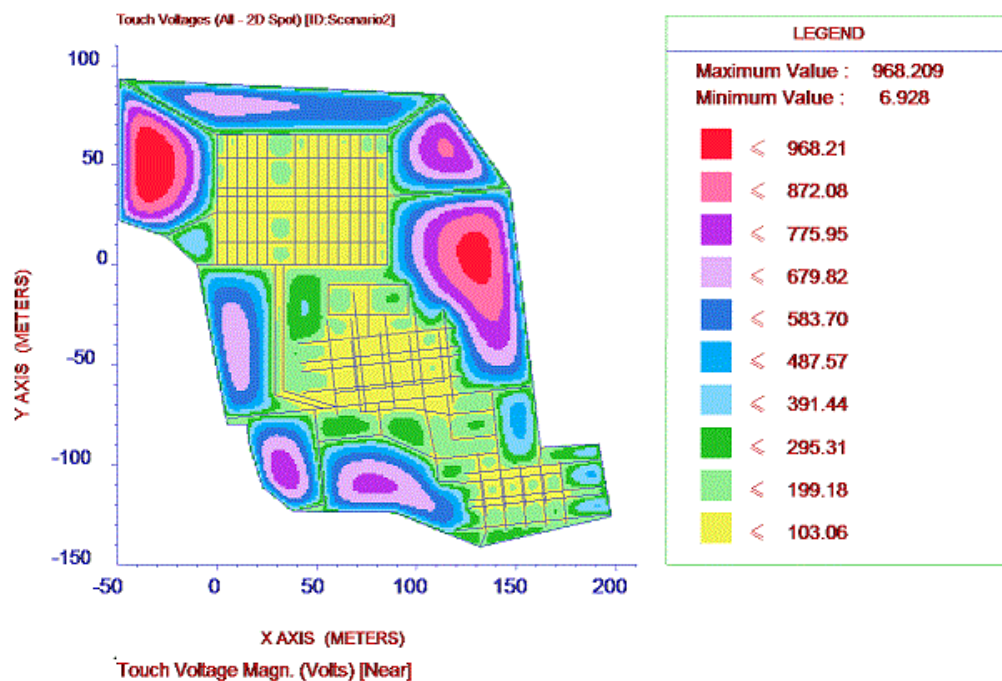


Figure 5-13 Scenario 2 U_T inside substation area

5.4.3 Scenario 3

The soil is still modeled as a two layer soil model, but the upper layer now has a higher resistivity than the bottom layer. This can be the case in real life due to higher moisture content deeper in the soil as a result of subsurface creeks or equivalent. The upper layer is set to $300 \Omega\text{m}$ and the bottom layer to $65 \Omega\text{m}$. These values are based on resistivity measurements listed in the AutoGrid Pro manual and may not be a realistic representation of Norwegian conditions. The upper layer thickness is set to 0.5 meter .

Based on the resistivity values it is according to theory expected an increase in U_T , U_S and I_g , while R_E should be reduced compared to Network 1. Figure 5-14 shows the distribution of touch voltages within the substation area.

For Scenario 3, $U_{Tp} = 160.8$ V and $U_{Sp} = 370$ V for $t_{\text{fault}} = 1$ second. Figure 5-14 shows that inside the switchyard bays the touch voltages are lower than U_{Tp} , but higher on the outside. $U_{S\text{max}} = 92.55$ V.

R_E is calculated to 0.19Ω , while I_g is calculated to 4612.2 A.

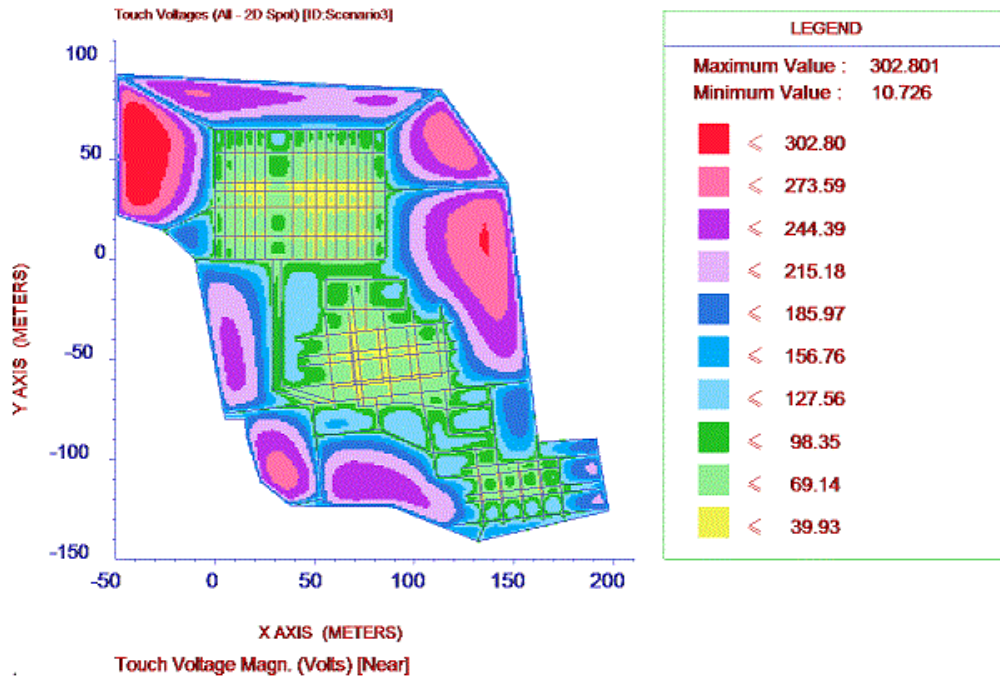


Figure 5-14 Scenario 3 U_T inside substation area

5.4.4 Scenario 4

The soil is modeled as a uniform soil model with a resistivity of $250 \Omega\text{m}$. This is an unrealistic scenario, but it is modeled to see the effects of a low resistivity uniform soil on the touch and step voltages.

Based on the resistivity of the soil, it is according to theory expected that a large portion of the fault current will flow in the substation grounding network. R_E should be decreased while U_T and U_S should be increased compared to Network 1. Figure 5-15 shows the distribution of touch voltages inside the substation area.

For Scenario 4, $U_{Tp} = 155.2$ V and $U_{Sp} = 347.5$ V for $t_{\text{fault}} = 1$ second. For this scenario there are touch voltages larger than U_{Tp} both inside and outside the switchyard bays, with $U_{T\text{max}} = 648.92$ V. $U_{S\text{max}}$, I_g and R_E was calculated to 195.21 V, 3276.1 A and 0.63Ω .

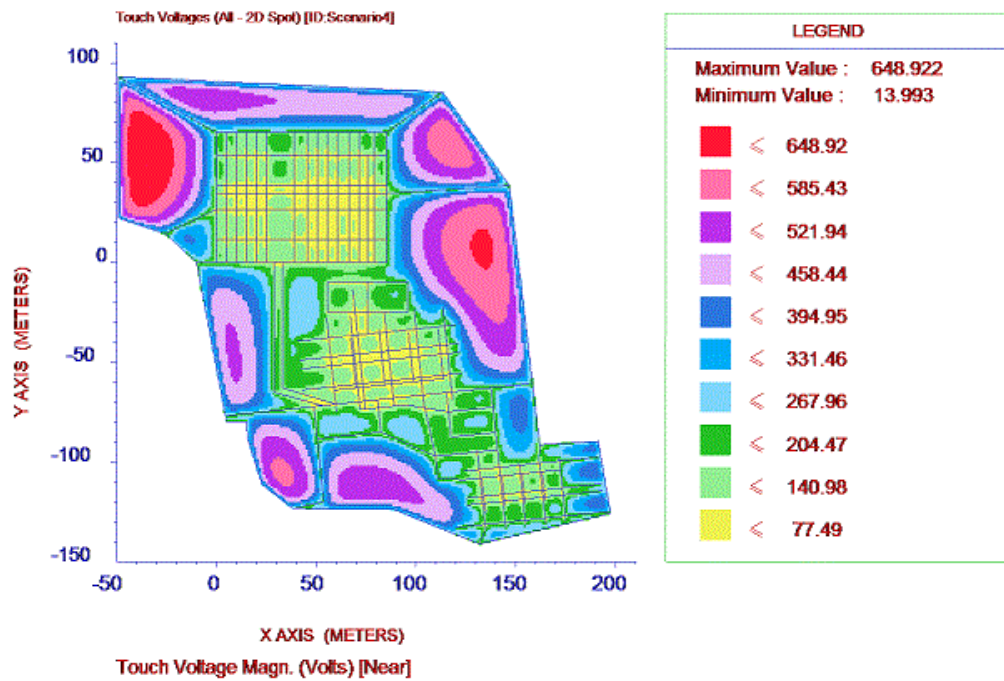


Figure 5-15 Scenario 4 U_T inside substation area

5.5 Varying R_E at adjacent substations

It is suspected that the resistance to earth for the grounding networks at adjacent substations will affect the touch and step voltages at the Samnanger substation. This is due to the fact that the current will choose the path of least resistance, thus a low resistance to earth for the adjacent substations will lead to large portions of the short circuit current flowing into these networks. The reason for these simulations is to find out how much the resistance to earth for adjacent substations contributes to touch and step voltages at Samnanger.

In Network 2 the resistance to earth for the grounding network at the adjacent substations was set to 2Ω . This value was based on ground resistance measurements of substation grounding networks in Norway.

Three scenarios with decreasing R_E for the adjacent substations have been simulated, shown in Table 5-5. The numbering of the scenarios starts at 5 to avoid any confusion with scenarios in chapter 5.4. Network 2 has been used as a basis for the simulations.

Table 5-5 Varying R_E values for adjacent substations to Samnanger

Scenario 5	R_E Sima_Mauranger = 0.5Ω	R_E remaining = 2Ω
Scenario 6	R_E Sima_Mauranger_Fana = 0.5Ω	R_E remaining = 2Ω
Scenario 7	R_E Sima_Mauranger_Fana_Evanger = 0.5Ω	R_E remaining = 2Ω

5.5.1 Scenario 5

Network 2 has been used as a basis for this scenario, with the only change being a reduction in R_E at Sima and Mauranger substation from 2Ω to 0.5Ω . Figure 5-16 shows the distribution of touch voltages inside the Samnanger substation area for Scenario 5.

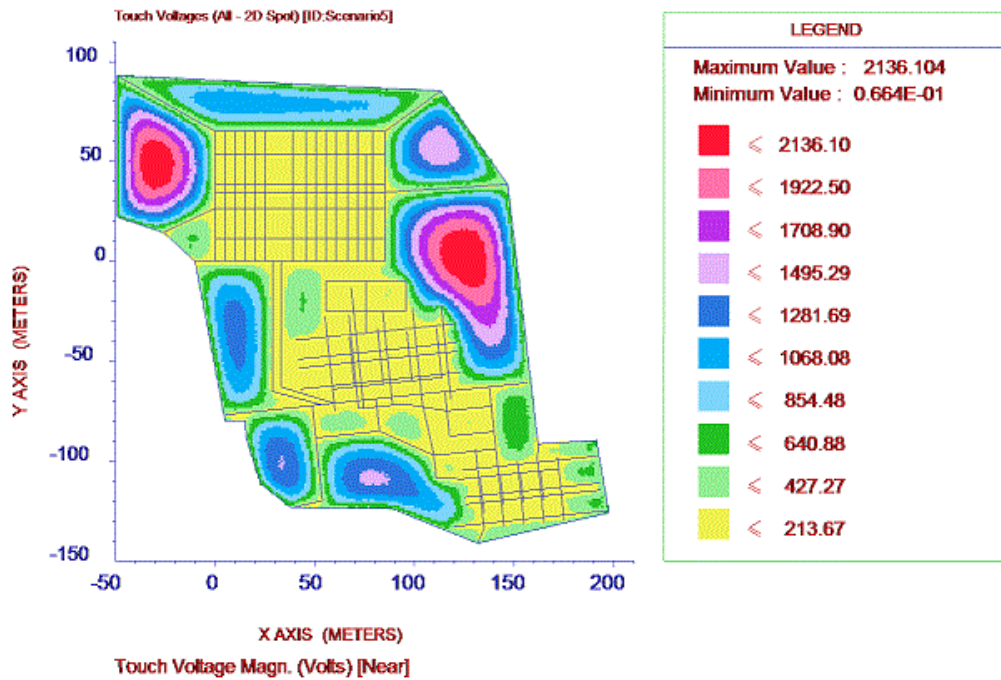


Figure 5-16 Scenario 5 U_T inside substation area

Figure 5-16 shows a deviation of U_T from Network 2 of 0 V. It is expected that the current flowing in the grounding network at Sima and Mauranger have increased compared to Network 2. Table 5-6 shows the currents flowing in the Samnanger, Sima and Mauranger substations grounding networks for Network 2 and for Scenario 5.

Table 5-6 Scenario 5 I_g

Substation	Network 2	Scenario 5	Change
Samnanger	$I_g = 1698.5 \text{ A}$	$I_g = 1698.5 \text{ A}$	0.00 A
Sima	$I_g = 1116.9 \text{ A}$	$I_g = 1479.7 \text{ A}$	362.80 A
Mauranger	$I_g = 2045.5 \text{ A}$	$I_g = 1251.7 \text{ A}$	793.80 A

5.5.2 Scenario 6

The resistance to earth for Fana substation has been reduced from 2Ω to 0.5Ω in Scenario 6, otherwise it is identical to Scenario 5. Having the results from Scenario 5 in mind it is expected a minor decrease, if any, in U_{Tmax} , while I_g at Fana substation should increase.

The simulation show that $U_{Tmax} = 2134.20 \text{ V}$, a decrease of 1.9 V compared to Scenario 5. Table 5-7 shows the currents flowing in the Fana substation for Network 2 and for Scenario 6. I_g for the other substations is unchanged.

Table 5-7 Scenario 6 I_g

Substation	Network 2	Scenario 6	Change
Fana	$I_g = 434.21 \text{ A}$	$I_g = 556.59 \text{ A}$	122.38 A

5.5.3 Scenario 7

The resistance to earth for Evanger substation has been reduced from 2Ω to 0.5Ω in Scenario 7, otherwise it is identical to Scenario 6. Based on the results from Scenario 6 it is expected a minor decrease in U_{Tmax} , and an increase in I_g at Evanger substation.

The simulation show that $U_{Tmax} = 2133.95 \text{ V}$, a decrease of 0.25 V compared to Scenario 6. Table 5-8 shows the currents flowing in the Evanger substation for Network 2 and for Scenario 7.

Table 5-8 Scenario 7 I_g

Substation	Network 2	Scenario 7	Change
Evanger	$I_g = 405.89 \text{ A}$	$I_g = 530.10 \text{ A}$	124.21 A

Simulations from Scenario 5, 6 and 7 show that the resistance to earth value for the substations adjacent to Samnanger have little to no effect on the touch voltage magnitude at Samnanger substation.

5.6 Varying R_t for overhead line towers

During a phase-to-earth fault some of the short circuit current will flow in the overhead line earth conductors, through the tower structure and into the soil along the overhead line trace. The amount of current entering the soil through the tower grounding arrangement is dependent on the resistance to earth (R_t) for the towers.

It is expected that a reduction of the values for R_t in Network 2 will lead to a decrease in I_g for the substations connected to the overhead lines. This should again lead to a decrease in the touch voltages at these substations, according to theory.

In Network 2 R_t is set to 60Ω . This value is based on simulations of tower ground electrodes in soils with low electric conductivity, as is the case for the tower ground electrodes along the overhead lines connected to Samnanger substation. Three scenarios have been simulated to see how R_t influences the touch voltages at Samnanger substation, shown in Table 5-9. The value of 25Ω is chosen based on the fact that the Statnett goal is $R_t \leq 25 \Omega$.

Table 5-9 Varying R_t values for overhead line towers

Scenario 8	$R_{t \text{ Sam-Sim}} = 25 \Omega$	$R_{t \text{ remaining}} = 60 \Omega$
Scenario 9	$R_{t \text{ all}} = 25 \Omega$	
Scenario 10	$R_{t \text{ all}} = 90 \Omega$	

5.6.1 Scenario 8

Network 2 has been used as a basis for this scenario, the only change being a reduction in the R_t -value for the Sima – Samnanger line from 60Ω to 25Ω . Figure 5-17 shows the distribution of touch voltages inside the Samnanger substation for Scenario 8.

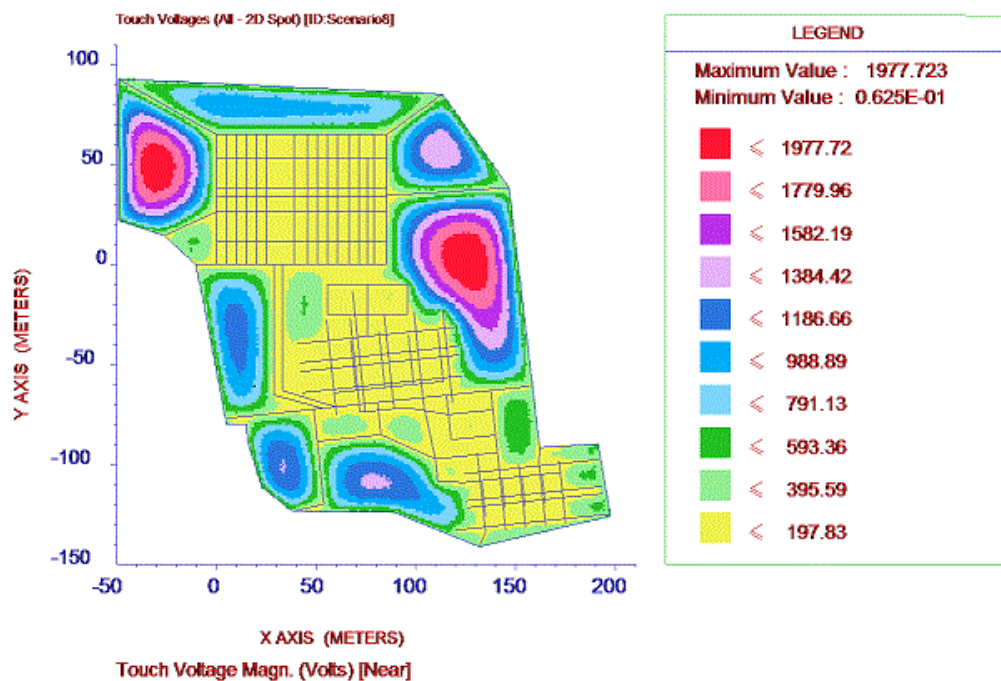


Figure 5-17 Scenario 8 U_T inside substation area

Compared to Network 2 U_{Tmax} has now been reduced with 158.38 V, and $I_g = 1572.6$ A compared to 1698.5 A. U_T are still higher than U_{Tp} in the “open” areas outside the switchyard bays.

5.6.2 Scenario 9

The resistance to earth for the towers on all overhead lines connected to Samnanger has been set to 25 Ω . Figure 5-18 shows the distribution of touch voltages inside the substation area for Scenario 9.

Figure 5-18 shows that $U_{Tmax} = 1590.75$ V, and $U_T > U_{Tp}$ in the “open” areas. The total current flowing in the main electrode is now $I_g = 1264.9$ A.

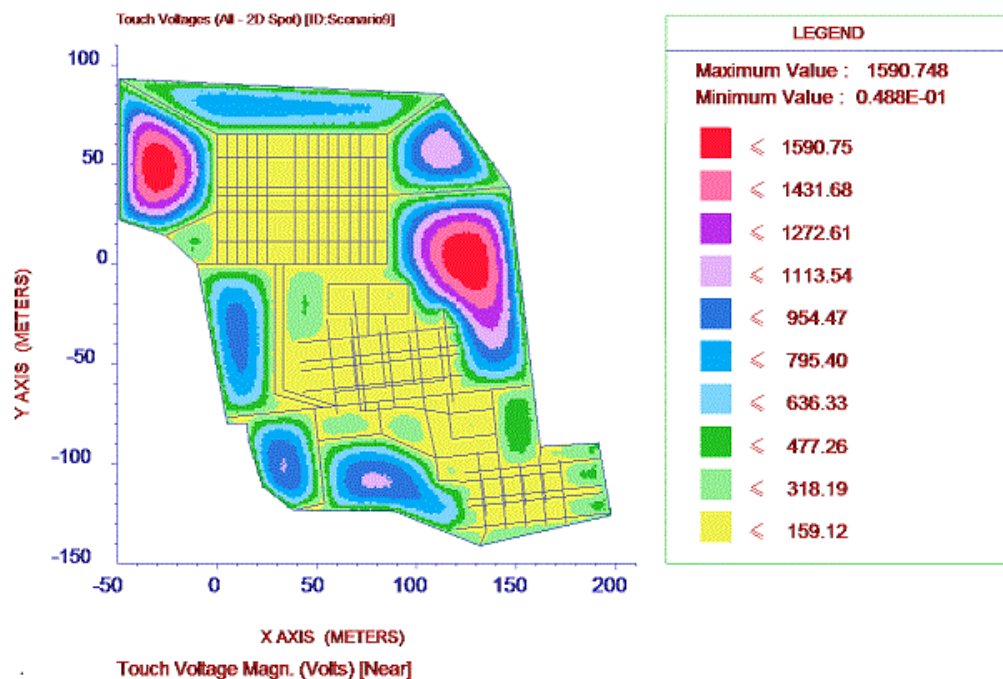


Figure 5-18 Scenario 9 U_T inside substation area

Table 5-10 shows the currents flowing in the main electrodes for Network 2 and Scenario 9. Reducing the R_t on all overhead line towers from 60 Ω to 25 Ω , a reduction of 58.33 %, leads to a reduction in I_g for nearly all adjacent substations of 12.38 – 19.52 %. The only exception is Frøland where I_g increases with 47.52 %. See chapter 6.6.2 for discussion.

Table 5-10 Scenario 9 I_g

Substation	Network 2	Scenario 9
Sima	$I_g = 1116.9 \text{ A}$	$I_g = 932.56 \text{ A}$
Mauranger	$I_g = 1022.7 \text{ A}$	$I_g = 891.95 \text{ A}$
Fana	$I_g = 434.21 \text{ A}$	$I_g = 349.46 \text{ A}$
Evanger	$I_g = 405.89 \text{ A}$	$I_g = 337.79 \text{ A}$
Norheimsund	$I_g = 566.56 \text{ A}$	$I_g = 496.40 \text{ A}$
Frøland	$I_g = 197.63 \text{ A}$	$I_g = 291.55 \text{ A}$

5.6.3 Scenario 10

The resistance to earth for the towers on all overhead lines connected to Samnanger has been set to 90Ω . This value is based on simulations of counterpoise electrodes in a two layer soil model. The upper layer was 10 cm thick and was given a resistivity of $200 \Omega\text{m}$, while the bottom layer resistivity was set to $15000 \Omega\text{m}$. This should illustrate typical mountainous Norwegian conditions.

Figure 5-19 shows the distribution of touch voltages exceeding U_{Tp} inside the substation area. U_{Tmax} is now 282.78 V higher than for Network 2. The total current flowing in the main electrode is now $I_g = 1923.4 \text{ A}$.

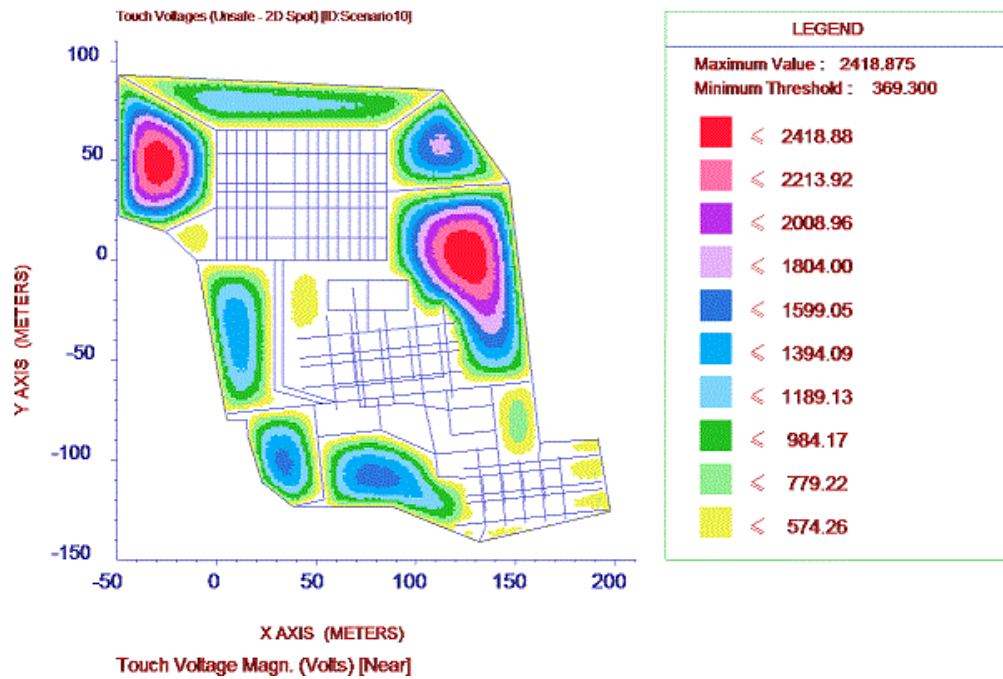


Figure 5-19 Scenario 10 $U_T > U_{Tp}$ inside substation area

Table 5-11 shows the currents flowing in the main electrodes for Network 2 and Scenario 10. Increasing the R_t on all overhead line towers from 60Ω to 90Ω , an increase of 50 %, leads to an increase in I_g for nearly all adjacent substations of 19.11 – 38.14 %. The only exception is Frøland where I_g decreases with 49.46 %. See chapter 6.6.3 for discussion.

Table 5-11 Scenario 10 I_g

Substation	Network 2	Scenario 9
Sima	$I_g = 1116.90 \text{ A}$	$I_g = 1192.40 \text{ A}$
Mauranger	$I_g = 1022.70 \text{ A}$	$I_g = 1073.20 \text{ A}$
Fana	$I_g = 434.21 \text{ A}$	$I_g = 482.73 \text{ A}$
Evanger	$I_g = 405.89 \text{ A}$	$I_g = 447.41 \text{ A}$
Norheimsund	$I_g = 566.56 \text{ A}$	$I_g = 591.28 \text{ A}$
Frøland	$I_g = 197.63 \text{ A}$	$I_g = 147.35 \text{ A}$

Figure 5-20 illustrates how I_g at the different substations changes with changing values of R_t . Notice the I_g -curve for Frøland.

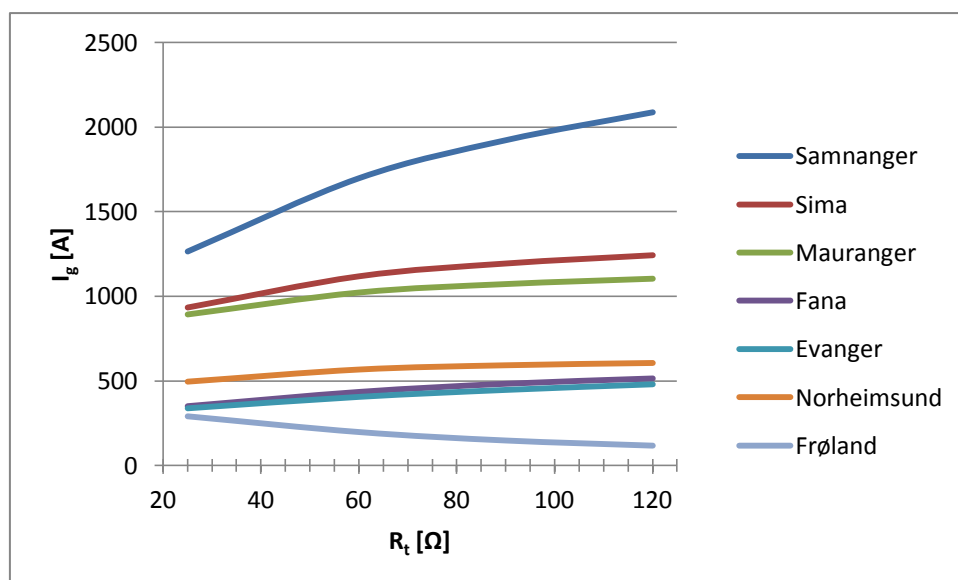


Figure 5-20 I_g as a function of changing R_t

5.7 Mesh density

The mesh density is decisive when it comes to touch and step voltages appearing in the switchyard bays. Denser meshes will create a more equipotential surface and reduce the touch and step voltages in these densely meshed areas. Two scenarios based on the comparison made in chapter 3 have been simulated, and are described in Table 5-12.

Table 5-12 Varying mesh density for 420 kV grounding network

Scenario 11	5x5 m meshes in 420 kV grounding network 120 mm ² Cu wire
Scenario 12	Electrodes along the switchyard bay dividing lines; extra transverse electrodes around measuring transformers and surge arresters. 70 mm ² Cu wire

5.7.1 Scenario 11

Figure 5-21 shows the simulated grounding network and the touch voltage distribution at Samnanger for Scenario 11. The meshes are now reduced to being 5x5 m, and equally distributed within the 420 kV switchyard. The remaining grounding network is kept unchanged from Network 2.

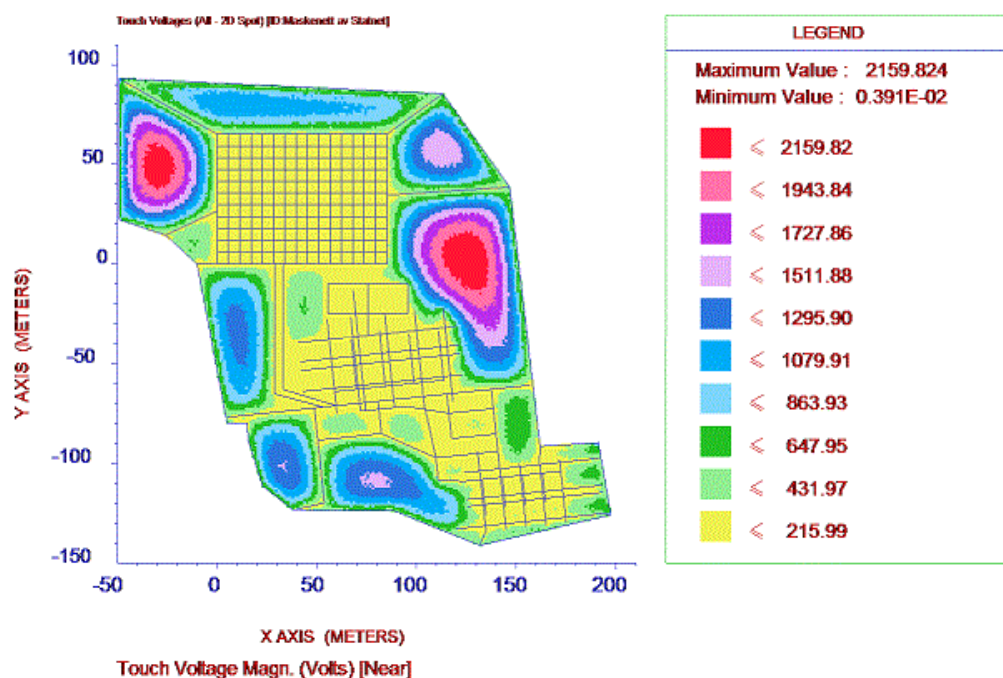


Figure 5-21 Scenario 11 Grounding network overview and U_T distribution inside substation area

By comparing Figure 5-5 and Figure 5-21 one can see that there is no real change in the touch voltage distribution inside the substation area. The potential touch voltages inside the 420 kV switchyard are practically of the same magnitude and distribution as for Network 2. Table 5-13 shows a comparison of bonding nodes and the magnitude of Cu wire used in Network 2 and Scenario 11.

Table 5-13 Comparison of Network 2 and Scenario 11

Nodes _{N1}	Nodes _{S11}	Cu _{N1} [m]	Cu _{S11} [m]
254	337	4855.8	5292.3

5.7.2 Scenario 12

Figure 5-22 shows the simulated grounding network and the touch voltage distribution at Samnanger for Scenario 12. Grounding electrodes are now installed along the dividing lines of the switchyard bays and along the outer perimeter of the 420 kV switchyard. Transverse electrodes are installed around the measuring transformers. These horizontal electrodes create an unevenly meshed grounding network. The remaining grounding network is kept unchanged from Network 2.

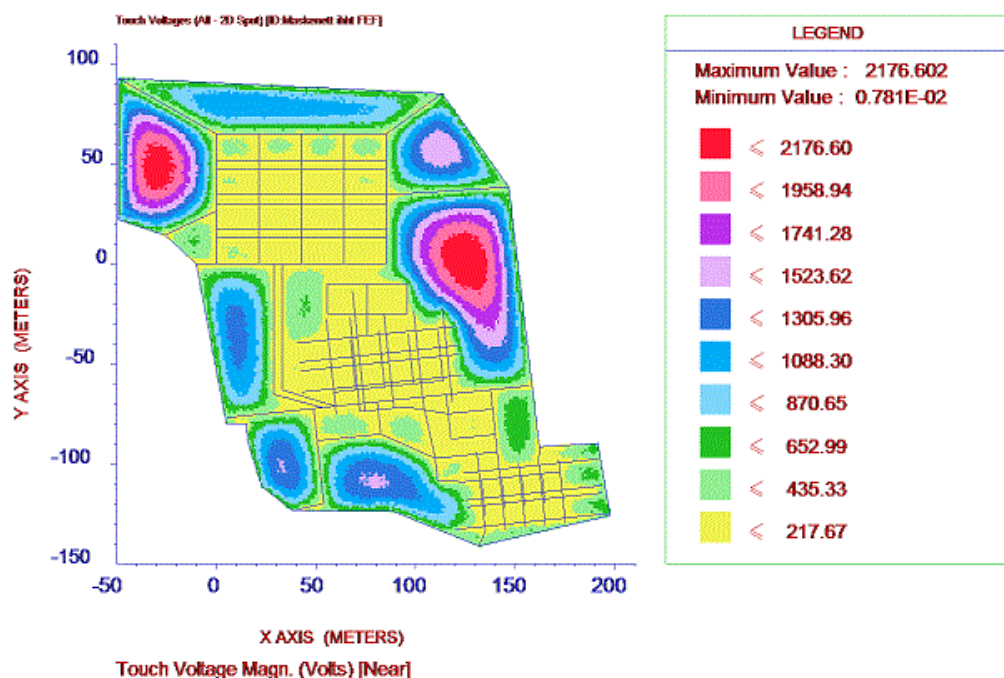


Figure 5-22 Scenario 12 Grounding network overview and U_T distribution inside substation area

By comparing Figure 5-5 and Figure 5-22 one can see that there is only a small change in the touch voltage distribution inside the substation area. The potential touch voltages inside the 420 kV switchyard are a little elevated in some areas compared to Network 2. The areas where $U_T > U_{Tp}$ are the same as in Network 2, and U_{Tmax} is 40.5 V higher in Scenario 12. Table 5-14 shows a comparison of bonding nodes and the magnitude of Cu wire used in Network 2 and Scenario 11.

Table 5-14 Comparison of Network 2 and Scenario 11

Nodes _{S_{N1}}	Nodes _{S_{S12}}	Cu _{N1} [m]	Cu _{S12} [m]
254	185	4855.8	4237.3

5.8 Cross sectional value of earth electrodes

According to published material about grounding system networks the cross sectional value of earth electrodes has little influence on the performance of the grounding system. It is mainly mechanical stress that is the dimensioning criteria for the cross section of grounding electrodes in high voltage substations, but demands listed in chapter 2.1.4 must be met.

Based on Network 2, simulations have been carried out where the cross sectional value of the complete grounding network was set to 70 mm², 50 mm² and 25 mm² in three scenarios. The objective of the simulations is to see how the grounding network performance changes with reduced cross sectional area of the grounding electrode. It is expected to see an increase in U_{Tmax} as a function of decreasing electrode cross section.

Figure 5-23 shows how U_{Tmax} inside the substation area changes with decreasing cross sectional area of the grounding electrode. From a cross sectional area of 120 mm^2 to 25 mm^2 , U_{Tmax} increases by 53.34 V. The largest step occurs between 25 mm^2 and 50 mm^2 , where U_{Tmax} increases by 19.79 V. $U_T < U_{Tp}$ inside the switchyard bays for all cross sections.

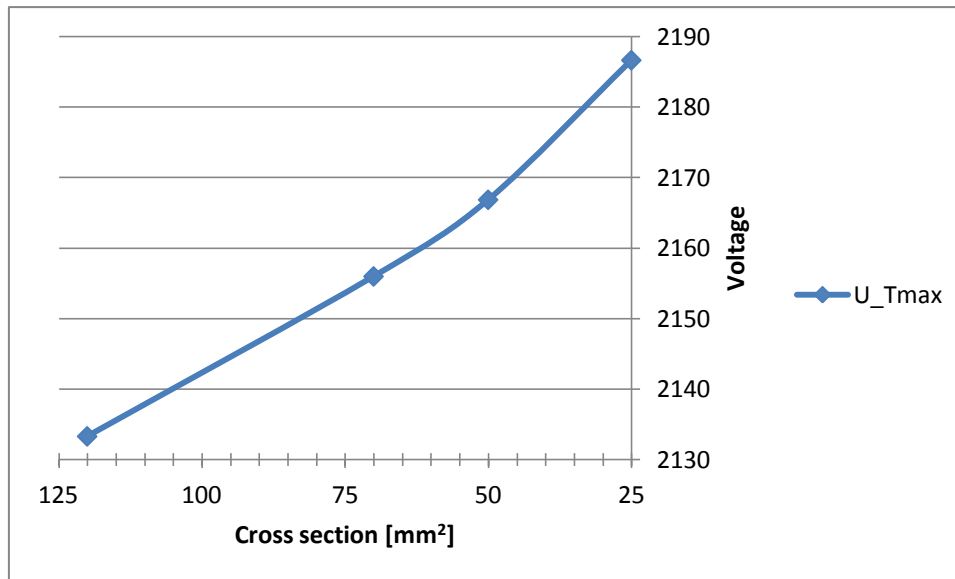


Figure 5-23 U_{Tmax} as a function of cross sectional area of grounding electrode at Samnanger

5.9 Vertical rods

Vertical, or inclined, rods are often used in combination with a meshed network to further reduce the resistance to earth for the grounding system. Vertical rods are beneficial when the surface soil resistivity is quite large compared to that of the deeper soil layers, and its thickness is small enough for vertical rods to penetrate into the deeper layers.

The objective of this simulation is to see how the grounding network performance changes with respect to U_{Tmax} , R_E and I_g . Material consumption compared to Network 1 will also be of interest. Network 1 is used as a basis for the simulations including vertical rods. Vertical rods are only added to the 420 kV grounding system, and to the earth conductor outside the fence. It is expected that an increasing number of grounding rods will lead to a reduced U_{Tmax} and R_E , while I_g should be increased. It is expected only minor changes due to the fact that $\rho_2 = 40 \times \rho_1$.

Figure 5-24 shows how U_{Tmax} decreases linearly with an increasing number of grounding rods. In the case with 30 grounding rods, 15 rods are distributed along the outer perimeter of the 420 kV grounding system and 15 rods are distributed along the earth conductor outside the fence. In the two other cases all grounding rods are distributed along the outer perimeter of the 420 kV grounding system. U_{Tmax} decreases by only 5.20 V when increasing the number of grounding rods from zero to 30.

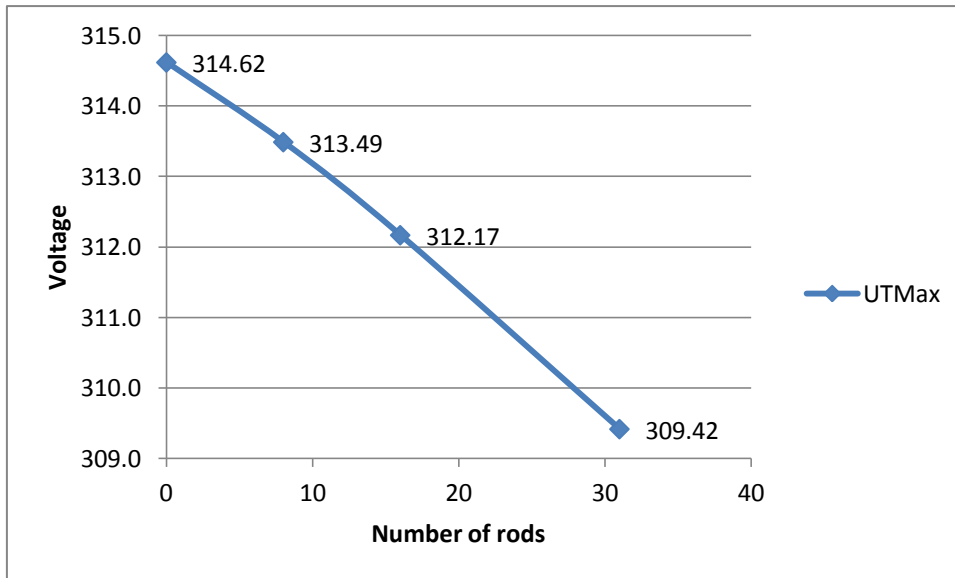


Figure 5-24 U_{Tmax} as a function of the number of grounding rods

Figure 5-25 shows how I_g and R_E changes with increasing number of grounding rods. The curves are exponential, and I_g increases while R_E decreases with increasing number of grounding rods. As can be seen from Figure 5-25 the changes in I_g and R_E are minimal.

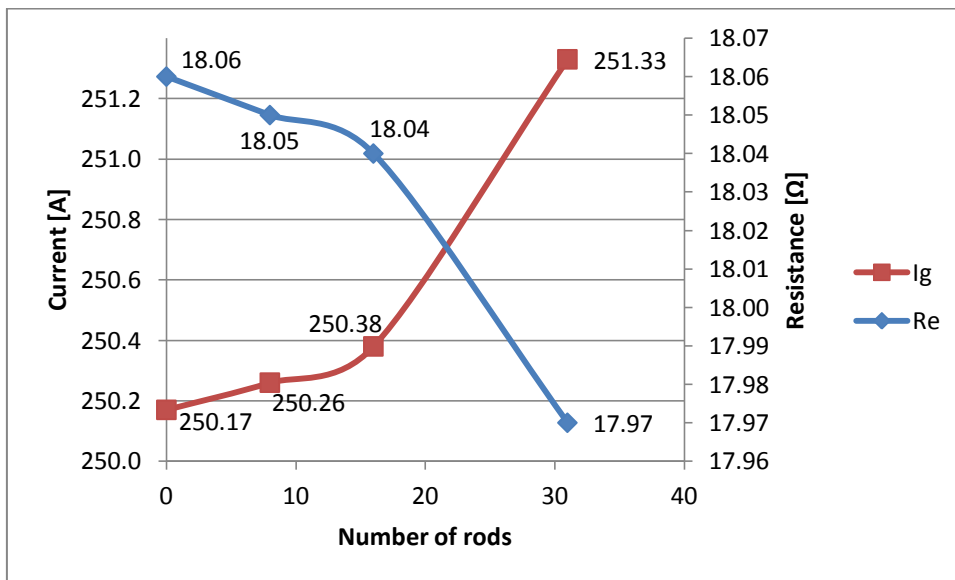


Figure 5-25 I_g and R_E as a function of the number of grounding rods

Figure 5-26 shows how the total length of Cu wires used in the grounding networks increases with an increasing number of grounding rods. From zero to 30 grounding rods, the Cu wire length increases with 300 meters.

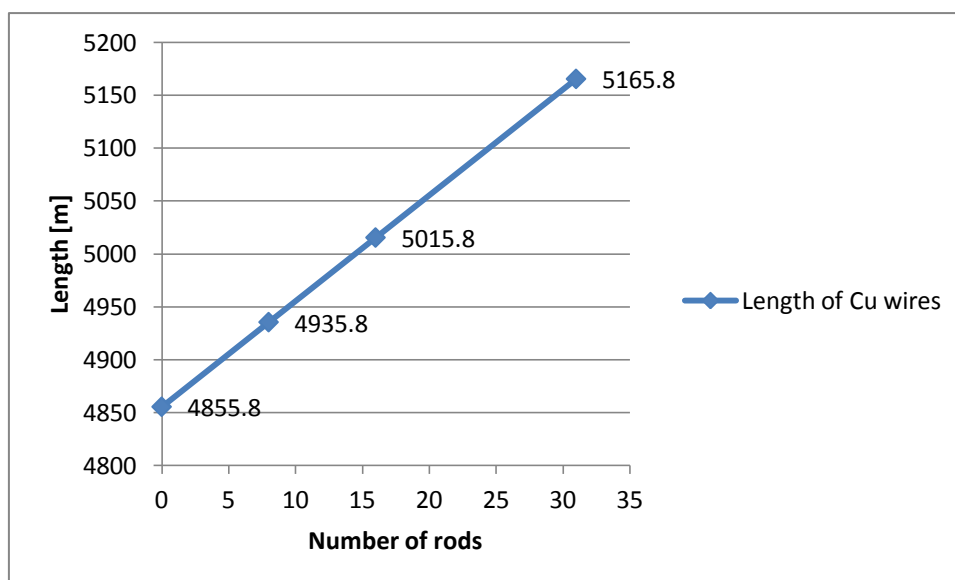


Figure 5-26 Length of Cu wires as a function of the number of grounding rods

As expected the changes in U_{Tmax} , I_g and R_E were only minimal due to the soil composition at Samnanger. To illustrate how grounding rods can substantially improve the performance of a grounding network, Network 1 has been modified by setting $\rho_1 = 15000 \Omega m$, $d_1 = 0.5 m$, $\rho_2 = 250 \Omega m$ and $d_2 = \infty$.

Table 5-15 shows how U_{Tmax} , I_g and R_E changes when using zero and 30 grounding rods, respectively. It must be emphasized that this is not a real example, but only an example to show how effective grounding rods may be where the lower soil layer has a higher electric conductivity than the upper soil layer.

Table 5-15 U_{Tmax} , I_g and R_E for zero and 30 ground rods

$U_{Tmax 0}$ [V]	$U_{Tmax 30}$ [V]	$I_{g 0}$ [A]	$I_{g 30}$ [A]	$R_{E 0}$ [Ω]	$R_{E 30}$ [Ω]
810.89	699.43	3049.8	3133.6	0.697	0.654

A simulation using 30 grounding rods and Network 2 as a basis was also conducted. Since R_E is set the only value that can change will be U_T . Simulations show that U_{Tmax} is reduced with 44.97 V.

5.10 Conductive additives

In areas where the soil mainly consist of rock or other matter of relatively high resistivity it may be beneficial to use vertical ground rods embedded in conductive additives like bentonite, petroleum coke, or other ground enhancement material. The procedure is to drill a hole in the rock ground, where $d_{hole} \gg d_{rod}$, place the rod in the hole and fill the hole with conductive

additives. The diameter and depth of the hole are dependent on the installation which the grounding system shall protect.

For these simulations Network 1 is used and the number of ground rods is increased in the same manner as in chapter 5.9. $d_{\text{hole}} = 25$ cm, $d_{\text{rod}} = 2.5$ cm and $h_{\text{hole}} = 10$ meters. It is not possible to define a conductive additive in AutoGrid Pro, but the conductive additive can be equated by defining $d_{\text{hole}} = d_{\text{rod}}$.

Figure 5-27 shows a comparison of $U_{T\text{max}}$ using grounding rods with and without conductive additives.

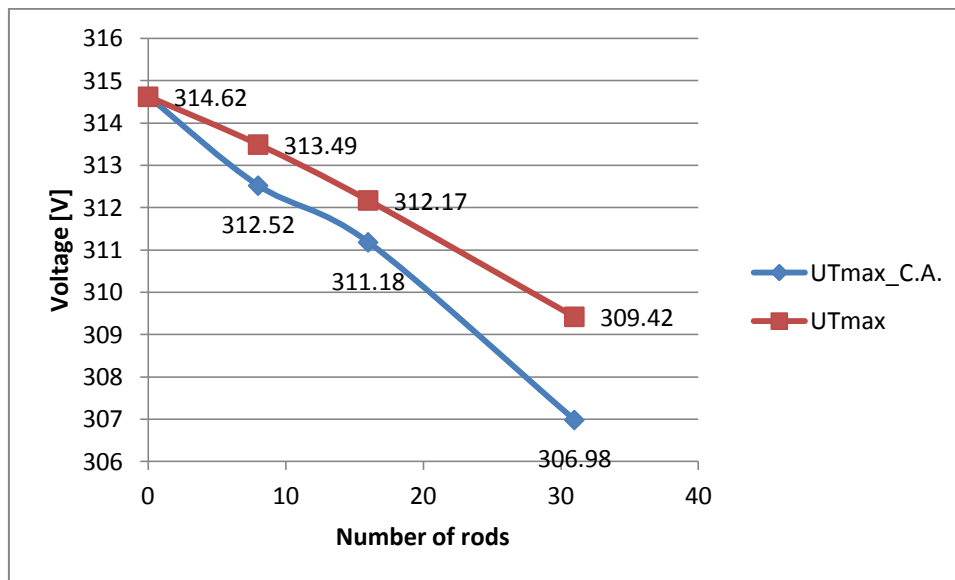


Figure 5-27 $U_{T\text{max}}$ using grounding rods with and without conductive additives

Figure 5-28 shows a comparison of I_g and R_E using grounding rods with and without conductive additives. Figure 5-27 and Figure 5-28 show a minor improvement in the grounding system performance, and it seems that deviation between the results using grounding rods with conductive additives compared to no additives increases with increasing number of grounding rods.

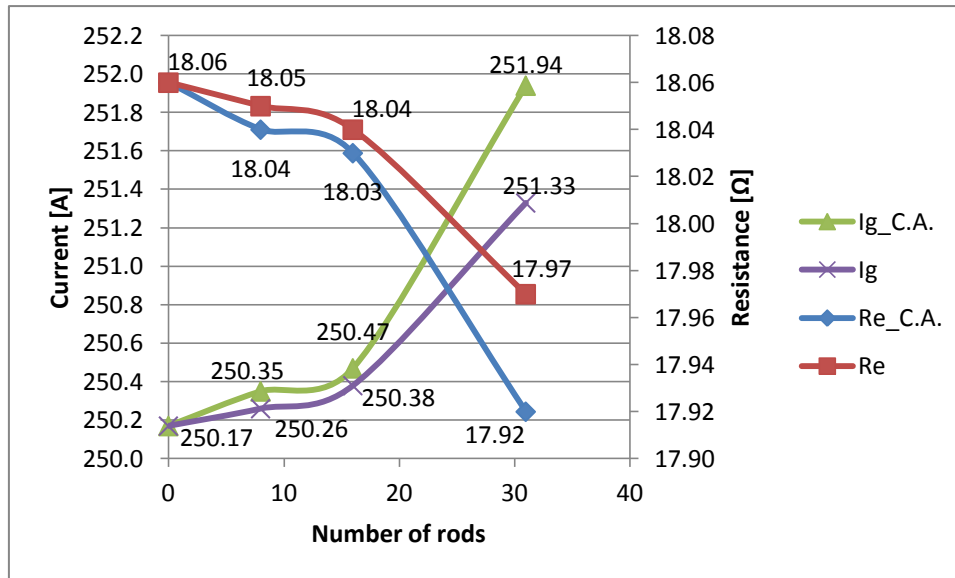


Figure 5-28 I_g and R_E using grounding rods with or without conductive additives

A simulation using 30 grounding rods and Network 2 as a basis was also conducted. Since R_E is set the only value that can change will be U_T . Simulations show that U_{Tmax} is reduced with 66.51 V.

5.11 Overhead earth conductors

So far the only currents considered have been the total fault current and the current flowing in the grounding network at the substation. Seeing as 1698.50 A of 10630 A flows in the substation grounding network in Network 2, a considerable amount must flow in the overhead earth conductors.

The objective of this simulation is to show how the overhead earth conductors affect the current flowing in the substation grounding network and U_{Tmax} . It is expected a noticeable increase in both values as the overhead earth conductors are sequentially disconnected. Network 2 must be modified in the following way to simulate one or more overhead lines without earth conductors:

1. Designate a special Terminal to model only transmission lines having no overhead line earth conductors (OHEC);
2. Specify the Energization Current for this terminal as the sum of the contributions from all transmission lines having no OHEC;
3. In the Neutral Connection frame, specify a large value for the Self Impedance, for example 999999 Ω , to ensure that no current returns back to the source through the OHEC;
4. Set any value for Ground Impedance, for example 0.1 Ω ;
5. Set the Number of Sections equal to 2;
6. The Section Length field can be set to any value (for example, set 300 meters);

7. Set the Tower Impedance field to some large value, for example 999999 Ω , to prevent a discharge of current there.
8. Define one phase (select an average height) wire and one shield wire using some typical conductors. This data will not have any influence on the computation; however they are required by the simulation program.

In the simulations the overhead lines for all lines connected to Samnanger substation are removed sequentially in the following order:

1. Sima
2. Mauranger
3. Fana
4. Evanger
5. Norheimsund
6. Frøland

Figure 5-29 shows how U_{Tmax} in the substation area changes with an increasing number of disconnected overhead earth conductors (OHEC). The increase is of a linear manner.

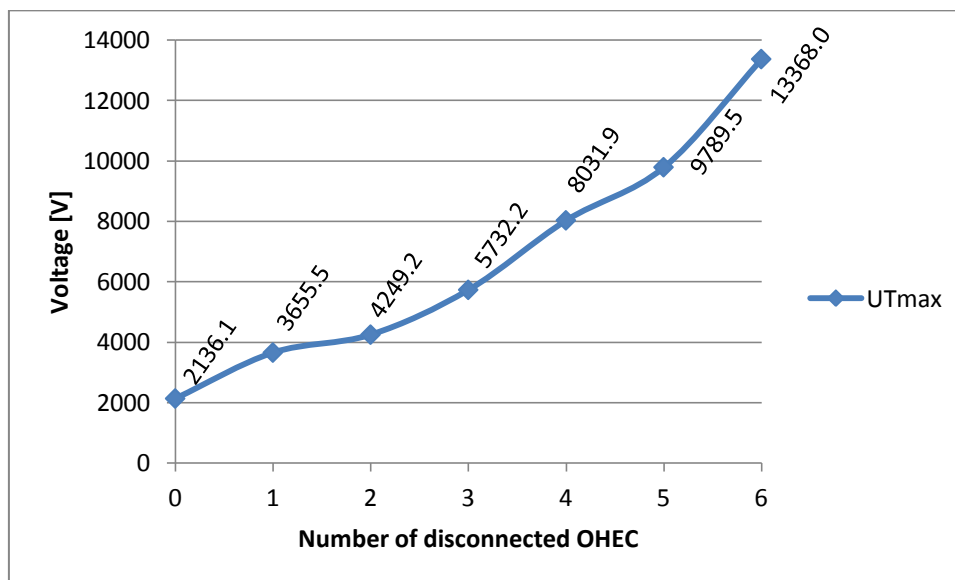


Figure 5-29 U_{Tmax} inside the substation area as a function of disconnected OHEC's

Figure 5-30 shows how I_g and the current flowing in the OHEC's, I_n , changes with an increasing number of disconnected OHEC's. The increase in I_g and the decrease in I_n are of a linear manner.

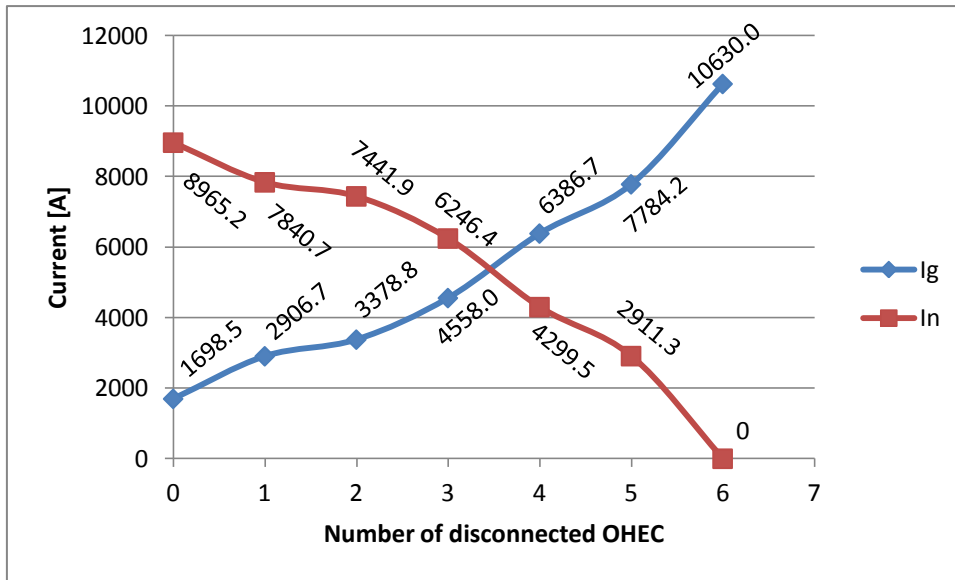


Figure 5-30 I_g and I_n as a function of the number of disconnected OHEC's

Figure 5-31 and Figure 5-32 show the unsafe touch voltages inside the substation area with five and six OHEC's disconnected. Notice that with five OHEC's disconnected $U_T > U_{Tp}$ in only a few areas within the switchyard bays, with $t_{\text{fault}} = 1$ second. When all OHEC's are disconnected, $U_T > U_{Tp}$ almost everywhere inside the substation area.

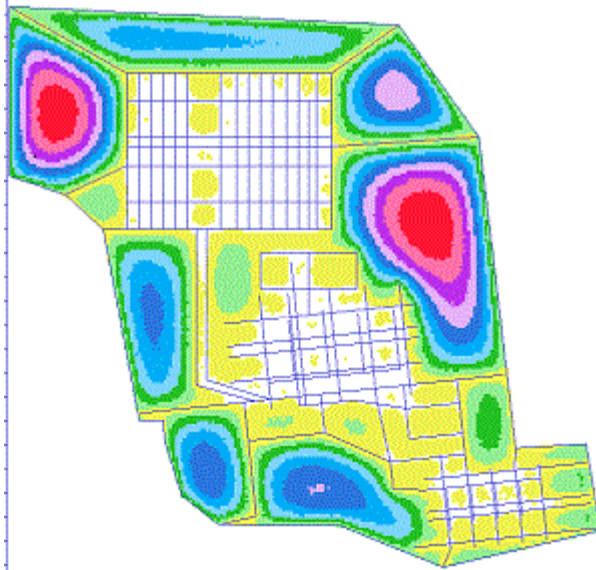


Figure 5-31 Unsafe U_T inside the substation area with five OHEC's disconnected

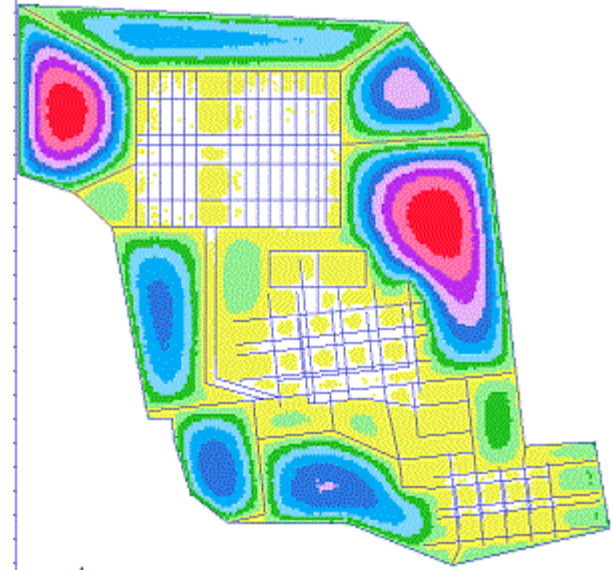


Figure 5-32 Unsafe U_T inside the substation area with all OHEC's disconnected

5.12 Increased single-phase-to-earth current

The single-phase-to-earth short circuit current (I_{k1}) used in the simulations so far is based on the network model Norden 2010, which includes the 420 kV overhead line Sima – Samnanger. Future plans to voltage upgrade the lines Mauranger – Samnanger, Fana – Samnanger and Evanger – Samnanger will lead to an increase in I_{k1} which the grounding network at Samnanger must be able to handle. The magnitude of the short circuit increase will be individual for each line, but for simulation reasons this increase is set to 30 % for every overhead line being voltage upgraded from 300 kV to 420 kV.

The objective of this simulation is to see how the grounding network performance is affected by an increase in I_{k1} on the three overhead lines mentioned in the above section, with respect to U_{Tmax} and I_g . I_{k1} is increased sequentially by 30 % on the overhead lines in the following manner:

1. Mauranger
2. Fana
3. Evanger

Figure 5-33 shows the results of the simulation with respect to U_{Tmax} and I_g . It is evident that U_{Tmax} and I_g increase in the same manner, and an increase in I_{k1} of 1455 A yields an increase in $U_{Tmax} = 293.20$ V and $I_g = 233.20$ A.

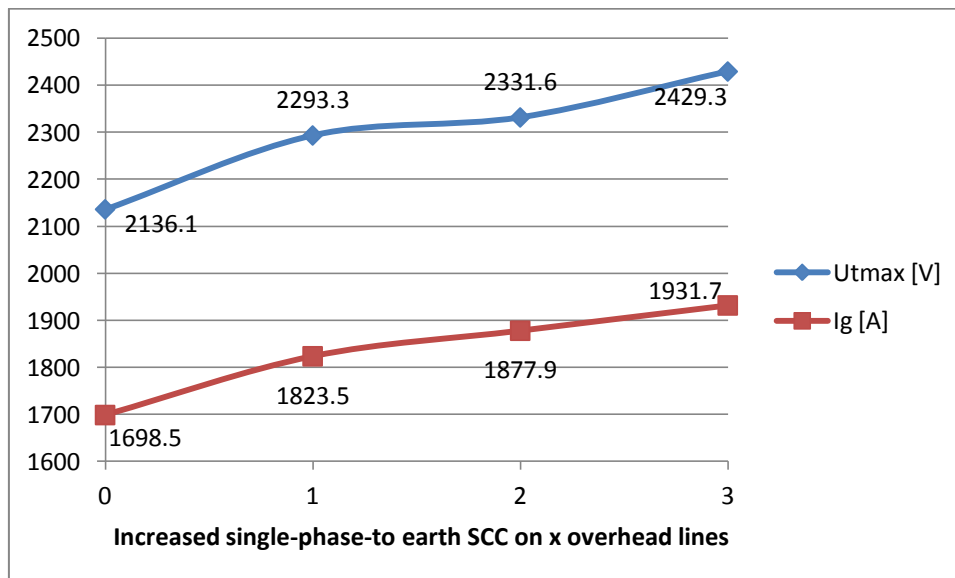


Figure 5-33 U_{Tmax} and I_g as a function of increasing I_{k1} on x-number of overhead lines

Figure 5-34 and Figure 5-35 show the distribution of the unsafe touch voltages within the substation area for an increase in $I_{k1} = 1455$ A, with a fault clearing time of 1 second and 0.06 second, respectively. Notice that there are no unsafe touch voltages within the substation area

when $t_{\text{fault}} = 0.06$ s. There are neither any unsafe touch voltages inside the switchyard bays when $t_{\text{fault}} = 1$ s, but the problematic areas are the “open areas” outside the bays as in Network 2.

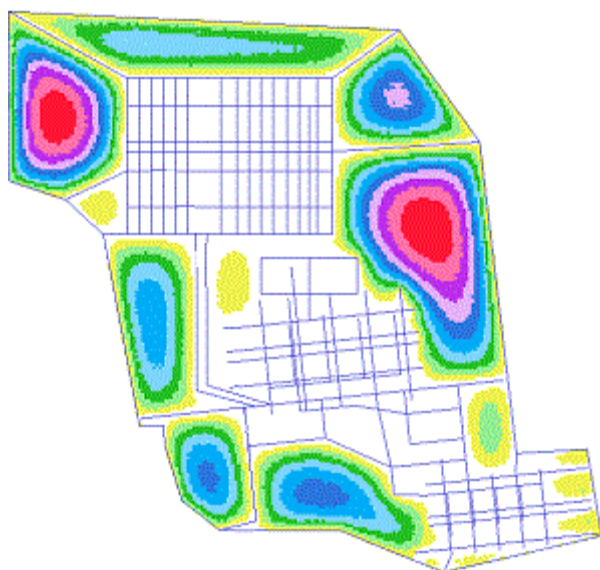


Figure 5-34 Unsafe U_T distribution for 30 % increase in I_{k1} , $t_{\text{fault}} = 1$ s

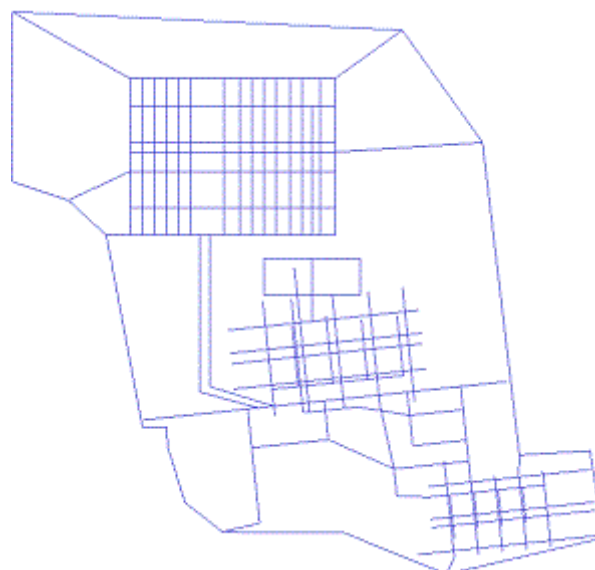


Figure 5-35 Unsafe U_T distribution for 30 % increase in I_{k1} , $t_{\text{fault}} = 0.06$ s

5.13 Three phase short circuit current

A three phase short circuit current (I_{k3}) on the installation connected to Samnanger substation may cause dangerous touch- and step voltages within the substation area. It is important that the grounding network can provide protection also in this event. Three phase short circuits shall be disconnected instantaneously, and control system engineers in ABB have stated that fault duration can be set to 0.06 s. Using Network 2 as a basis and setting $t_{\text{fault}} = 0.06$ s yields $U_{Tp} = 2999.8$ V and $U_{Sp} = 10400.7$ V.

The highest I_{k3} at Samnanger is simulated to 16.1 kA and occurs in the event of a short circuit on the 300 kV busbar, with current distribution as follows:

Mauranger	-	3.8 kA
Fana	-	2.4 kA
Evanger	-	3.5 kA
From T1 (300/132)	-	0.6 kA
From autotransformer (300/420)	-	5.8 kA

Due to the future voltage upgrading of the 300 kV overhead lines one must take into account an increase in I_{k3} , which has been set to 30 % in the simulations. The objective of the simulation is to see how the grounding network performance is affected by a three phase short circuit at the 300 kV busbar for the present and future network.

Figure 5-36 shows the distribution of unsafe U_T within the substation area for I_{k3} . $U_T > U_{Tp}$ in only two areas, again in the “open” areas.

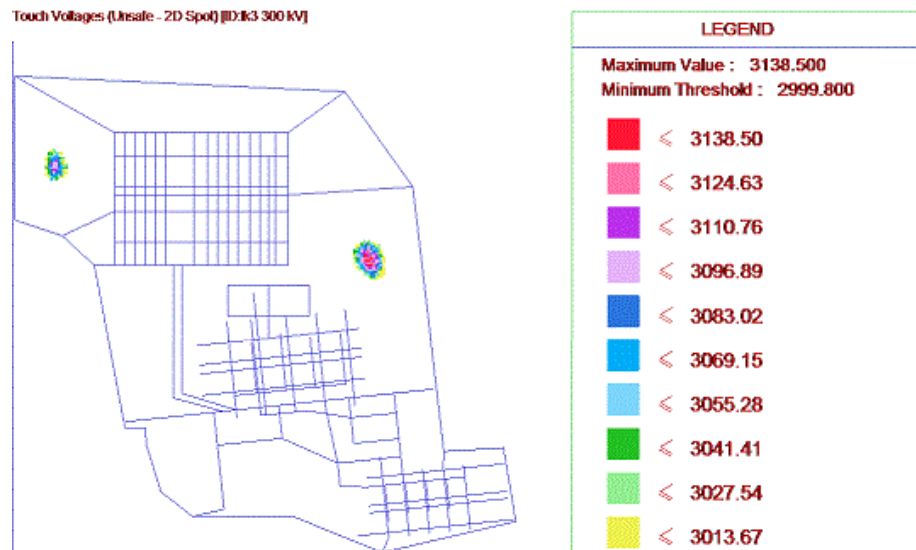


Figure 5-36 U_T distribution within the substation area for I_{k3}

Figure 5-37 shows the distribution of U_S inside the substation area during a three phase short circuit. $U_{Smax} < (U_{Tmax} \cap U_{Sp})$. U_{Smax} occurs outside the grounding network at the top left- and bottom right corner.

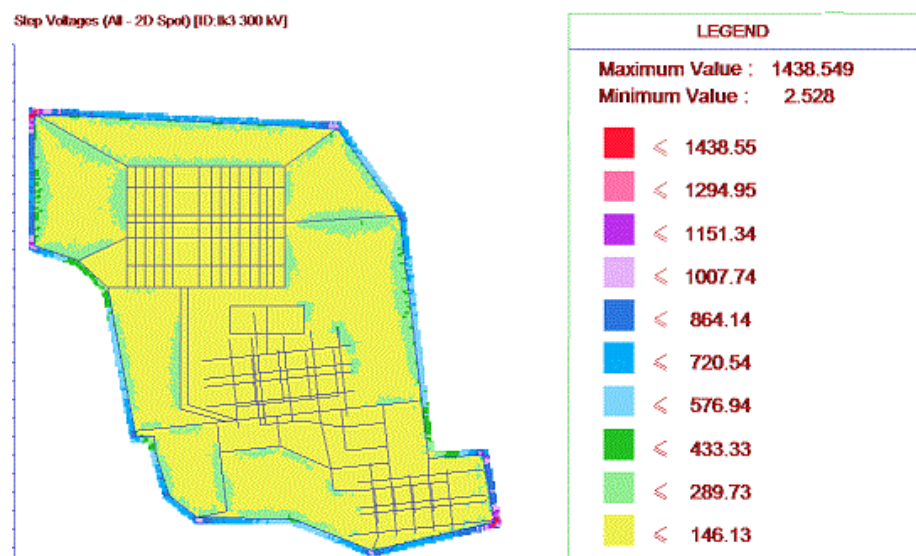


Figure 5-37 U_S distribution within the substation area for I_{k3}

Figure 5-38 shows the touch voltage distribution within the substation area when the short circuit contributions from Mauranger, Fana and Evanger have been increased by 30 %. $U_{Tmax} = 3755.84$ V, which is an increase of 19.67 %, and $U_{Tmax} > U_{Tp}$ in two areas outside the switchyard bays. $U_{Smax} = 1721.51$ V, which is lower than U_{Sp} .

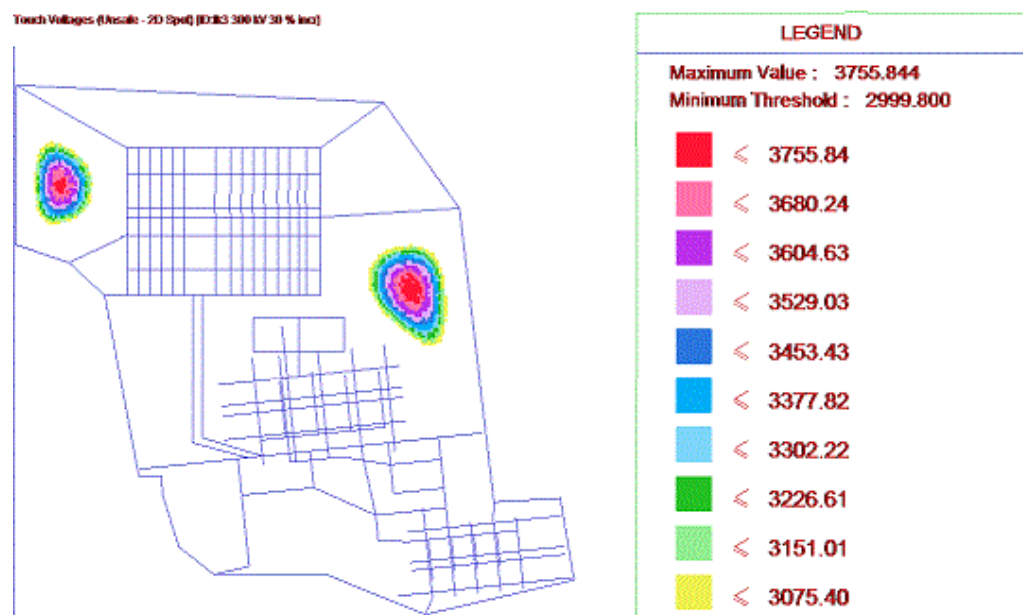


Figure 5-38 U_T distribution inside substation area for I_{k3} increased 30 %

6 DISCUSSION

This chapter presents the discussion of the simulation results shown in chapter 5. The subchapters are divided in the same manner as in chapter 5 for reader simplicity.

6.1 Initial modeling

Network 1 was modeled with a two layer soil, where $\rho_1 = 250 \Omega\text{m}$, $d_1 = 0.5 \text{ m}$, $\rho_2 = 10000 \Omega\text{m}$ and $d_2 = \infty$. Network 2 was modeled with the same soil type and an insulating surface layer of $\rho = 3000 \Omega\text{m}$, but R_E was set to 2Ω . The simulated single-phase-to-earth short circuit current occurred at the 420 kV busbar with a value of 10.63 kA, and $t_{\text{fault}} = 1$ second.

The simulation results for Network 1 and Network 2 showed that the touch voltages inside the switchyard bays did not exceed the permissible touch voltages, but unsafe touch voltages occurred in some of the “open” areas inside the substation. The touch voltages calculated by AutoGrid Pro are potential touch voltages and not real touch voltages, and in these “open” areas there will be no real touch voltages during normal situations since there are no metallic structures to touch. See Nomenclature list for the definition of touch voltage.

However, the potential touch voltages in the “open” areas may become real touch voltages when grounded equipment is brought into these areas during for example maintenance work. Such equipment can be a drill connected to a grounded extension cord, thus dangerous potential differences can occur between the hands and feet of the person holding the equipment. Therefore, considerations should be made to prevent dangerous potential touch voltages. A common measure is to install an insulating surface layer with a higher resistivity than the underlying soil layer.

The single-phase-to-earth fault is of a magnitude that implies immediate disconnection of the fault. Using $t_{\text{fault}} = 0.06 \text{ s}$ yields no unsafe touch nor step voltages inside the substation area for Network 1 and Network 2. $U_S < U_{Sp}$ also for $t_{\text{fault}} = 1$ second.

6.2 Insulating surface layer

Network 1 was used as a basis and modified with a 10 cm insulating surface layer with $\rho = 3000 \Omega\text{m}$. This lead to $U_T < U_{Tp}$ in all areas inside the substation. Figure 5-8 showed that for each 500 Ωm increase in the insulating surface layer resistivity, U_{Tp} increased by 38.6 V on average. This proves that installing an insulating surface layer is an effective measure to provide protection against touch voltages.

It must be emphasized that the touch voltages do not decrease when an insulating surface layer is installed, but it is the permissible touch voltages that increase. This is due to the fact that the

insulating surface layer provides an additional resistance to the body impedance and shoe resistance, which in total limits the current through the body that can cause auricular fibrillation.

6.3 Varying fault duration

In this simulation AutoGrid Pro was used to calculate the permissible touch- and step voltages as a function of varying fault duration. The simulation program uses the input data as a basis for the calculations, with respect to soil conditions and additional resistances. A foot resistance of 1000 Ω was used, as in Network 1 and Network 2.

The results showed that U_{Tp} and U_{Sp} decreases exponentially with an increasing fault duration, and stabilizes at 114.0 V and 244.3 V, respectively. The curve for U_{Tp} in Figure 2-1 stabilizes at 80 V. The reasons for the deviation between Figure 2-1 and Figure 5-9 are that AutoGrid Pro takes into consideration the upper soil layer and additional resistances. It can be stated that the curve in Figure 2-1 is conservative.

6.4 Varying soil conditions at Samnanger substation

Four scenarios with different soil conditions were developed for these simulations. Network 1 was used as a basis for the simulations and the grounding network performance as a function of varying soil conditions was presented.

6.4.1 Scenario 1

The resistivity of the bottom soil layer was changed from 10000 Ωm to 15000 Ωm , while the rest of the network was kept unchanged. According to theory for an isolated grounding network the touch and step voltages should increase in this case due to an increased soil resistivity.

The results showed that U_T and U_S was reduced by 85.65 V and 18.94 V, which is contradictory to what could be expected. The reason for this decrease is that the current flowing in the grounding network is decreased due to an increased resistance to earth. R_E is increased by 7.15 Ω , which leads to a reduction in I_g of 68.95 A. The result is that more of the fault current flows in the overhead line earth conductors and into the soil along the overhead line trace and adjacent substations.

6.4.2 Scenario 2

The resistivity of the upper soil layer was changed from 250 Ωm to 2000 Ωm , while the rest of the network was kept unchanged from Network 1. Based on the discussion in 6.4.1 one should expect, based on the increased soil resistivity, a decrease in U_T , U_S and I_g , while R_E should increase.

The results showed that R_E increased with 4.61Ω and I_g decreased with 49.33 A , but $U_{T_{\max}}$ and $U_{S_{\max}}$ increased by 616.21 V and 141.03 V compared to Network 1. It is suspected that this occurs because I_g does not distribute in the soil as well as in Network 1 where the upper soil was $250 \Omega\text{m}$. This leads to that the current density is very high in and close to the grounding network, which again leads to large potential differences between the grounding network and metallic structures above ground.

In Network 1 more of I_g distributes in the upper soil layer, creating a more homogenous surface which leads to lower potential differences between the grounding network and metallic structures above ground, thus lower U_T and U_S .

6.4.3 Scenario 3

The simulations were conducted with the following soil parameters: $\rho_1 = 300 \Omega\text{m}$, $d_1 = 0.5 \text{ m}$, $\rho_2 = 65 \Omega\text{m}$ and $d_2 = \infty$. The remaining network was kept as in Network 1. The expected simulation results were an increase in U_T , U_S and I_g , while R_E should be reduced compared to Network 1.

The results showed that R_E decreased with 17.87Ω and I_g increased with 4362.03 A . $U_{T_{\max}}$ decreased with 11.82 V , while $U_{S_{\max}}$ decreased by 29.46 V . $U_{T_{\max}}$ was calculated to be 302.80 V which may seem low considering $I_g = 4612.2 \text{ A}$. The reason for $U_{T_{\max}}$ not being higher is due to the fact that the soil has a relatively low resistivity, which in turn leads to I_g being distributed well throughout the soil, most of it in the lower soil layer. This yields a soil with smaller potential differences than in Network 1, which is illustrated in the fact that $U_{S_{\max}}$ decreases. See Nomenclature list for the definition of step voltage.

6.4.4 Scenario 4

The soil was modeled as a uniform soil with a resistivity of $250 \Omega\text{m}$. It was expected that a large portion of the fault current would flow in the grounding network due to a reduced R_E compared to Network 1, which again should lead to an increase in U_T and U_S .

The results showed that R_E was reduced with 17.42Ω and I_g increased with 3025.93 A . $U_{T_{\max}}$ and $U_{S_{\max}}$ increased with 334.3 V and 51.0 V , respectively. Since the soil was modeled as a uniform soil with low resistivity, I_g will be distributed throughout the soil with the highest density in the upper parts of the soil around the grounding network.

Compared to Scenario 3 in chapter 5.4.3 one could expect that U_T and U_S would be equally low for the uniform soil case, but I_g for the case in 5.4.3 was mainly distributed in the lower soil layer which lead to a lower potential for the upper soil layer. For 5.4.4 the largest part of I_g is distributed in the upper part of the soil, creating a soil with a high potential compared to Network

1, causing the U_{Tmax} increase. Even though the soil potential is high, the potential differences in the upper parts of the soil do not create an equally large increase in U_{Smax} as in U_{Tmax} .

6.5 Varying R_E at adjacent substations

Three scenarios with reduced R_E for adjacent substations were developed for these simulations. Network 2 was used as a basis for the simulations and the grounding network performance as a function of R_E of adjacent substations was presented.

6.5.1 Scenario 5

R_E at Sima and Mauranger was changed from 2Ω to 0.5Ω , while the rest of the network remained as in Network 2. The simulations showed that U_T at Samnanger was unchanged, and the only difference was an increase in I_g at Sima and Mauranger of 362.80 A and 793.80 A, respectively. This is due to the fact that a larger part of the fault current contribution from Sima and Mauranger flows into their respective grounding networks because of the reduced R_E . This in turn leads to a reduced fault current flowing in the overhead line earth conductors of the Sima - Samnanger and Mauranger – Samnanger lines.

6.5.2 Scenario 6

R_E at Sima, Mauranger and Fana was set to 0.5Ω , while the rest of the network remained as in Network 2. The simulations showed that U_{Tmax} decreased by 1.9 V and I_g at Fana substation increased by 122.38 A. The increased I_g is due to the reduced R_E , which in turn leads to a lower part of the fault current contribution from Fana flowing in the Fana – Samnanger line.

6.5.3 Scenario 7

R_E at Sima, Mauranger, Fana and Evanger was set to 0.5Ω , while the rest of the network remained as in Network 2. The simulation showed that U_{Tmax} further reduced by 0.25 V and I_g at Evanger substation increased by 124.21 A. The increased I_g is due to the reduced R_E , which in turn leads to a lower part of the fault current contribution from Evanger flowing in the Evanger – Samnanger line.

Based on 6.5.1, 6.5.2 and 6.5.3 it can be concluded that the R_E at adjacent substations have very little impact on the grounding network performance at Samnanger. The only real effect is seen in the increased I_g flowing in the grounding networks at the substations where R_E has been reduced.

6.6 Varying R_t for overhead line towers

Three scenarios with varying R_t for the overhead line towers were developed for these simulations. Network 2 was used as a basis for the simulations and the grounding network performance as a function of R_t was presented.

6.6.1 Scenario 8

R_t of the Sima – Samnanger line was reduced from 60 Ω to 25 Ω , while the rest of the network remained as in Network 1. It was expected a decrease in U_{Tmax} and I_g . The simulations showed that U_{Tmax} was reduced with 158.38 V (7.41 %), and I_g was reduced with 125.9 A (7.41 %). This is due to the fact that a larger part of the fault current flows in the overhead line earth conductors and into the soil along the Sima – Samnanger line trace because of the reduced R_t . I_g at the other substations was unchanged.

6.6.2 Scenario 9

R_t for the towers on all overhead lines connected to Samnanger was set to 25 Ω , while the rest of the network remained as in Network 2. The simulations showed that U_{Tmax} was reduced by 545.36 V (25.53 %) at Samnanger, while I_g at all substations was reduced, except for Frøland where an increase in I_g of 47.52 % was calculated.

It is suspected that this occurs because the Frøland – Samnanger line is only 2.3 km long and has only 10 towers. A possible reason for the increase in I_g at Frøland is that when R_t is reduced, an increased current will flow in the overhead line earth conductors. Because of the limited amount of towers there will be a limited amount of the current in the OHEC flowing through the towers and into the ground. The remaining current will thus flow into the grounding network at Frøland, leading to an increased I_g compared to Network 2.

6.6.3 Scenario 10

R_t for the towers on all overhead lines connected to Samnanger was set to 90 Ω , while the rest of the network remained as in Network 2. The simulations showed that U_{Tmax} was increased by 282.78 V (13.24 %) compared to Network 2, while I_g at all substations was increased, except for Frøland where a decrease in I_g of 49.46 % was calculated.

Again, it is suspected that this occurs because of the limited number of towers on the Frøland – Samnanger line. When R_t is increased a reduced current compared to Network 2 will flow in the overhead line earth conductors. Because the current in the OHEC is reduced a larger part of it will flow in the tower structures and into the ground along the overhead line trace. The

remaining current will flow in the grounding network at Frøland, but this will be lower than in Network 2.

It is suspected that the reason for this not happening on the longer lines is that induction from the faulted phase “traps” larger parts of the fault current, and keeps it at a constant level.

Simulation of the Frøland – Samnanger line with 2.3 km length and 50 towers results in similar results for I_g as for the rest of the substations, both in Scenario 9 and Scenario 10. This indicates that the number of towers is the reason for the original results.

Based on 6.6.1, 6.6.2 and 6.6.3 it can be concluded that R_t for the overhead line towers have a substantial impact on the grounding network performance of the substations connected the lines in question.

6.7 Mesh density

Two scenarios with different mesh densities for the grounding network were developed for these simulations; one using Statnett Earthing Guidelines and one using FEF 2006. Both simulations showed neglectable deviations compared to Network 2 in consideration to how much the grounding network was modified in the two scenarios. The only substantial difference between the two scenarios and Network 1 are the amount of material and labor hours used to install the grounding network.

Based on these simulations it can be questioned if the Statnett Earthing Guidelines are too conservative. They provide a fast and easy way of engineering large grounding networks, but the material consumption and labor required for installing the grounding network is a cost that must be considered. Likewise the cost of simulation programs and engineering labor must be considered, and weighed against a more expensive installation. It must be emphasized that the considerations in this discussion is based on simulations of only one substation, and are not necessarily correct for other substations and installations. Neither are transient conditions caused by lightning considered.

6.8 Cross sectional value of earth electrodes

The cross sectional area of the grounding network electrodes was reduced in three steps for these simulations; 70 mm², 50 mm² and 25 mm². The rest of the network remained as in Network 2.

The simulations showed that U_{Tmax} increased by 53.34 V (2.5%) when using a 25 mm² electrode compared to a 120 mm² electrode, with the largest step in U_{Tmax} between 25 mm² and 50 mm².

It is evident that the cross sectional area of the grounding network electrodes has little influence on the performance of the grounding network. It can be concluded that for the performance of

the grounding network a 25 mm² cross sectional area is sufficient, but due to the mechanical stresses it is subjected to, especially during substation construction work and short circuits, the cross sectional area of the grounding network should be at least 70 mm². For example, Statnett use 120 mm² in their 300 kV and 420 kV substations.

6.9 Vertical grounding rods

The grounding network was modified with an increasing number of vertical grounding rods, while the rest of the network remained as in Network 1. 5, 10, 15 and 30 vertical grounding rods were used in the simulations.

The simulations showed that U_{Tmax} decreased by 5.2 V (1.65 %) when using 30 grounding rods compared to none. For the same scenario R_E decreased with 0.09 Ω (0.5 %), while I_g increased with 1.16 A (0.46 %). From zero to 30 grounding rods the grounding electrode length increased by 300 meters. It is evident that such an increase in material usage cannot be justified when considering the minor changes in the grounding network performance. It was also expected that using grounding rods in Network 1 would be inefficient due to the high resistivity of the lower soil layer.

Table 5-15 showed that grounding rods were more efficient in the case where the lower soil layer resistivity was 250 Ωm , and the upper soil layer resistivity was 15000 Ωm . U_{Tmax} decreased by 111.46 V (13.75 %) when using 30 grounding rods compared to none. This is due to the fact that more of I_g flows into the lower soil layer, leading to a reduced potential of the grounding network.

Simulating Network 2 with 30 grounding rods showed a decrease in U_{Tmax} of 44.97 V (2.11 %). This is due to the fact that more of I_g flows deeper into the soil as a function of the grounding rods. Using grounding rods was not efficient for this case either, as expected.

6.10 Conductive additives

The grounding network was modified with an increasing number of vertical grounding rods embedded in a conductive additive, while the rest of the network remained as in Network 1. The simulations were conducted using 5, 10, 15 and 30 grounding rods. The conductive additive was modeled by setting the diameter of each grounding rod equal to the diameter of the hole they were installed in, as stated in the AutoGrid Pro manual.

The simulations showed that U_{Tmax} was reduced by 7.64 V (2.43 %) when using 30 grounding rods compared to none. Figure 5-27 indicated that the deviation between using grounding rods with and without conductive additives increased with an increasing number of grounding rods. Figure 5-28 showed the same trend for R_E and I_g .

A simulation using Network 2 with 30 grounding rods embedded in conductive additives showed a decrease in U_{Tmax} of 66.51 V (3.11 %).

It was expected that modeling the grounding rods embedded in conductive additives would lead to larger changes in the grounding network performance. It is suspected that the way conductive additives are modeled in these simulations does not produce accurate enough results.

6.11 Overhead line earth conductors

The simulations were carried out by sequentially disconnecting the overhead line earth conductors to see the impact on the grounding network performance. The rest of the network was kept as in Network 2.

The simulations showed that U_{Tmax} increased in a linear manner for each set of overhead line earth conductors that were disconnected. When all OHEC were disconnected U_{Tmax} had increased by 11231.9 V (526 %). The simulations also showed that I_g increased in a linear manner, with a total increase of 8931.5 A (526 %).

Figure 5-31 showed that there were only a few places within the switchyard bays where $U_T > U_{Tp}$ when 5 of 6 OHEC were disconnected. This shows that the grounding network is able to create an equipotential surface even for relatively large currents when the meshes are as dense as in Network 2. One can further conclude that the OHEC have a large impact on the touch voltages within a substation, and the amount of fault current that flows in the grounding network. It is therefore extremely important that one should try to obtain as low as possible R_t for the overhead line towers, and to implement measures that will reduce the probability of an OHEC failure.

6.12 Increased single-phase-to-earth current

These simulations were conducted while sequentially increasing I_{k1} by 30 % on Mauranger, Fana and Evanger to Samnanger overhead lines, to see the impact on the grounding network performance. The rest of the network was kept as in Network 2.

The results showed that an increase in I_{k1} of 1455 A compared to network one, yielded an increase in U_{Tmax} of 293.20 V (13.73 %). Figure 5-35 showed that when $t_{fault} = 0.06$ second, no unsafe touch voltages inside the substation area occurred. It can be concluded that the designed grounding network at Samnanger can bare the increased short circuit contribution that will arise when the 300 kV overhead lines are voltage upgraded to 420 kV. It is emphasized that this conclusion is based on the conditions used in this master thesis work.

6.13 Three phase short circuit current

These simulations were conducted while sequentially increasing I_{k3} by 30 % on Mauranger, Fana and Evanger to Samnanger overhead lines, to see the impact on the grounding network performance. The rest of the network was kept as in Network 2.

The simulation results showed that an increase in I_{k3} of 2910 A compared to original I_{k3} -value yielded an increase in U_{Tmax} of 617.34 V (19.67 %). Almost all touch voltages were inside the permissible values due to the short fault duration time of 0.06 s, except for two small areas outside the switchyard bays. All step voltages were within permissible limits.

It can be concluded that the designed grounding network at Samnanger can bare both the original I_{k3} and the increased I_{k3} as a result of voltage upgrading of the 300 kV lines. No unsafe touch- or step voltages occur inside the substation area when using a 3500 Ω m-20 cm insulating surface layer. It is emphasized that this conclusion is based on the conditions used in this master thesis work.

7 CONCLUSION

To study the performance of the grounding network at Samnanger, and the effect of varying different parameters suspected to influence the grounding network performance, thirteen different simulations were created. Different scenarios were created in these simulations to show how an increase or decrease of a parameter affected the grounding network performance. Based on the simulation results and the discussion of these, the following conclusions have been drawn:

- The potential touch voltages (U_T) at Samnanger substation for the designed grounding network will be lower than permitted for the following events when $R_E = 2 \Omega$ and $t_{\text{fault}} = 0.06$ second:
 - For an $I_{k1} = 10.63$ kA when using a 3000 Ωm -10 cm insulating surface layer.
 - For an increase in I_{k1} of 30 % when using a 3000 Ωm -10 cm insulating surface layer. Larger increases have not been simulated.
 - For an $I_{k3} = 16.10$ kA when using a 3000 Ωm -15 cm insulating surface layer.
 - For an increase in I_{k3} of 30 % when using a 3500 Ωm -20 cm insulating surface layer. Larger increases have not been simulated.
- $U_T < U_{Tp}$ inside the switchyard bays for $t_{\text{fault}} = 1$ second, for all cases when the electrical network is intact.
- The potential step voltages (U_S) are lower than permissible values for all conducted simulations.
- Permissible touch and step voltages decreases exponentially with an increasing fault duration.
- An increase in the bottom soil layer resistivity will lead to a decrease in touch- and step voltages, when $\rho_1 \ll \rho_2$, and $d_1 \ll d_2$.
- An increase in the top soil layer resistivity will lead to an increase in U_T and U_S , when $\rho_1 \ll \rho_2$, and $d_1 \ll d_2$.
- Large currents flowing in the substation grounding network (I_g), i.e. kA, will not cause equally large U_T and U_S for a two layer soil when $\rho_1 \cap \rho_2$ are low, i.e. 50 – 300 Ωm , and $\rho_2 < \rho_1$.
- Large I_g can cause equally large U_T for a uniform soil layer of low resistivity, i.e. 50 – 300 Ωm .
- The resistance to earth (R_E) for adjacent substations has very little to neglectable effect on the grounding network performance at the substation in question.
- The resistance to earth (R_l) for overhead line towers has a large effect on the grounding network performance at the substations connected to the overhead line.
- I_g at substations connected to short lines with fewer than 50 towers may have an opposite change as a function of varying R_l than substations connected to lines with more than 50 towers.

- Based on the conditions used in this master thesis, the recommended mesh density in the Statnett Earthing Guidelines seems too conservative when considering 50 Hz grounding.
- The cross sectional value of the grounding network electrodes has little effect on the grounding network performance. The cross sectional value is set based on mechanical stress subjected to the grounding network.
- Vertical grounding rods have little effect in soils with high resistivity, i.e. $> 10000 \Omega\text{m}$, compared to the material consumption.
- It is suspected that the modeling method of conductive additives used in AutoGrid Pro is inaccurate.
- Disconnection of overhead line earth conductors leads to large increases in U_T , i.e. 1-10 kV.
- CDEGS is a very powerful and comprehensive simulation tool, and to learn to use it effectively will take more than 21 weeks of self study.

8 FUTURE WORK

This chapter includes a list of possible future work to be conducted on the basis of this master thesis work and results.

- The grounding system performance during transient conditions should be investigated.
- Attention to ground potential rise (EPR) along the overhead line trace should be given, along with EPR at adjacent substations during fault conditions.
- A different method on simulating vertical rods embedded in conductive additives should be investigated.
- R_E for the substation grounding network at Samnanger should be measured.

REFERENCES

- [1] Morstad A. Grounding of high voltage substations [Fall project]. Trondheim: NTNU; 2011
- [2] Norsk Elektroteknisk Komité. FEF 2006 – Forskrift om Elektriske Forsyningsanlegg med veiledning. 1. utgave – 3. opplag. Lysaker: Pronorm AS; 2010
- [3] Norsk Elektroteknisk Komité. NEK 440 – Stasjonsanlegg over 1 kV. 2. utg. Lysaker: Standard Online; 2011
- [4] Brede A.P., Høidalen H.K., Pleym A., Rørvik O., Seljeseth H. Underlag for beregninger og målinger på jordelektroder i forskjellige elkraftanlegg. Trondheim: EFI SINTEF-gruppen; 1995.
- [5] Ohnstad T. Veileder for jording av Statnetts stasjoner. Rev 1A. Oslo: Statnett; 2010.
- [6] Gremmel H, Kopatsch G. ABB Switchgear Manual. 11th edition. Berlin, Germany: Cornelsen Verlag Scriptor GmbH & Co; 2006.
- [7] Gärtner T. Ground Resistance Measurements on Transmission Towers with Overhead Ground Wires [Master thesis]. Trondheim: NTNU; 2007.
- [8] Norsk Elektroteknisk Komité. NEK IEC/TS 60479-1. 4. utg. Lysaker: Pronorm; 2005.

FIGURE LIST

Figure 2-1 Permissible touch voltage U_{Tp} [3].....	4
Figure 2-2 Two layer soil model.....	9
Figure 2-3 User interface of the Safety module.....	11
Figure 2-4 Report module interface.....	12
Figure 2-5 Soil module interface	13
Figure 2-6 Circuit module interface.....	14
Figure 4-1 Location of Samnanger substation in relation to Bergen city centre	17
Figure 5-1 Grounding network as modeled in CDEGS	25
Figure 5-2 Initial modeling U_T inside substation area	27
Figure 5-3 $U_T > U_{Tp}$ inside substation area.....	28
Figure 5-4 U_S within the substation area	29
Figure 5-5 U_T within the substation area when $R_E = 2 \Omega$	30
Figure 5-6 $U_{T_{\text{unsafe}}}$ within the substation area when $R_E = 2 \Omega$	30
Figure 5-7 U_S within the substation area when $R_E = 2 \Omega$	31
Figure 5-8 U_{Tp} and U_{Sp} as a function of 10 cm top layer resistivity	32
Figure 5-9 U_{Tp} and U_{Sp} as a function of fault duration	32
Figure 5-10 Scenario 1 U_T inside substation area.....	33
Figure 5-11 Change of $U_{T_{\text{max}}}$ as a function of bottom layer resistivity	34
Figure 5-12 Change of R_E and I_g as a function of bottom layer resistivity.....	34
Figure 5-13 Scenario 2 U_T inside substation area.....	35
Figure 5-14 Scenario 3 U_T inside substation area.....	36
Figure 5-15 Scenario 4 U_T inside substation area.....	37
Figure 5-16 Scenario 5 U_T inside substation area.....	38
Figure 5-17 Scenario 8 U_T inside substation area.....	40

Figure 5-18 Scenario 9 U_T inside substation area.....	41
Figure 5-19 Scenario 10 $U_T > U_{Tp}$ inside substation area.....	43
Figure 5-20 I_g as a function of changing R_t	44
Figure 5-21 Scenario 11 Grounding network overview and U_T distribution inside substation area	45
Figure 5-22 Scenario 12 Grounding network overview and U_T distribution inside substation area	46
Figure 5-23 U_{Tmax} as a function of cross sectional area of grounding electrode at Samnanger ...	47
Figure 5-24 U_{Tmax} as a function of the number of grounding rods	48
Figure 5-25 I_g and R_E as a function of the number of grounding rods	48
Figure 5-26 Length of Cu wires as a function of the number of grounding rods	49
Figure 5-27 U_{Tmax} using grounding rods with and without conductive additives.....	50
Figure 5-28 I_g and R_E using grounding rods with or without conductive additives	51
Figure 5-29 U_{Tmax} inside the substation area as a function of disconnected OHEC's	52
Figure 5-30 I_g and I_n as a function of the number of disconnected OHEC's	53
Figure 5-31 Unsafe U_T inside the substation area with five OHEC's disconnected	53
Figure 5-32 Unsafe U_T inside the substation area with all OHEC's disconnected	53
Figure 5-33 U_{Tmax} and I_g as a function of increasing I_{k1} on x-number of overhead lines.....	54
Figure 5-34 Unsafe U_T distribution for 30 % increase in I_{k1} , $t_{fault} = 1$ s	55
Figure 5-35 Unsafe U_T distribution for 30 % increase in I_{k1} , $t_{fault} = 0.06$ s	55
Figure 5-36 U_T distribution within the substation area for I_{k3}	56
Figure 5-37 U_S distribution within the substation area for I_{k3}	56
Figure 5-38 U_T distribution inside substation area for I_{k3} increased 30 %	57

TABLE LIST

Table 2-1 Specific resistance of different soils.....	9
Table 3-1 Comparison of Statnett guidelines and norms and regulations	15
Table 4-1 Substations connected to Samnanger substation	20
Table 4-2 Overhead lines connected to Samnanger substation	21
Table 5-1 Project settings.....	23
Table 5-2 Values of soil layers	25
Table 5-3 Terminal data input.....	26
Table 5-4 Varying soil scenarios at Samnanger	33
Table 5-5 Varying R_E values for adjacent substations to Samnanger.....	37
Table 5-6 Scenario 5 I_g	38
Table 5-7 Scenario 6 I_g	39
Table 5-8 Scenario 7 I_g	39
Table 5-9 Varying R_t values for overhead line towers	40
Table 5-10 Scenario 9 I_g	42
Table 5-11 Scenario 10 I_g	43
Table 5-12 Varying mesh density for 420 kV grounding network	44
Table 5-13 Comparison of Network 2 and Scenario 11	45
Table 5-14 Comparison of Network 2 and Scenario 11	46
Table 5-15 U_{Tmax} , I_g and R_E for zero and 30 ground rods.....	49

APPENDICES

- Appendix A Conventional time/current zones of effects of a.c. currents (15 Hz to 100 Hz) on persons for a current path corresponding to left hand to feet [8].
- Appendix B Materialvalg og minste dimensjoner for jordelektroder, som sikrer deres mekaniske styrke og korrosjonsmotstand [3].
- Appendix C Tabell 1 – Relevante strømmmer for utførelse av jordingsanlegg [3].
- Appendix D Earthing system design flow chart [8].
- Appendix E Samnanger substation grounding network technical drawing
- Appendix F Written report from CDEGS – AutoGrid Pro

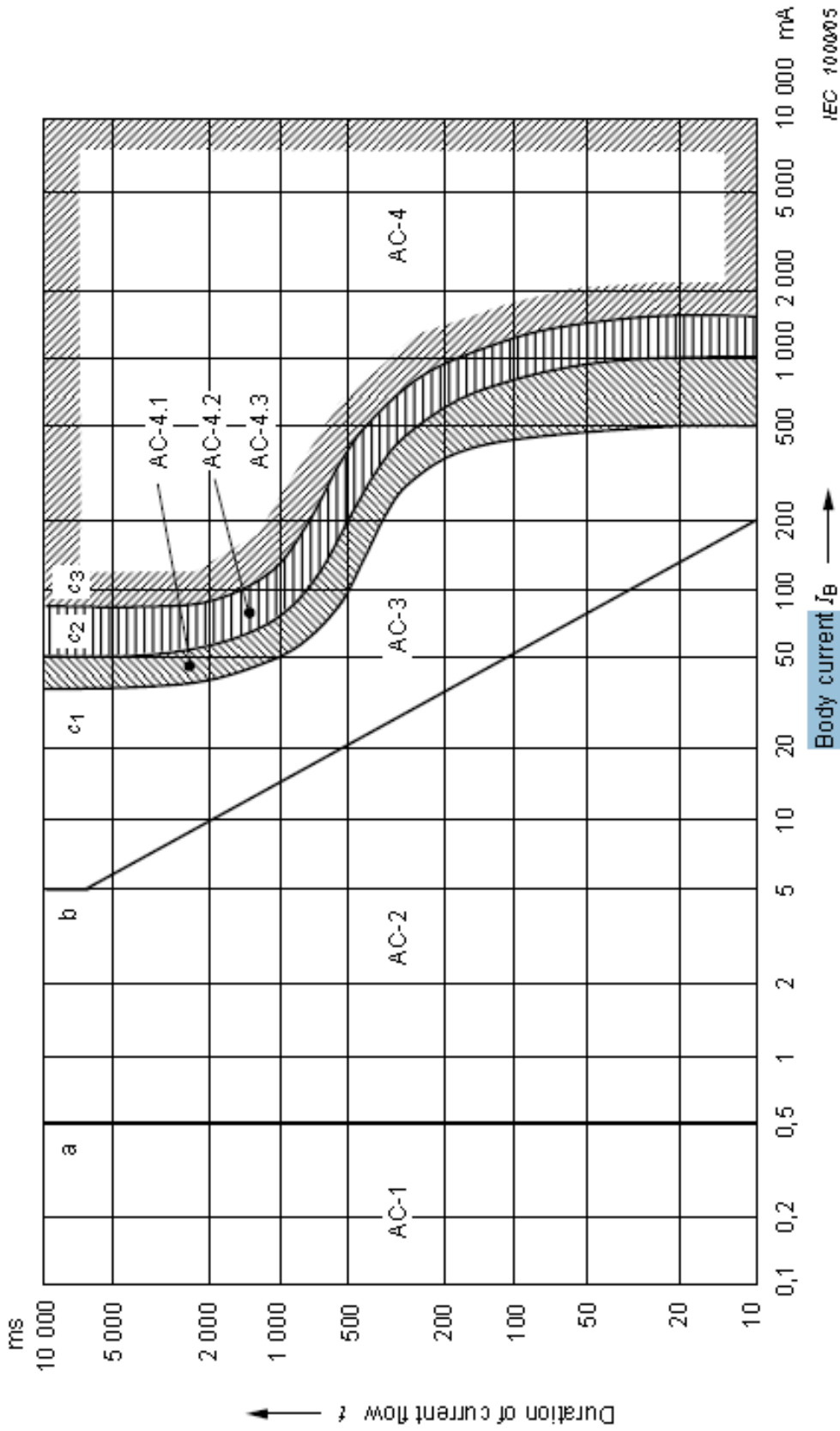


Figure 20 – Conventional time/current zones of effects of a.c. currents (15 Hz to 100 Hz) on persons for a current path corresponding to left hand to feet (for explanation see Table 11)

Tillegg C

(normativt)

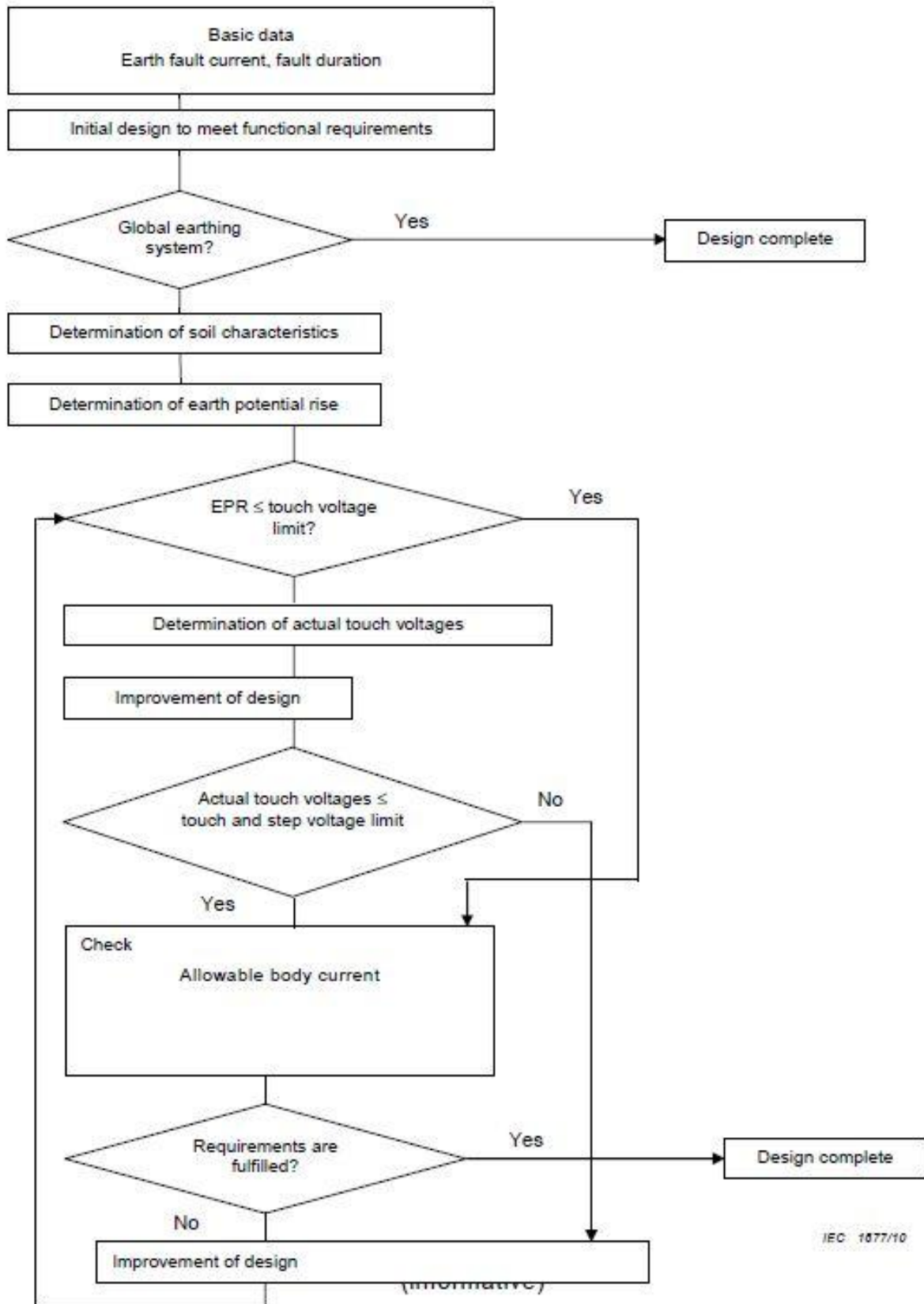
Materialvalg og minste dimensjoner for jordelektroder, som sikrer deres mekaniske styrke og korrosjonsmotstand

Materiale		Type av elektrode	Minste størrelse				
			Leder			Belegg/mantel	
			Dia- meter (mm)	Tverr- snitt (mm ²)	Tykkelse (mm)	Enkelt- verdier (µm)	Middelverdier (µm)
Stål	Varm-galvanisert	Bånd ^b		90	3	63	70
		Profil (inkl. plater)		90	3	63	70
		Rør	25		2	47	55
		Rund stang for jord- elektrode (jordspyd)	16			63	70
		Rund leder for horisontal jord- elektrode	10				50
	Med blymantel ^a	Rund leder for horisontal jord- elektrode	8			1000	
	Med ekstrudert kobbermantel	Rund stang for jord- elektrode (jordspyd)	15			2000	
	Med elektrolytisk kobbermantel	Rund stang for jord- elektrode (jordspyd)	14,2			90	100
Kobber	Blank	Bånd		50	2		
		Rund leder for horisontal jord- elektrode		25 ^c			
		Flertrådet leder	1,8 ^d	25			
		Rør	20		2		
	Fortinnet	Flertrådet leder	1,8 ^d	25		1	5
	Galvanisert	Bånd		50	2	20	40
	Med blymantel ^a	Flertrådet leder	1,8 ^d	25		1000	
		Rund leder		25		1000	
		<p>^a Ikke egnet for direkte innstøping i betong. Bruk av bly er ikke anbefalt av miljøgrunner.</p> <p>^b Bånd, rullet eller avklippet med avrundede kanter</p> <p>^c Ved ekstreme forhold hvor erfaring viser at risiko for korrosjon og mekanisk skade er svært liten kan 16 mm² anvendes.</p> <p>^d For enkelt leder</p>					

Tabell 1 - Relevante strømmer for utførelse av jordingsanlegg

Type høyspenningssystem		Relevant for termisk belastning ^{a e}		Relevant for jordpotensialstigning og berøringsspenninger
		Jord elektrode	Jordingsleder	
Systemer med isolert nøytralpunkt				
		I_{kEE}	I_{kEE}	$I_E = r \cdot I_C$ ^b
Systemer med spolejordet nøytralpunkt				
Inkluderer kort tids jording for påvisning				
	Sekundærstasjoner uten slukkespoler ^f	I_{kEE}	I_{kEE}	$I_E = r \cdot I_{RES}$ ^b
	Sekundærstasjoner med slukkespoler	I_{kEE}	I_{kEE}^c	$I_E = r \cdot \sqrt{I_L^2 + I_{RES}^2}$ ^{b h}
Systemer med lavimpedansjordet nøytralpunkt				
Inkluderer korttids jording for tripping ^g				
	Sekundærstasjon uten nøytral jording	I_{k1}	I_{k1}	$I_E = r \cdot I_{k1}$
	Sekundærstasjon med nøytral jording	I_{k1}	I_{k1}	$I_E = r \cdot (I_{k1} - I_N)$ ^d
<p>a Hvis flere strømbaner er mulige kan en oppsplitting vurderes.</p> <p>b Om det ikke er automatisk utkobling av jordfeil, er behovet for å vurdere dobbel jordfeil avhengig av driftserfaringer.</p> <p>c Jordlederen på Petersen spolen må bli dimensjonert i forhold til spolestrømmen.</p> <p>d Det må sjekkes om ekstern feil er avgjørende.</p> <p>e Minimums tverrsnitt i tillegg C må vurderes.</p> <p>f I et ikke velkompensert system må den reaktive komponent av reststrømmen vurderes i tillegg.</p> <p>g Korttidsjording for systemer med spolejording starter automatisk innen 5 sek. etter påvisning av jordfeil.</p> <p>h I tilfeller av feil I understasjonen må kapasitiv jordfeilstrøm I_C vurderes. I tilfeller med ytterligere spoler utenfor understasjonen kan disse bli tatt i betraktning.</p> <p>Tegnforklaring</p> <p>I_C Beregnet eller målt kapasitiv jordfeilstrøm.</p> <p>I_{RES} Jordfeil reststrøm (Figur 3b). Hvis den eksakte verdi ikke forefinnes kan det antas 10 % av I_C.</p> <p>I_L Summen av merkestrømmene for de parallelle slukningsreaktorene i den aktuelle stasjonen.</p> <p>I_{kEE} Feilstrøm ved dobbelt jordfeil beregnet i henhold til NEK EN 60909 (for I_{kEE} kan 85 % av den initiale symmetriske kortslutningsstrøm brukes som en høyeste verdi).</p> <p>I_{k1} Initiell symmetrisk kortslutningsstrøm for en linje-til-jord kortslutning, beregnet i samsvar med NEK EN 60909.</p> <p>I_E Strøm til jord (se Figur 2).</p> <p>I_N Strøm via nøytral jording av transformator (se Figur 2).</p> <p>r Reduksjonsfaktor (se Tillegg L).</p> <p>Hvis ledninger og kabler som går ut fra stasjonen har forskjellige reduksjonsfaktorer må den relevante strømmen bestemmes (i henhold til Tillegg L).</p>				

Earthing system design flow chart



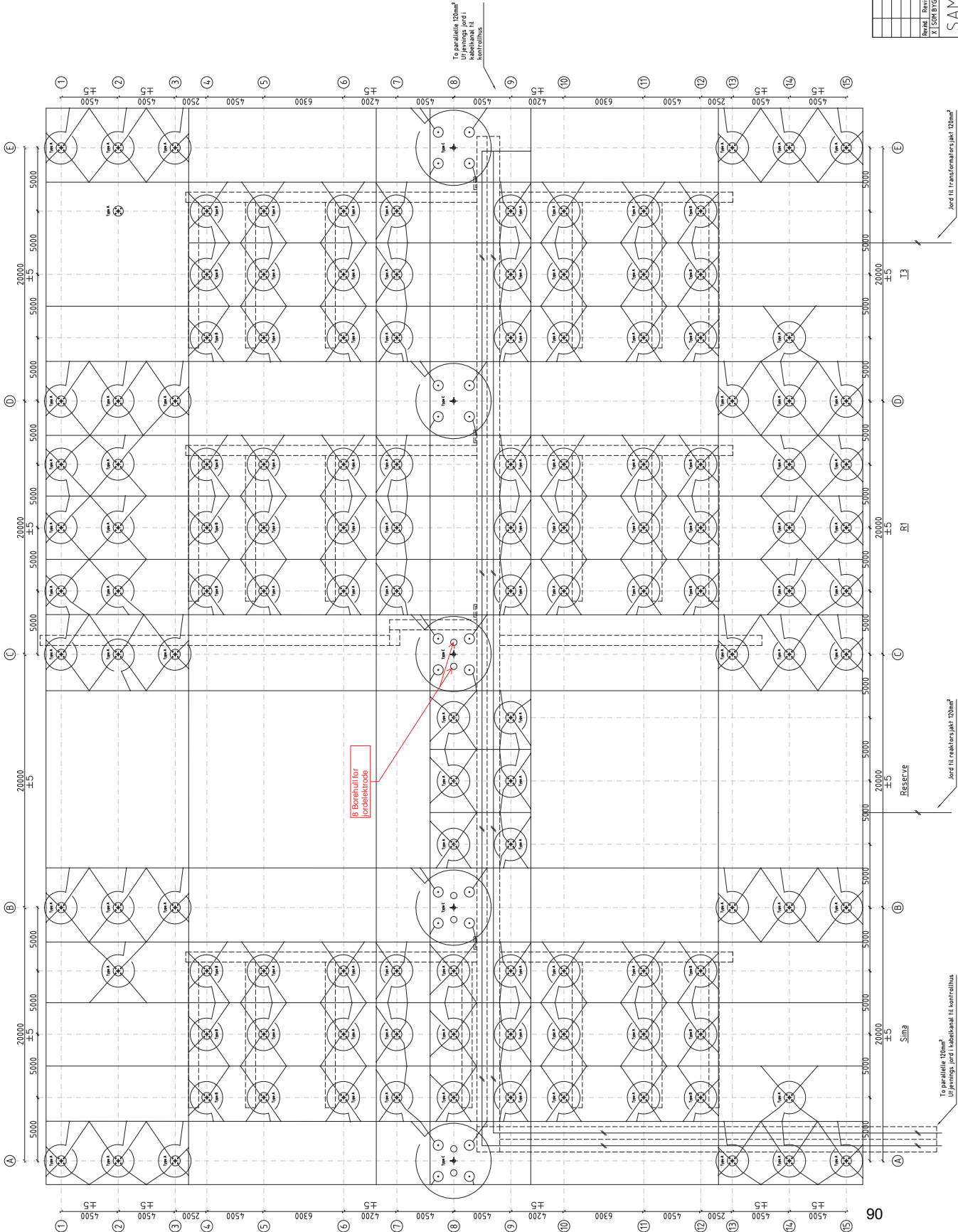
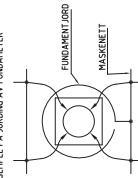
Appendix E2

Type	Lengde i meter
Hovedjordring for 420kV anlegg	2250
Fundamentjord for 420kV anlegg	3450
Total antall meter 120mm ² Cu jordlinjer	5700
Total antall stk. C-pressklemmer	632

GENERELLE RETNINGSLINJER FOR JORDING

- All jording skal utføres med 120 Cu line, type KGF.
- Jordingslapp som føres opp langs fundament. (for jording av stativ med kabesko)
- To jordingslinjer.
- Kortforbindelse. Cimpet forbindelse for agnering NB! To pressinger.
- Ledningsring lagt under/rundt og ført opp langs jordfundament.
- Kortslutningsstrøm 1420kV anlegget 24kA
- Det vises for øvrig til Montasjeveiledning Jording av Stativets støtstøper del 2, utførelse. Dok nr: 1406379
- Borehull for jordrelektroder
- 13stk fundament for innslekta a1v.

EKSEMPEL PÅ JORDING AV FUNDAMENTER



Revidert	Revisjonen gjelder	Dato/Sign.	Kontrollert
X	ISOK BYGGET I 10/2011		FORLEGGING TEGNING
	AREBEGG TEGNING	IMBEG/REVISJON	
	Målestokk	Kontinert	10.0.11. IN 7/02
	1:150	Tegnet	11.0.11. ASB88
		Kontrollert	
SAMNANGER		Erstatning av	
TRANSFORMATORSTASJ.		122258	
420kV apparatanlegg		Revisjons	
Jordnett		Blad nr.	
Kabelkanaler inntegnet stiple		Grupper nr.	
		Prosjekt nr.	
		Kategori	
		AT	



Fault Current

01-juni-2012 14:57:10

Report #1:

```
*****
*****
```

AUTOGRID PRO USER INPUT DATA REPORT

Creation Date/Time: 1 jun 2012/14:53:02

```
*****
*****
```

Input Data Summary Reports

System Data Summary

C:\Data\Morstad\Skole\Masteroppgave\CDEGS\Samnanger\Samnanger 420
kV\Network 1\Results\System Input.rep

Requested Computation Reports and Plots

C:\Data\Morstad\Skole\Masteroppgave\CDEGS\Samnanger\Samnanger 420
kV\Network 1\Results\User Input.rep-----
Graphics option chosen

Computation Plots

Touch Voltages

Show All Values

Show Unsafe Values Above Selected Safety Threshold

Step Voltages

Show All Values

Show Unsafe Values Above Selected Safety Threshold

Electric Network Configuration

Fault Current Distribution

Section Span Currents

Shunt Tower Currents

Shunt Tower Potentials

One Terminal Plot

Terminal Number 6

All Sections Selected

Configuration Plots

Grounding System Configuration

Types of plot selected

Computation Plots

2D Spot

Configuration Plots

Top View

End of Report #1

Report #2:

```

*****
*****
AUTOGRID PRO SYSTEM INPUT DATA REPORT
Creation Date/Time:      1 jun 2012/14:53:02
*****
*****

```

 Project Summary

```

-----
Run Identification ..... Network 1
System of Units ..... Metric
Radius Measured in ..... Meters
Frequency ..... 50 Hz

```

 Soil Structure (use specified soil structure characteristics)

 Soil type.....Horizontal - 2 Layer

Layer	Resistivity (Ohm-Meters)	Thickness (Meters)
Air	1E+18	0
Top	250	0,5
Bottom	10000	Infinite

 Network Fault Current Distribution

```

-----
Average soil characteristics along electric lines:
  Resistivity(Ohm-m) ..... 10000
  Relative Permeability (p.u.) ..... 1

```

Central site definition:

```

  Name ..... Samnanger
  Ground Impedance (To be deduced from grounding computations)

```



```
-----
Safety
-----
```

```
Determine Safety Limits for Touch and Step Voltages
```

```
  Safety Threshold for Touch Voltages ..... 369,3 V
```

```
  Safety Threshold for Step Voltages ..... 1203,9 V
```

```
Generation of observation points is user-defined.
```

```
  Grid Border Offset for Step Voltages ..... 3 m
```

```
-----
The computation results are written in the following reports:
-----
```

```
Ground Grid Performance
```

```
  C:\Data\Morstad\Skole\Masteroppgave\CDEGS\Samnanger\Samnanger 420
kV\Network 1\Results\Ground Grid Performance.rep
```

```
Fault Current Distribution
```

```
  C:\Data\Morstad\Skole\Masteroppgave\CDEGS\Samnanger\Samnanger 420
kV\Network 1\Results\Fault Current.rep
```

```
Safety Assessment
```

```
  C:\Data\Morstad\Skole\Masteroppgave\CDEGS\Samnanger\Samnanger 420
kV\Network 1\Results\Safety.rep
```

```
Report for Ampacity Function
```

```
  C:\Data\Morstad\Skole\Masteroppgave\CDEGS\Samnanger\Samnanger 420
kV\Network 1\Results\Ampacity.rep
```

```
List of Materials
```

```
  C:\Data\Morstad\Skole\Masteroppgave\CDEGS\Samnanger\Samnanger 420
kV\Network 1\Results\Bill of Materials.rep
```

```
End of Report #2
```

```
Report #3:
```

```
*****
```

```
List of Materials
```

```
Creation Date/Time:      1 jun 2012/14:53:02
```

```
*****
```

```
Interconnection / Bonding Nodes ..... 254
```

```
Extent of Grounding System ..... 36976,6 (Square
Meters)
```

```
Surface Layer Thickness ..... 10 (Centimeters)
```

```
Volume of Insulating Layer ..... 3697,66 (Cubic
meters)
```

```
Wet Resistivity of Insulating Surface Layer ..... 3000 (Ohm-m)
```

```
Grounding System Data
```

```
Number of Rods              Length (m)          Diameter (m)
```

```
-----
```

```
None
```

```
-
```

```
-
```

```
Number of Grid Conductors   Length (m)          Diameter (m)
```

```
-----
```

```
1
```

```
16,26
```

```
0,00944
```

```
1
```

```
47,9
```

```
0,00944
```

```
1
```

```
152,374
```

```
0,00944
```

4	80	0,00944
1	55,19	0,00944
3	25,3044	0,00944
1	28,3645	0,00944
5	47,45	0,00944
2	60,64	0,00944
3	68	0,00944
1	48,33	0,00944
1	75,0001	0,00944
1	18,02	0,00944
3	14,9399	0,00944
2	22,41	0,00944
1	31,2	0,00944
1	9,73	0,00944
1	22,47	0,00944
1	27,3827	0,00944
1	22,85	0,00944
1	32,08	0,00944
1	21,8415	0,00944
1	29,9474	0,00944
1	11,42	0,00944
1	13,2983	0,00944
1	39,99	0,00944
3	31,64	0,00944
1	56,6159	0,0124
1	34,6318	0,0124
1	3,18907	0,0124
2	7,81056	0,0124
1	16,02	0,0124
1	61,6699	0,0124
1	28,493	0,0124
1	10,059	0,0124
63	5	0,0124
7	14	0,0124
7	6,5	0,0124
14	6	0,0124
22	4	0,0124
6	3,5	0,0124
31	11,5	0,0124
35	15	0,0124
16	8	0,0124
1	7,5	0,0124
2	40	0,0124
1	10,9806	0,0124
1	63,1195	0,0124
1	27,9375	0,0124
1	65,3637	0,0124
1	25,2121	0,0124
1	70,77	0,0124
1	162,492	0,0124
1	57,5066	0,0124
1	131,08	0,0124
1	29,3363	0,0124
1	36,6872	0,0124
1	67,4405	0,0124
1	46,1453	0,0124
1	10	0,0124
1	8,19661	0,0124
1	24,2033	0,0124
1	19,789	0,0124
1	50,686	0,0124
1	21,4168	0,0124
1	24,6803	0,0124

1	81,3093	0,0124					
Total Length of Grid Conductors (m)		Diameter (m)					
1846,65		0,00944					
3009,15		0,0124					
End of Report #3							
Report #4:							
Date of run (Start) = fredag,01 juni 2012							
Starting Time = 14:53:02							
>>Safety Calculation Table							
System Frequency.....	:	50.000(Hertz)					
System X/R.....	:	20.000					
Surface Layer Thickness.....	:	10.000(cm)					
Number of Surface Layer Resistivities.....	:	10					
Starting Surface Layer Resistivity.....	:	500.00(ohm-m)					
Incremental Surface Layer Resistivity.....	:	500.00(ohm-m)					
Equivalent Sub-Surface Layer Resistivity.....	:	250.00(ohm-m)					
Body Resistance Calculation.....	:	IEC					
Body Resistance Exceeded by.....	:	50%					
Percent of Hand-to-Hand Resistance.....	:	75.000 %					
Fibrillation Current Calculation.....	:	IEC c2 curve					
Foot Resistance Calculation.....	:	IEEE Std.80-2000					
User Defined Extra Foot Resistance.....	:	1000.0 ohms					
=====							
===							
Fault Clearing Time (sec)		0.060 0.100 8.000					
+-----+							
-+							
Decrement Factor		1.378 1.269 1.004					
Fibrillation Current (amps)		0.880 0.773 0.049					
Body Resistance (ohms)		834.61 840.13 1448.65					
=====							
===							
=====							
Surface Layer Resistivity (ohm-m)	Fault Clearing Time						Foot Resistance
	0.060 sec.		0.100 sec.		8.000 sec.		
	Step	Touch	Step	Touch	Step	Touch	1 Foot
	Voltage	Voltage	Voltage	Voltage	Voltage	Voltage	Resistance
	(Volts)	(Volts)	(Volts)	(Volts)	(Volts)	(Volts)	(ohms)
500.0	3537.4	1284.0	3377.8	1228.2	299.0	127.5	1353.1
+-----+							

1000.0	4931.7	1632.5	4707.9	1560.7	405.1	154.0	2445.1
1500.0	6305.3	1975.9	6018.2	1888.3	509.6	180.2	3520.9
2000.0	7672.7	2317.8	7322.6	2214.4	613.6	206.2	4591.8
2500.0	9037.4	2659.0	8624.5	2539.9	717.5	232.1	5660.7
3000.0	10400.7	2999.8	9925.0	2865.0	821.2	258.1	6728.4
3500.0	11763.1	3340.4	11224.7	3189.9	924.9	284.0	7795.4
4000.0	13125.1	3680.9	12523.9	3514.7	1028.5	309.9	8862.1
4500.0	14486.6	4021.3	13822.7	3839.4	1132.1	335.8	9928.5
5000.0	15847.9	4361.6	15121.3	4164.1	1235.7	361.7	10994.6

* Note * Listed values account for short duration asymmetric waveform decrement factor listed at the top of each column.

End of Report #4

Report #5:

DATE OF RUN (Start)= DAY 1 / Month 6 / Year 2012
STARTING TIME= 14:53: 2:99

=====
>===== < G R O U N D I N G (SYSTEM INFORMATION SUMMARY)
>=====

Run ID.....: Network 1
System of Units: Metric
Earth Potential Calculations.....: Single Electrode Case
Type of Electrodes Considered.....: Main Electrode ONLY
Soil Type Selected.....: Uniform or Two-Layer
Horizontal
SPLITS/FCDIST Scaling Factor.....: 0.25017
1

EARTH PARAMETERS FOR HORIZONTALLY-LAYERED SOIL

TOP LAYER RESISTIVITY = 250.00 ohm-meters
BOTTOM LAYER RESISTIVITY = 10000. ohm-meters
REFLECTION COEFFICIENT = 0.951219 per unit
TOP LAYER HEIGHT = 0.50000 METERS

1

CONFIGURATION OF MAIN ELECTRODE
=====

Original Electrical Current Flowing In Electrode..: 1000.0 amperes
Current Scaling Factor (SPLITS/FCDIST/specified)..: 0.25017
Adjusted Electrical Current Flowing In Electrode..: 250.17 amperes

```

Number of Conductors in Electrode.....: 278
Resistance of Electrode System.....: 18.055      ohms

```

SUBDIVISION

=====

```

Grand Total of Conductors After Subdivision.: 3658

```

```

Total Current Flowing In Main Electrode.....: 250.17      amperes
Total Buried Length of Main Electrode.....: 4855.8      meters

```

EARTH POTENTIAL COMPUTATIONS

=====

```

Main Electrode Potential Rise (GPR).....: 4516.9      volts

```

```

End of Report #5

```

```

Report #6:

```

```

DATE OF RUN (Start)= DAY 1 / Month 6 / Year 2012
STARTING TIME= 14:53: 3: 8

```

```

===== < FAULT CURRENT DISTRIBUTION ( SYSTEM INFORMATION SUMMARY )
>=====

```

```

Run ID.....: Network 1

```

```

Central Station Name.....: Samnanger
Total Number of Terminals.....: 6
Average Soil Resistivity.....: 10000.      ohm-meters
Printout Option.....: Detailed

```

1

```

Central Station: Samnanger

```

```

Ground Resistance.....: 18.055      ohms
Ground Reactance.....: 0.0000      ohms

```

1

```

Terminal No. 1 : Sima

```

```

Number of Sections.....: 264
Ground Impedance.....: 2.0000      +j 0.0000      ohms
Source Current.....: 4170.0      Amps / -79.150
degrees

```

```

Neutral Connection Impedance....: 0.0000      +j 0.0000      ohms
Span Length.....: 349.60      m

```

1

```

Terminal No. 2 : Mauranger

```

```

Number of Sections.....: 117
Ground Impedance.....: 2.0000      +j 0.0000      ohms
Source Current.....: 1615.0      Amps / -79.760
degrees

```

```

Neutral Connection Impedance....: 0.0000      +j 0.0000      ohms
Span Length.....: 406.80      m
1
Terminal No.      3 : Evanger

Number of Sections.....: 96
Ground Impedance.....: 2.0000      +j 0.0000      ohms
Source Current.....: 1615.0      Amps / -79.760
degrees
Neutral Connection Impedance....: 0.0000      +j 0.0000      ohms
Span Length.....: 393.80      m
1
Terminal No.      4 : Fana

Number of Sections.....: 70
Ground Impedance.....: 2.0000      +j 0.0000      ohms
Source Current.....: 1615.0      Amps / -79.760
degrees
Neutral Connection Impedance....: 0.0000      +j 0.0000      ohms
Span Length.....: 470.00      m
1
Terminal No.      5 : Norheimsund

Number of Sections.....: 55
Ground Impedance.....: 2.0000      +j 0.0000      ohms
Source Current.....: 807.50      Amps / -79.760
degrees
Neutral Connection Impedance....: 0.0000      +j 0.0000      ohms
Span Length.....: 274.50      m
1
Terminal No.      6 : Frøland

Number of Sections.....: 9
Ground Impedance.....: 2.0000      +j 0.0000      ohms
Source Current.....: 807.50      Amps / -79.760
degrees
Neutral Connection Impedance....: 0.0000      +j 0.0000      ohms
Span Length.....: 255.60      m
1
TERMINAL GROUND SYSTEM (Magn./Angle)
Term: 1 Total Earth Current...: 1116.9      Amps / 99.011      deg.
      Earth Potential Rise...: 2233.9      Volts / 99.011      deg.
Term: 2 Total Earth Current...: 1022.7      Amps / 91.838      deg.
      Earth Potential Rise...: 2045.5      Volts / 91.838      deg.
Term: 3 Total Earth Current...: 408.34      Amps / 102.83      deg.
      Earth Potential Rise...: 816.68      Volts / 102.83      deg.
Term: 4 Total Earth Current...: 442.26      Amps / 102.48      deg.
      Earth Potential Rise...: 884.53      Volts / 102.48      deg.
Term: 5 Total Earth Current...: 565.99      Amps / 94.042      deg.
      Earth Potential Rise...: 1132.0      Volts / 94.042      deg.
Term: 6 Total Earth Current...: 75.347      Amps / 102.22      deg.
      Earth Potential Rise...: 150.69      Volts / 102.22      deg.
Average Resistivity.....: 10000.      Ohm-meters
Grid Impedance.....: 18.055      +j 0.0000      Ohms
      < Magnitude / Angle >
Total Fault Current.....: 10630.      Amps / -79.521      degrees
Total Neutral Current.....: 10393.      Amps / -79.952      degrees
Total Earth Current.....: 250.17      Amps / -61.290      degrees
Ground Potential Rise (GPR)...: 4516.9      Volts / -61.290      degrees

End of Report #6

```

Report #7:

Report for Ampacity Function
Creation Date/Time: 1 jun 2012/14:53:03

CDEGS Conductor Ampacity Calculation (per IEEE Standard 80)

Computation Results

Use 250°C if mechanical considerations do not allow annealing for the conductor(e.g., connections of aboveground conductors), no matter how the connections are made. Also for pressure type connections if no temperature data is available:

Minimum Conductor Size:

=====
86,4571 MCM
43,7979 mm²
0,1470 in (radius)
3,7339 mm (radius)

Use 450°C for brazed conductors:

Minimum Conductor Size:

=====
69,7433 MCM
35,3310 mm²
0,1320 in (radius)
3,3536 mm (radius)

Other temperatures may apply for pressured type conductors

Use fusing temperature of conductor otherwise (e.g., direct-buried conductors with exothermic welded joints):
1083,0000 °C (fusing temperature)

Minimum Conductor Size:

=====
54,1023 MCM
27,4074 mm²
0,1163 in (radius)
2,9537 mm (radius)

Input Data:

=====
Symmetrical RMS Current Magnitude: 10,63 kA
Maximum Fault Duration: 0,5 s
Ambient Temperature: 20 °C
Conductor Type: Copper, annealed soft drawn (100% conductivity)
Decrement Factor: 1,0517
X/R: 20
Frequency: 60 Hz

Material Constants of Conductor:

=====
Name: Copper, annealed soft drawn (100% conductivity)
Reference Temperature for Material Constants: 20 °C
Thermal Coefficient of Resistivity at Reference Temperature: 0,00393 1/°C

Fusing Temperature of Conductor: 1083 °C
Resistivity of Conductor at Reference Temperature: 1,72 mW×cm
Thermal Capacity per Unit Volume: 3,42 J/cm³ · °C

End of Report #7